Incorporation of Developability into Cell Line Selection

An EngD Thesis submitted to

University College London

by

John Paul James Betts

Declaration

I, John Betts, confirm that the work presented in this thesis is my own. Where information has been derived from other sources, I confirm that this has been indicated in the thesis.

Acknowledgments

I would like to thank my supervisors from UCL, Gary Lye and Frank Baganz for all their support and advice throughout this project. In addition, I would like to thank my supervisors Steve Warr, Gary Finka and Mark Uden for welcoming me into the BiopharmR&D group, for all their assistance and for providing an invaluable collaborative opportunity. Furthermore, I would like to thank the EPSRC and GSK for funding my studies.

There are too many people at UCL to thank for their help and friendship but I would especially like to acknowledge members of the Mammalian Cell Group for their support, in particular Rich, Andy, Lourdes, Eduardo, Dougie, Daria and Nick. I would like to thank everyone in the Vineyard office, especially Sara and Jayan. Finally, I would like to thank Rooni and Akin for always adventurous Friday nights.

I would like to thank everyone from the BiopharmR&D group at GSK; in particular Katy, Jai, Yuen-Ting and Pete for their support and making me feel so welcome. I would also like to acknowledge UCL Public Policy for giving me the opportunity to undertake a secondment to the Department of Business, Innovation and Skills. This was a fantastic addition to my studies and I would like to thank Shami, Harry and Ollie for their friendship and with sadness, Ron who was a great inspiration.

Finally, I would like to thank all my friends and family who have supported me so absolutely throughout this project. I could not have done any of this without you.

Abstract

The pharmaceutical industry is under increasing pressure to deliver new medicines quickly and cost effectively; traditional small molecule product pipelines have dried up and companies are increasingly investing into biopharmaceuticals. To date, the most successful biopharmaceuticals have been monoclonal antibodies. The ability to construct common manufacturing platforms for a range of antibody products has underpinned this interest. Antibodies are most often produced as heterologous proteins at large scale in stirred tank reactors. However, at manufacturing scale there is limited opportunity to undertake process development and optimisation. If a manufacturing process can be 'scaled down' experiments could be carried out at much greater throughput and occur in parallel throughout the entire product lifecycle. In creating a small scale model, the fundamental challenge lies in accurately recreating the engineering environment experienced at large scale in order to yield process relevant data.

In this thesis a miniature, single use, 24-well shaken bioreactor platform was investigated as a small scale cell culture device. This plate format can operate either using direct (REG plate) or headspace sparging (PERC plate) i.e. with either the presence or absence of a dispersed gas phase. Initial work involved the experimental and theoretical characterisation of the novel, miniature bioreactor (7 mL) and the conventional stirred bioreactors (1.5 L), themselves mimics of pilot scale GSK cell culture processes. Under typical operating conditions in the miniature bioreactor, measured mixing times were 0.8 – 13 s and apparent $k_L a$ values in the range 5 – 50 hr^{-1}.

Based on these findings, cell culture kinetics were investigated. A methodology for consistent, parallel cell cultures was first established and then used to determine the

impact of the dispersed gas phase on culture kinetics of a model CHO cell line. Cultures performed with head space aeration showed the highest viable cell density (15.2×10^6 cells mL^{-1}) and antibody titre (1.58 g L^{-1}). Final cell density in the PERC plate was nearly 40 % greater than shake flask cultures due to the improved control of process conditions. In contrast, cultures performed with direct gas sparging showed a 25 – 45% reduction in cell growth and 40 – 70 % reduction in antibody titre. The platform nature of the system was confirmed with similar findings obtained using a second antibody and cell line cultured under different conditions. The miniature bioreactor was then investigated for use as an early stage, cell line selection tool. A strong positive correlation between PERC and shake flask data was found (0.88), indicating the suitability of the platform for this application. In contrast, selection results in the REG plate format differed notably, highlighting the fact that the presence of a dispersed gas phase can significantly alter cell culture kinetics; and potentially cell line selection.

A panel of four CHO clones was then investigated alongside bench scale bioreactors, operating at matched mixing times; the REG plate format provided the most comparable match in terms of cell growth and product titre. Primary recovery studies investigated use of a small scale depth filtration tool to analyse material generated previously with regards to ease of processing. Data showed that cells cultures in the presence of a dispersed gas phase yielded the most accurate prediction of primary recovery data. Subsequently, detailed product quality analysis confirmed consistent product quality attributes across the different cell culture formats.

In summary, this work shows the utility of miniature bioreactor systems for high throughput strain selection under process relevant conditions.

Table of contents

List of Tables

List of Figures

Nomenclature

Abbreviation	**Description**
ADCC	Antibody-dependent cellular cytotoxicity
BCR	B-cell receptor
BHK	Baby hamster kidney cells
C	Ig constant region
CD	Chemically defined
CDC	Complement-dependent cytotoxicity
CDR	Complementarity determining regions
CD-CHO	Chemically defined CHO cell line media
CFD	Computational fluid dynamics
CHO	Chinese hamster ovary cells
CHO-A	CHO DG44 (*dhfr*$^{-/-}$) cell line expressing an IgG1 mAb in a non-chemically defined process
CHO-B	CHO DG44 (*dhfr*$^{-/-}$) cell line expressing an IgG1 mAb in a chemically defined process
Da	Daltons
dAb	Domain antibody
dhfr$^{-/-}$	Dihydrofolate reductase deficient cell line
DMSO	Dimethyl sulphoxide
DNA	Deoxyribonucleic acid
DO	Dissolved oxygen
DoE	Design of experiments
DOT	Dissolved oxygen tension
DPBS	Dulbecco's phosphate buffered saline
DTT	Dithiothreitol
EPO	Erythropoietin
ER	Endoplasmic reticulum
fAb	Fragment antibody
FACS	Fluorescent activated cell sorting
G-CSF	Granulocyte colony-stimulating factor
GFP	Green fluorescent protein
GHT	Glycine, hypoxanthine, and thymidine

GOI	Gene of interest
GS	Glutamine synthetase
GSK	GlaxoSmithKline
H Chain	Ig heavy chain
HBSS	Hank's balanced salt solution
HEK-293	Human embryo kidney cell line
HEPES	4-(2-hydroxyethyl)-1-piperazineethanesulfonic acid buffer
HPLC	High performance liquid chromatography
HTE	High throughput experimentation
HTS	High throughput system
Ig	Immunoglobulin
L Chain	Ig light chain
µ24	Miniature, single use, 24 well, shaken bioreactor format
mAb	Monoclonal antibody
MALDI	Matrix-assisted laser desorption/ionization
mRNA	Messenger ribonucleic acid
MSX	Methionine sulfoximine
MTX	Methotrexate
NGHC	Non-glycosylated heavy chain
NIR	Near-infrared
NS0	Mouse myeloma cell line
PBS	Phosphate buffered saline
PBT	Pitched blade turbine
PEG	Polyethylene glycol
PERC	Headspace sparged miniature bioreactor plate format
Per.C6	Human retinal derived cell line
PES	Polyethylene sulfone
PPG media	Proprietary production growth media
PTV	Particle tracking velocimetry
Q-TOF	Quantitative Time of Flight
R&D	Research and Development
Rec	Recombinant
REG	Direct sparged miniature bioreactor plate format
RO	Reverse osmosis

scFv	Single-chain variable fragments
SEC	Size exclusion chromatography
SELDI	Surface-enhanced laser desorption/ionization
SF	Shake flask
SP2/0	Mouse myeloma cell line
SRW	Standard round well microtitre plate
STR	Stirred tank reactor
SUB	Single use bioreactor
TNF	Tumour necrosis factor
TOF	Time-of-flight
UPR	Unfolded protein response
USD	Ultra scale-down
V	Antibody molecule variable region
v/v	Concentration volume by volume
VVM	Gas volume flow per unit of liquid volume per minute
wv	Working volume

Symbol	Description	Unit
A	Constant used in equation 1.6	-
A_{280}	Absorption at 280 nm	Absorbance Units
a	Term used in equation 2.8	-
a	Area	m^2
Ab	Antibody titre	$g\ L^{-1}$
b	Term used in equation 2.8	-
Bo	Bond number ($\rho g d_w^2/W$)	Dimensionless
c	Constant used in equation 1.3	-
C	Constant used in equation 1.10	-
c_1	Constant used in equation 1.14	m^{-1}
cIVC	Cumulative integral of viable cell concentration	10^6 cells.day mL^{-1}
C_P	Normalised dissolved oxygen concentration	%
d_f	Inner diameter of shaken vessel	m
D_i	Impeller diameter	m
D_{O2}	Oxygen diffusion coefficient	$m^2\ s^{-1}$
d_s	Shaker diameter	m
D_T	Tank diameter	m
d_w	Microwell diameter	m
Fr	Froude number ($d_s(2\pi N)^2/2g$)	Dimensionless
g	Gravitational acceleration	$m\ s^{-2}$
[glucose]	Glucose concentration	$g\ L^{-1}$
h_L	Displaced liquid height	m
H_T	Tank height	Tank height, m
IVC	Integral of viable cell concentration	10^6 cells.day mL^{-1}
k_La	Volumetric oxygen mass transfer coefficient	hr^{-1}
k_La_{app}	Apparent volumetric oxygen mass transfer coefficient	hr^{-1}
N	Agitation rate	s^{-1}
N_{crit}	Critical shaking frequency	rpm
OD_{600}	Optical density at 600 nm	Absorbance Units
P	Power input	W
P_g	Gassed power input	W
Ph	Phase number as defined in equation 1.11	Dimensionless
P_o	Power number ($P/\rho N_3 D_i^5$)	Dimensionless
P'_o	Modified power number as defined in equation 1.9	Dimensionless
P_{og}	Gassed power number	Dimensionless

t	Timepoint	Days
t_m	Mass transfer time	$k_L a^{-1}$, s
t_m	Mixing time	s
Q	Volumetric airflow rate	$m^3\ s^{-1}$
$Q_{gluc\ (avg)}$	Average specific glucose consumption rate	ng $cell^{-1}$ day^{-1}
Q_P	Instantaneous cell specific productivity	pg $cell^{-1}$ day^{-1}
Q_S	Specific impeller pumping rate ($\propto ND^3/V_L$)	s^{-1}
Sc	Schmidt number ($\mu/\rho D_{O2}$)	Dimensionless
U	Tip speed (πND)	m s^{-1}
V_L	Liquid volume	m^3
v_s	Superficial gas velocity	m s^{-1}
W	Wetting tension	N m^{-1}
W_b	Impeller blade width	m
x	Viable cell density	10^6 cells mL^{-1}
Z	Term used in equation 2.3	-

Greek symbol	Description	Unit
α	Constant used in equation 1.6	-
β	Constant used in equation 1.6	-
$\bar{e}$	Average energy dissipation rate	W kg^{-1} or W m^{-3}
ε	Local energy dissipation rate	W kg^{-1}
ε_I	Energy dissipation rate in the impeller discharge zone	W kg^{-1}
ε_b	Energy dissipation rate in the bulk liquid	W kg^{-1}
ε_{Tg}	Total energy dissipation rate in a gassed bioreactor	W kg^{-1} or W m^{-3}
ε_{ig}	Gassed energy dissipation rate from the impeller	W kg^{-1} or W m^{-3}
ε_{sg}	Energy dissipation rate as a result of gas sparging	W kg^{-1}
$\bar{\gamma}$	Average shear rate	s^{-1}
λ_K	Kolmogorov microscale of turbulence	m
ν	Kinematic viscosity (μ/ρ)	$m^2 s^{-1}$
μ	Viscosity	N m^{-2} s
r	Density	kg m^{-3}
σ	Liquid surface tension	N m^{-1}
τ_P	Probe response time	s

Chapter 1. Introduction

1.1. Pharmaceutical industry overview

Whilst the value of the pharmaceutical market is continuing to increase with time, the rate of growth is declining (Figure 1.1). This is as a result of the limitations of the 'big pharma' blockbuster drug business model. Currently, development pipelines are failing to create products to meet the needs of the therapeutic market since most of the 'easier' indications have already been targeted and older product patents are expiring leading to generic drug competition.

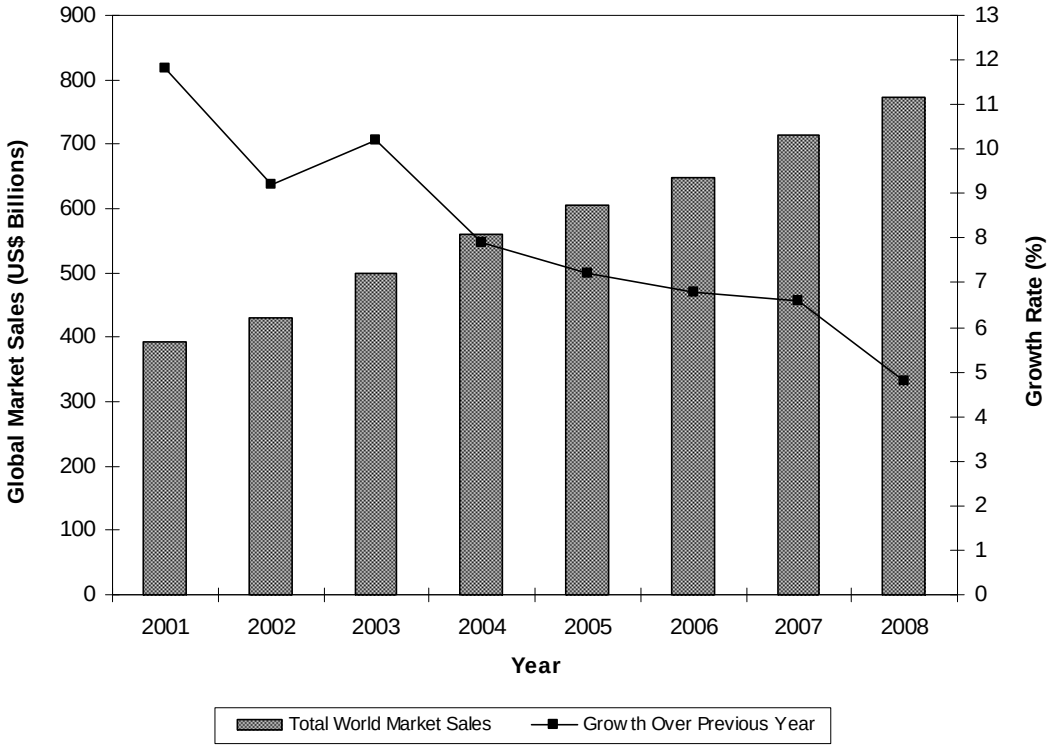

Figure 1.1. Global pharmaceutical industry sales (bars, US$ billions) against sector growth rate (lines, %) (2001-2008). Raw data current as of 2009 (IMS Health Market Prognosis) is presented in Appendix C.

A recent article from IMS Health indicated three challenges to existing pharmaceutical companies which helps explain the current surge in investment in biological therapeutics; a transition in growth rate, market segment and research and development (R&D) focus. Firstly, the global growth rate has decreased; major markets have moderated whilst “pharmerging” markets, e.g. China, Brazil, Mexico and Turkey have rapidly increased (IMS Health, 21st Century Pharma). This creates a shift in the indications that pharmaceutical companies need to target.

The focus of pharmaceutical markets has also altered dramatically. Traditionally, the focus was on large numbers of patients within the primary care sector, with treatments for conditions such as infectious diseases, high cholesterol or blood pressure. However, this has realigned towards small niche groups of patients, requiring innovative, molecularly targeted products for more complicated diseases such as cancer or rheumatoid arthritis (Nelson et al. 2010). Finally, pharmaceutical companies have relied heavily on the blockbuster drug model; at the middle of the last decade 44.3% of growth was attributed to blockbusters; thus blockbuster drugs were at the centre of R&D strategy. However, as blockbuster R&D targets have decreased, pharmaceutical companies need to expand their product portfolios and redirect R&D budgets (IMS Health, 21st Century Pharma). The decline in growth in the market and recent successes with biologics, in particular antibody based therapeutics, has resulted in a huge investment of traditional ‘big pharma’ companies in biopharmaceuticals.

1.2. Biopharmaceutical industry

Pharmaceutical companies are becoming increasingly reliant on biopharmaceuticals, or biologics, product sales as a means of generating revenue (Figure 1.2). This is largely due to recent successes in the field, hence driving up sales and interest in these products.

Global prescription sales of biopharmaceutical products increased 12.5% in 2007 to more than $75 billion, and the global biotech market grew at nearly double the rate of the global pharmaceutical market, which increased only 6.4% that same year (IMS Health, Press Release). More recently, the global biopharmaceutical market value is estimated to account for 15.6% of the total pharmaceutical market, reaching a global market value of $138 billion in 2011 and is expected to increase to more than £320 billion by 2020 (GBI Research, 2012).

In 2007, 22 biopharmaceuticals generated sales exceeding $1 billion, compared with just 6 products in 2002; and in 2007, biopharmaceuticals represented 25% of the total pharmaceutical drug development pipeline (IMS Health, Press Release). One attractive feature of biotechnology products is the perceived lower associated risk; a recent analysis showed that the success rate of biopharmaceutical medicines had an overall higher success rate over chemically-derived medicines at 30% compared to 21.5% (Simoens, 2009). However, it should also be noted that biopharmaceutical products had a lower Phase III clinical trial success rate (Simoens, 2009).

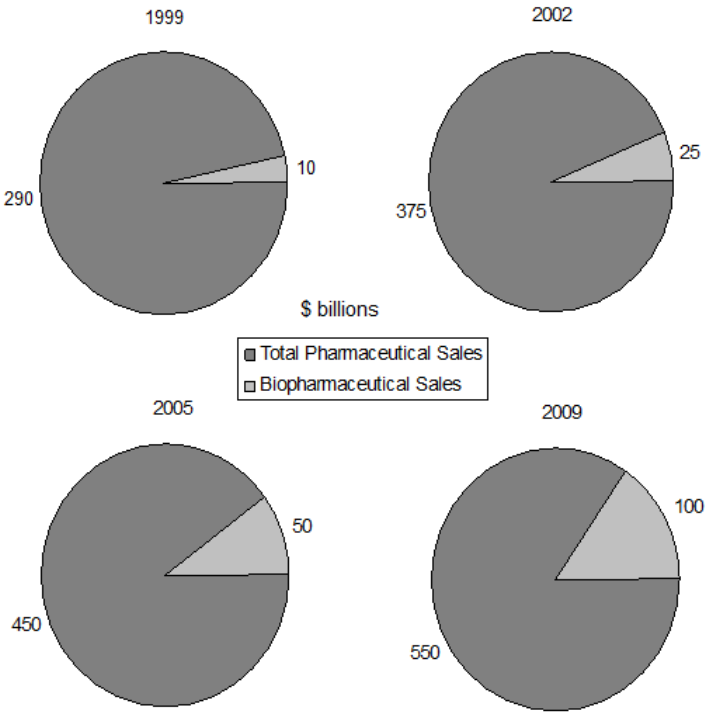

Figure 1.2. Total pharmaceutical sales (*dark grey*), biopharmaceutical sales (*light grey*), values in US$ billions. (Adapted from IMS Health; Biogenerics: A Difficult Birth).

The demand for antibody therapeutics triggered parallel efforts to increase production capacity through construction of large bulk manufacturing plants as well as improvements in cell culture processes to raise product titres (Kelley, 2009). Factors such as fermentation titre and overall yield are deemed critical determinants of economic success (Farid, 2007).

There is now increased pressure for the cost-effective manufacture of antibodies, given the fact they are administered at high doses and show an increasing market potential (Farid, 2007). However, biopharmaceutical products are expensive and time-consuming to develop (Section 1.6.). This highlights the need to establish and implement an efficient, small scale, cell culture model in a high throughput format that can be used to screen for high producing, high potency cell lines and rapidly advance them through development.

1.3. Overview of cell culture processes

The advent of genetic manipulation led to the ability to manufacture heterologous protein products in a variety of cell lines (Rai and Padh, 2001). The choice of cell line largely depends on the nature of the product. These different cell lines have varying characteristics which can be advantageous for certain product types, but can also present different engineering challenges, e.g. in terms of the design of the production scale vessel and subsequent purification of the product. Many different cell types have been investigated for the production of heterologous proteins as therapeutic agents (Lee and Lee, 2005; Walsh, 2001). It is paramount that the cell line selected is not only capable of producing the protein properly, i.e. correctly folded with the necessary post-translational modifications required for clinical efficacy, but also in sufficient quantities per manufacturing run so that production costs are not excessive. Table 1.1 summarises some of the commonly used cell types along with some brief comparisons between them with regard to heterologous protein production as therapeutic agents.

Table 1.1. Summary of different cell line characteristics with respect to the manufacture of heterologous protein products. Table adapted from Lee and Lee (2005) with information from Rai and Padh (2001).

Cell Type	Advantages	Disadvantages
Bacterial	– High growth rate – High cell densities achievable – Inexpensive media	– Misfolds large or complex protein products – No post-translational modifications or protein glycosylation – Must ensure removal of bacterial endotoxins from final product
Insect	– High growth rate – Correct folding of proteins – Correct protein glycosylation	– High culture cost – Currently no manufacturing facilities or regulatory experience for this cell type
Yeast	– High growth rate – High cell densities achievable – Inexpensive media – Certain post translational modifications achievable	– Often hypermannosylates the protein product rendering it ineffective
Plant	– Already used to make some pharmaceuticals	– Slow growth rate – Expensive to culture
Mammalian	– Correct (‘human like’) folding of proteins – Correct protein glycosylation – Correct post-translational modification	– Expensive media – Slow growth rate – ‘Shear sensitive’ cells due to lack of cell wall

For the production of heterologous proteins for use as biopharmaceuticals, especially in the case of full length monoclonal antibody (mAb) molecules, it is often necessary to use mammalian cells. This is because these protein products are often difficult to fold and require significant amounts of post-translational modifications, not always possible in other cell types. Ideally, recombinant glycoprotein products will have high structural fidelity with the ‘natural’ product. Alterations to the protein in, for example, protein

folding and post-translational modifications could cause the product to actually become immunogenic, consequently resulting in an anti-therapeutic antibody response which can impact therapeutic efficacy, i.e. reduced circulation time in blood, and perhaps more significantly might precipitate an adverse reaction (Jefferis, 2009). Thus, whilst screening cells as potential manufacturing scale candidates, it is not only essential to analyse for high productivity in terms of amount of protein expressed, but also in terms of the quality of the protein expressed. Very high titres can be offset by the fact that the protein product itself is not therapeutically active or in fact immunogenic.

One significant development with regard to recombinant glycoprotein production is the work of Glycofi Inc. (owned by Merck). This company is genetically engineering yeast cells to perform the necessary glycosylation post-translational modifications equivalent to human cells (Hamilton and Gerngross, 2007). This group have pioneered the glycoengineering of the yeast *Pichia pastoris*, which has led to the production of fully humanized sialylated glycoproteins (Hamilton and Gerngross, 2007). As described in Table 1.1, yeast cells have very high growth rates and inexpensive media requirements. If the ability to perform human-like glycosylation protein modifications could be integrated into this host line, then this is potentially the one future expression system that could rival mammalian cell culture for the production of recombinant glycoprotein products, in particular mAb therapeutics.

Biopharmaceuticals may be produced in a range of mammalian cell types, e.g. immortalized Chinese hamster ovary (CHO) cells, mouse myeloma (NS0), baby hamster kidney (BHK), human embryo kidney (HEK-293) and human retinal derived cells, i.e. Per.C6 (Butler, 2005; Wurm, 2004). However, all currently licensed mAb products are manufactured in one of three mammalian cell lines: CHO, NSO or mouse

Sp2/0 myeloma cells (Jefferis, 2009). To date, no other mammalian cell lines, for example, the mammalian BHK line or human Per.C6 line, have been licensed for the production of mAbs (Flickenger, 2013). The industrial advantage to using CHO and NSO cells is that these are well-characterised platform technologies, which allow for transfection, amplification and selection of high-producer clones rapidly for a range of different products (Butler, 2005). There is further evidence that both NSO and Sp2/0 perform unusual glycosylation; inserting additional oligosaccharide residues in some recombinant mAb products, but CHO cell lines do not and therefore may be preferred over these alternative mammalian cell hosts (Jefferis, 2009).

The industrial scale culture of cells expressing a product of interest will most often occur in a bioreactor, in which conditions for growth of the cells and expression of the desired product are optimised. There are many reactor types that may be employed, but the most frequently used format is the stirred tank reactor (STR) (Doran, 1999). An STR is able to adequately mix, even at large volumes, providing homogenous culture conditions for the cells, i.e. uniform temperature, pH, dissolved oxygen, and nutrients. When using ‘fragile’ mammalian cells, there have been fears that high hydrodynamic shear, especially in the impeller discharge zone, may damage the cells. This led to the development of airlift reactors. Airlift reactors have to be very tall in order to operate effectively, and thus are awkward to install in manufacturing facilities. While they do not generate particularly efficient mixing they do have the capacity for high gas transfer rates. However, with the advent of shear protectants, like Pluronic F-68, airlift reactors have largely been made redundant in favour of STR’s (Nienow, 2006). In addition, research has suggested that cell death is more dependent on energy dissipation released as a result of bubble bursting rather than shear as a result of the impeller (Figure 1.3) (Heath and Kiss, 2007; Nienow, 2006). The chosen bioreactor may also be operated

under a variety of fermentation strategies, e.g. batch, fed-batch and perfusion, whereby the aim of the latter methods are to extend the culture length and thus increase the amount of time the cells are at their highest density and producing large amounts of the product of interest (Bailey and Ollis, 1986).

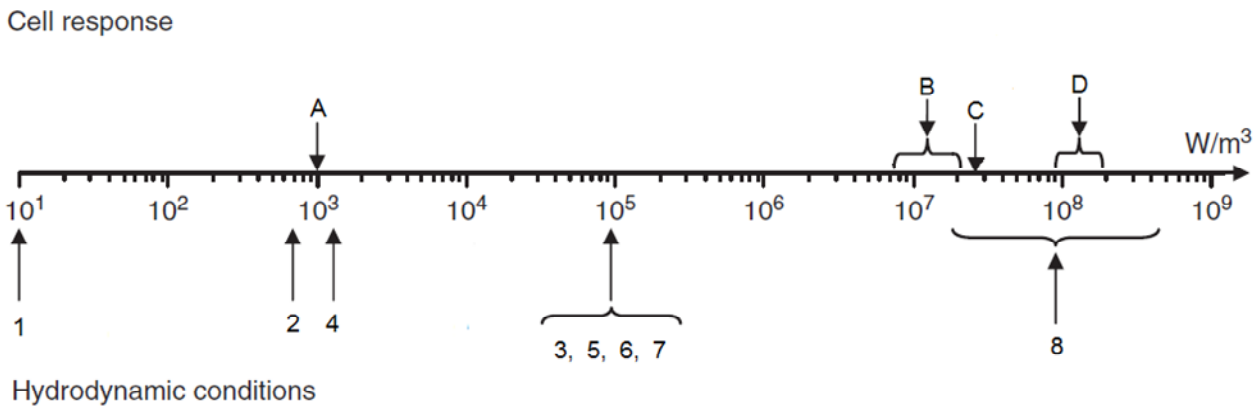

Cell Response			
Symbol	**Mode of growth**	**Cell line**	**Effect**
A	Anchored	CHO-K1	Necrosis
B	Suspension	Hybridoma	Necrosis
C	Suspension	Mouse myeloma	Necrosis
D	Suspension	CHO-K1	Necrosis
Hydrodynamic Conditions			
Symbol	**Process**	**Description**	**Energy Dissipation Rate**
1	Agitation	Typical animal cell bioreactors	Average
2	Agitation	10 L STR (Rushton, 700 rpm)	Average
3	Agitation	10 L STR (Rushton, 700 rpm)	Maximum
4	Agitation	22,000 L STR (Rushton, 240 rpm)	Average
5	Agitation	22,000 L STR (Rushton, 240 rpm)	Maximum
6	Flow through a micropipette tip	Flow through a 200 µL tip in 0.2 s	N/A
7	Bubble rupture	Pure water, bubble diameter 6.32 mm	N/A
8	Bubble rupture	Pure water, bubble diameter 1.7 mm	N/A

Figure 1.3. Effects of various energy dissipation values on mammalian cells (Adapted from Godoy-Silva et al., 2010). 'Maximum' refers to the peak energy dissipation rate observed in a stirred tank bioreactor, i.e. in the impeller discharge zone, whereas 'average' refers to the average energy dissipation rate observed in the bulk of the liquid.

The successful manufacture of a heterologous protein in a production scale bioreactor will require significant optimisation before full productivity can be reached. It would be costly and time consuming to perform all process development and optimisation at large scale, therefore small scale mimics of large scale bioreactors have been developed to allow process assessment and optimisation before scaling up to production conditions.

1.4. Monoclonal antibodies

Within the biopharmaceutical sector there has been a range of highly successful products; however, the overriding driver in the sector has been as a result of the success of mAbs (Pavlou and Belsey, 2005). Nearly 40 recombinant antibody molecules have been licensed for therapeutic indications in Europe or the United States (2013), largely for cancers and chronic diseases (Dübel and Reichart, 2014). Table 1.2 highlights the number of mAbs that exist within the top 10 biopharmaceuticals in the world market.

As shown in Table 1.2, over half of the top 10 biopharmaceutical products are mAb therapies, and together these 10 products account for half the total global biotechnology market. In addition it is estimated that 30% of new drugs to be licensed in the next decade will be based on antibody products (Jefferis, 2009).

Table 1.2. Top 10 biopharmaceutical products (2013). rHU = recombinant humanised, EPO = erythropoietin, PEG = Polyethylene glycol, G-CSF = Granulocyte colony-stimulating factor, TNF = Tumour necrosis factor. Adapted from Walsh, 2014.

Ranking	**Product**	**Type**	**Indication**	**Sales ($ billions)**	**Company**
1	Humira (adalimumab)	Whole human mAb (anti-TNFa)	Autoimmune diseases	11	AbbVie & Eisai
2	Enbrel (etanercept)	Fusion Protein (anti-TNFa)	Autoimmune diseases	8.76	Amgen, Pfizer, Takeda Pharmaceuticals
3	Remicade (infliximab)	Whole chimeric mAb (anti-TNFa)	Autoimmune diseases	8.37	J&J, Merck & Mitsubishi Tanabe Pharma
4	Lantus (insulin glargine)	Insulin analogue	Diabetes	7.95	Sanofi
5	Rituxan/MabThera (rituximab)	Whole chimeric mAb (anti-CD20)	Lymphomas/leukemia/ autoimmune diseases	7.91	Biogen-IDEC, Roche
6	Avastin (bevacizumab)	Whole humanised mAb (anti-VEGF)	Angiogenesis inhibitor (cancer)	6.97	Roche/Genentech
7	Herceptin (trastuzumab)	Whole humanised mAb (anti-HER2)	Metastatic breast cancer	6.91	Roche/Genentech
8	Neulasta (pegfilgrastim)	PEGylated rHu G-CSF	Neutropenia	4.39	Amgen
9	Lucentis (ranibizumab)	Humanised fAb (anti-VEGF)	Anti-angiogenic (wet AMD)	4.27	Roche/Genentech, Novartis
10	Epogen/Procrit/Eprex/ESPO (epoetin alfa)	rHu EPO	Anaemia (renal failure/ chemotherapy)	3.35	Amgen, J&J, KHK

Antibodies are complex protein molecules (Figure 1.4.a), which have the ability to bind to foreign entities, thus targeting them for destruction by other agents of the immune system. In order to combat the vast array of pathogens that an individual may encounter, lymphocytes of the adaptive immune system have evolved to recognise a great range of antigens, small protein fragments (Janeway et al., 2005; Lodish et al., 2004; Mathews et al., 2000) that might either be on the surface of, or within, a pathogenic organism. The antigen-recognition molecules of B cells are the immunoglobulins (Ig), which are themselves produced in a vast range of antigen specificities, with each B cell producing an Ig of a single specificity (Janeway et al., 2005; Mathews et al., 2000). Ig molecules can be membrane bound on the surface of B cells, and are thus known as B-Cell Receptors (BCR's) or secreted from terminally differentiated B cells, or plasma cells, as antibody molecules (DeFranco et al., 2007).

Antibody molecules have two distinct functions; the first is to bind specifically to antigens of the pathogen, whether it is, for example, a viral surface protein or a bacterial toxin. The second function is to recruit other cells or molecules of the immune system to destroy the pathogen once the antibody has bound to it (Lodish et al., 2004), as well as bind to molecules that determine the biodistribution of the antibody (Brekke and Sandlie, 2003). As such, the antibody molecule is composed of two different regions (Figure 1.4.c), one that binds the antigen and the other that brings about a certain response. The variable region, or V-region, is the antibody binding domain. The great degree of variation that occurs in this part of the protein structure means that a huge range of antigens may be recognised by the antibody (Lodish et al., 2004). The region that brings about the effector functions is much less varied and is therefore known as the constant region, or C region. The most common effector functions are complement-

dependent cytotoxicity (CDC), phagocytosis and antibody-dependent cellular cytotoxicity (ADCC) (Brekke and Sandlie, 2003).

All antibodies are composed from paired heavy and light polypeptide chains, and within these immunoglobulins there are five classes based on their different constant regions: IgM, IgD, IgG, IgA and IgE, with IgG being the most abundant form (DeFranco et al., 2007; Mathews et al., 2000), and therefore the most relevant as a therapeutic agent. IgG molecules are approximately 150 kilo Daltons (Da) and are composed of two different polypeptide chains: the Heavy or H chain is approximately 50 kDa and the Light or L chain is approximately 25 kDa (Janeway et al., 2005; Mathews et al., 2000). Each IgG molecule is constructed from two light chains and two heavy chains, with disulphide bonds linking the two heavy chains, and each heavy chain to a light chain (Brekke and Sandlie, 2003; DeFranco et al., 2007). The IgG molecule is a Y-shape with each variable, antigen binding domain at the ends of the arms of the Y-shape. In this way, the antibody molecule is also capable of cross-linking antigens and binding to them more stably (Janeway et al., 2008).

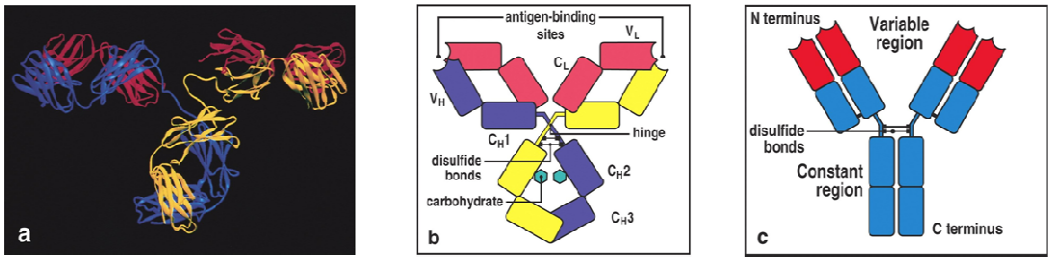

Figure 1.4. Illustrations of typical features of an antibody, as represented in the form of an IgG molecule; firstly by a) ribbon diagram highlighting how the heavy and light chains interact, b) block diagram showing the structural features of the antibody where C = Constant Region, V = Variable Region, L = Light Chain and H = Heavy Chain and c) simplified block diagram highlighting the key features of an antibody. Adapted from Janeway et al., 2005.

1.4.1. Fragment antibodies

Whilst mAb's have proven very successful as therapeutic agents, there has been further innovation in the field which has led to the development of variations of these Ig molecules, including fragment antibodies (fAb's) and single-chain variable fragments (scFv's) (Brekke and Sandlie, 2003). With a mass of approximately 57 kDa, a Fab fragment comprises a V_H–C_H1 polypeptide disulphide-bonded to a V_L–C_L polypeptide and at 27 kDa, a scFv fragment contains only the V_H domain fused to the V_L domain via a polypeptide linker (Holt et al., 2003). Figure 1.5 shows some of the different isoforms generated as therapeutic agents, which have been molecularly engineered from natural Ig molecules (Enever et al., 2009), and are currently on the market or in development. Figure 1.5 also shows some novel antibody variations, often combining multiple components from different Ig molecules and/or synthetic components.

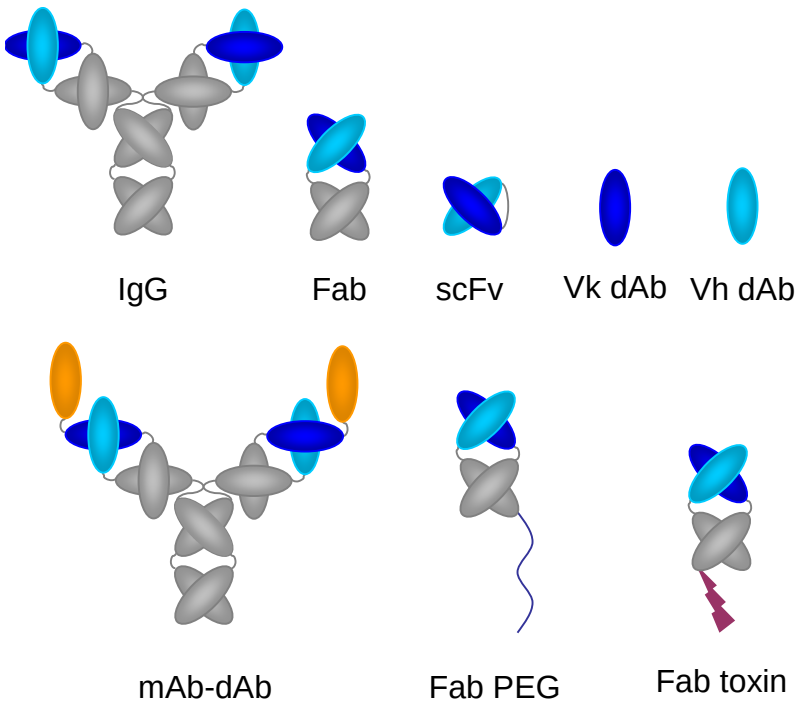

Figure 1.5. Schematic representation of different antibody molecules that have been identified as potential therapeutic agents (Adapted from Enever et al., 2009). PEG = Polyethylene glycol.

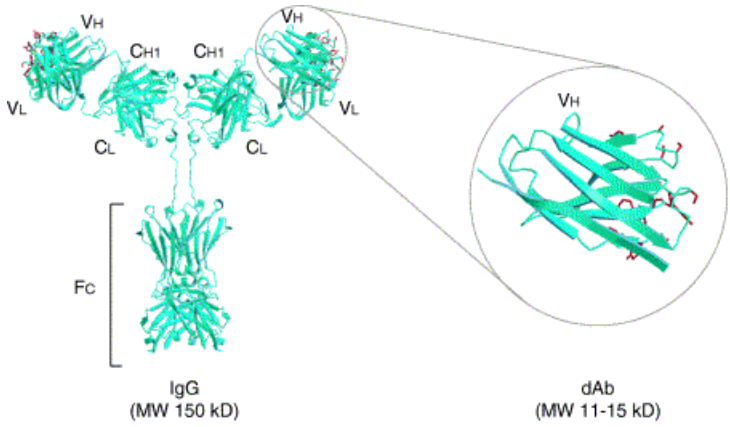

Figure 1.6. Schematic representation of a domain antibody. (Adapted from Holt et al., 2003).

Domain antibodies, dAbs are between 11 – 15 kDa and can either exist as an isolated antibody V_H domain, as shown in Figure 1.6 or as an isolated antibody V_L domain (Holt et al., 2003). Each dAb will therefore retain three of the six naturally occurring complementarity determining regions, CDRs, (Lodish et al., 2004) from the original V_H–V_L pairing; these CDRs are highlighted in red in Figure 1.6.

Domain antibodies are a relatively new development in antibody technologies as they can be used independently as a therapeutic agent but also may be employed as a way of augmenting mAb mode of action and pharmacokinetics. In the former context, a human dAb product is, for example, being investigated for HIV treatment, and it is thought that due to the small molecular weight of the product that the agent may be capable of penetrating into virally infected tissues (Dimitrov and Chen 2008; Chen et al., 2008). However, using a dAb as an independent therapeutic agent may cause problems with 'stickiness' due to their high binding capacity yet small size (Ward et al., 1989). In terms of using dAbs as molecule or in, this context, mAb modulators, dAbs which are capable of specifically binding to serum albumin could be used to enhance the half-life and efficacy of any molecule attached to them (Domantis Patent, 2006). This could help

in terms of product efficacy, lower product dosage and reduce the number of doses required, for example.

1.5. Cell culture process development

Due to the high manufacturing costs associated with mammalian cell culture (Lee and Lee, 2005; Rai and Padh, 2001) there is a great demand to improve cell growth and increase fermentation titres. Historically, process development for biopharmaceutical products, has occurred in incremental stages. Long development periods can mean that by the time the manufacturing process is optimised, the product patent may be coming to the end. This highlights the need for faster, higher throughput development pathways. Figure 1.7 shows a historical case study for the process development of a mAb product, illustrating the kind of process improvements that can be achieved over time.

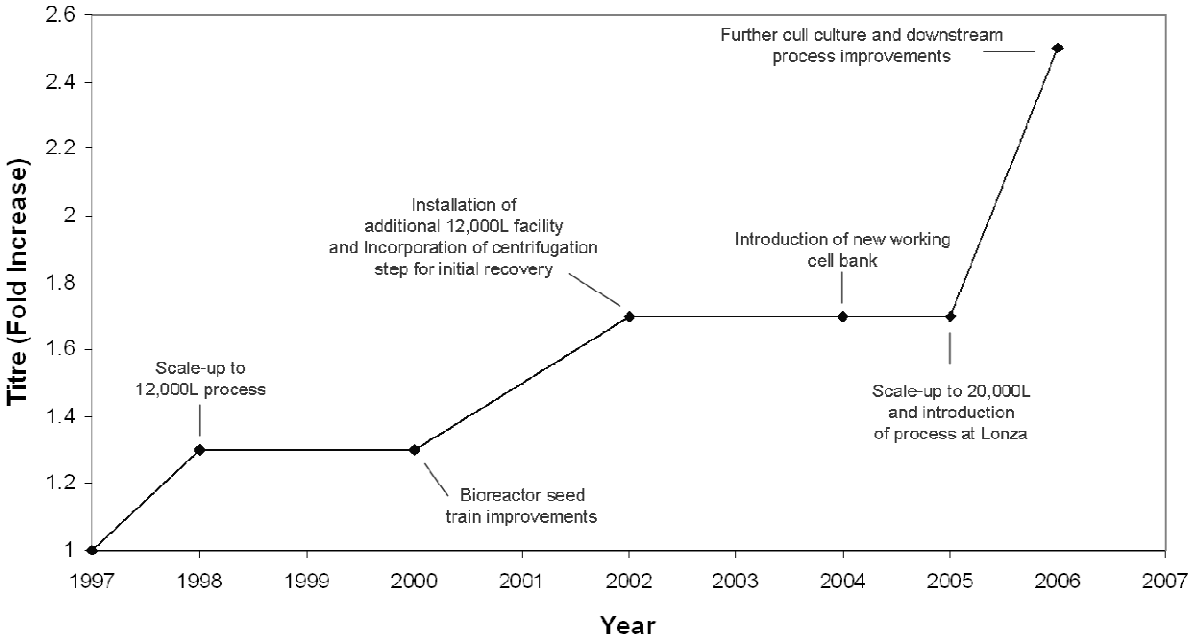

Figure 1.7. Cumulative enhancement in mAb titre and bioreactor productivity (Figure produced from data compiled from a Genentech presentation given at Cell Culture Engineering X, 2006).

With regard to recombinant protein biopharmaceuticals, and in particular antibody manufacturing, industrial production typically takes place in mammalian cell lines, for reasons described previously. For recombinant protein products, the gene of interest, GOI, will be cloned into an expression vector, which is then used to transfect the cells (Lodish, 2004). The expression vector will typically combine a promoter sequence with some form of selection marker, e.g. antibiotic resistance or auxotrophic selection, i.e. an enzyme conferring the ability to synthesise a metabolite not present in the culture media, which can therefore be utilised to select cells that have stably integrated the exogenous genes (Lodish et al., 2004; Matasci et al., 2008). The cell line chosen must be able to efficiently transcribe the recombinant protein genes; this is determined by the expression vector used. It must be capable of translating the GOI's messenger ribonucleic acid (mRNA) efficiently, assembling and modifying the GOI mRNA at high rates with minimal accumulation of incorrectly processed material. Also, the cell line must be able to achieve high cell densities within acceptable production timeframes and achieve desired product quality (Birch and Racher, 2006).

There are two main expression vector systems used for mammalian cell production of recombinant proteins; Glutamine Synthetase (GS) System (Lonza Biologics) and those based on dihydrofolate reductase (DHFR) genes (Birch and Racher, 2006). Methotrexate (MTX) and Methionine Sulfoximine (MSX) are inhibitors of DHFR and GS, respectively (Matasci et al., 2008). Cells can be transfected with the expression construct using a variety of methods including viral vectors, lipofection, electroporation and chemical methods, e.g. $CaPO_4$. Successive rounds of increased enzyme inhibitor can also be applied in such a selection system in gene amplification strategies, attempting to amplify the amount of integrated deoxyribonucleic acid (DNA) and increase productivity (Matasci et al., 2008). One example of an industrially used CHO

cell line that lacks DHFR activity is CHO-DG44. The CHO-DG44 cell line was generated from a proline dependent CHO-pro3$^-$ strain, itself a derivative of the original CHO line, through mutagenesis to yield CHO-DG44. This cell line has deletions of both *dhfr* alleles; requiring glycine, hypoxanthine, and thymidine (GHT) for growth (Hacker et al., 2009).

Transfected cells next undergo a screening process in order to select clones that exhibit the desired characteristics as described previously. The main difficulty is that the creation of a clone that exhibits all the desired characteristics is a very rare event, thus there are large numbers of cells to sort through in order to select high producing cell lines; making the process slow and labour intensive. One way to reduce the number of cell lines involved in screening is to increase the selection pressure (Hacker et al., 2009). Additionally, a high throughput screening mechanism can be applied. One example cotransfects the cells with the GOI and a gene for the green fluorescent protein (GFP); thus, if the genes are genetically linked, the amount of GFP expressed will correlate with the expression of the desired protein product, allowing single cells to be selected based on expression of this fluorescent protein using fluorescent activated cell sorting (FACS) (Mancia et al., 2004; Matasci et al., 2008). Another example involves immobilisation of cells in a semi-solid matrix containing a fluorescent protein conjugated anti-antibody molecule, which then allows for the highest antibody producing cells to be selected by the relative amounts of stained antibody expressed into the matrix surrounding the individual cell, e.g. the ClonePix system (Genetix Ltd) (Hacker et al., 2009; Hanania et al., 2005).

A case study from Wurm (2004) has shown the significant improvements that have occurred in a mAb process. In this article a theoretical process from 1986 is compared

to data from an actual industrial process in 2004. In 1986, cells typically reached a maximal density of ~2 × 10^6 cells mL^{-1}; the product titre reached approximately 50 mg L^{-1} during a 7 day batch production process with a specific productivity of ~10 pg $cell^{-1}$ day^{-1}. In the 2004 process, the culture rapidly grew from a seeding density of 2 × 10^5 to more than 1 × 10^7 cells mL^{-1}; the accumulative yield over the three week fed-batch process reached ~4.7 g L^{-1} with a specific productivity up to ~90 pg $cell^{-1}$ day^{-1}. The author attributes the significant improvements in bioprocess productivity to a better understanding of gene expression, metabolism, growth and apoptosis delay in mammalian cells. Ongoing research in the field has led to improvements in vectors, host cell engineering, medium development, screening methods and process engineering and development (Wurm, 2004) particularly with respect to feeding strategies (Hacker et al., 2009).

Crucially, as discussed earlier, processes have historically been developed incrementally, in a step-wise manner (Figure 1.7). However, with increasing pressure for the biopharmaceutical sector to develop products, process development times must be shortened. Therefore there is an increased priority for high throughput, small scale unit operation mimics to investigate and optimise multiple process choices simultaneously; thus acquiring an optimised manufacturing process much earlier in the product lifetime. Such high-throughput systems for a cell culture process will require accurate scaling down of the manufacturing scale bioreactor thus providing a representative environment to perform process development and optimisation. In doing so, cells can be grown, transfected, screened and selected in an environment that reflects that in which they will be cultured at the manufacturing scale. This will allow for much more accurate selection of high producing clonal lines and further precision in optimisation studies for media and feed development or process optimisation studies.

1.6. Commercial drivers to accelerate product/process development

Herceptin, a mAb therapeutic agent used in the treatment of metastatic breast cancers, costs in the region of $60,000 per patient per year (Waltz, 2005). Whilst there is increasing pressure from government and health bodies to decrease prices, manufacturers argue they must recoup their losses from product failures in clinic and expensive R&D procedures. It is reported that it costs on average $1.2 billion and takes approximately 10 years to develop a new biopharmaceutical (Tufts CSDD, Press Release). Furthermore, as shown in Figure 1.8, the top 10 pharmaceutical companies spend, on average, approximately one sixth of total revenue on R&D. Therefore, to meet such pressures yet remain economically viable, companies must find a way to accelerate their R&D programs and increase product pipeline throughput. To highlight this factor, even when looking at the top 10 biopharmaceutical products it takes, on average, approximately two years before development costs are recouped, assuming an average development cost of a biologic product of $1.2 billion (Purvis, 2009; La Merie, Top 20 Biologics 2008). Should selling prices need to fall, reaching break-even point would take even longer, and might even make some of these products non-viable. All these factors are driving for increased throughput in the R&D process, without losing quality of data that might risk product safety and therefore patient well-being, which could negatively affect public and private confidence, and thus investment in the sector.

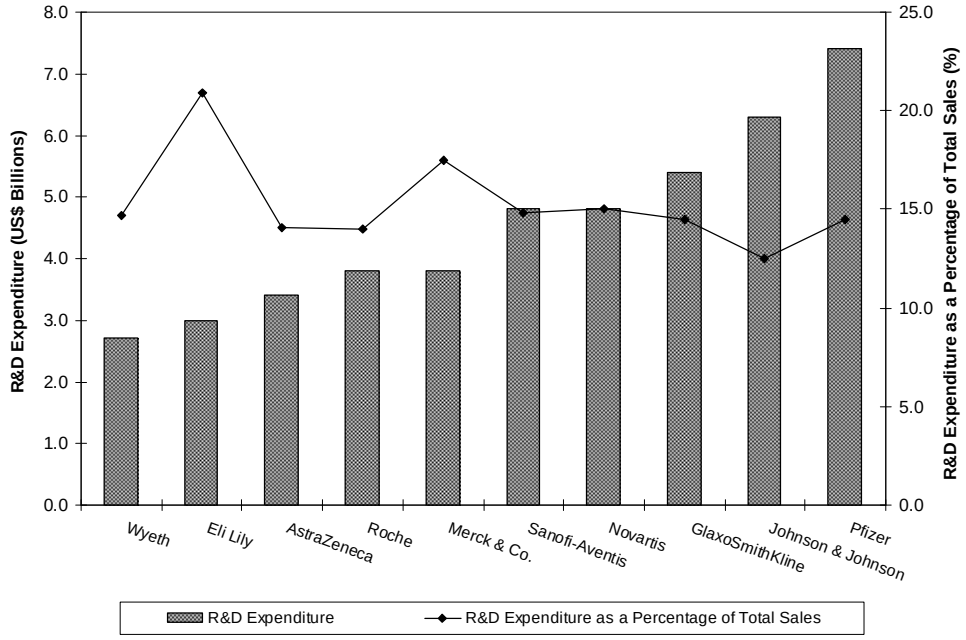

Figure 1.8. Illustration of the significant investment required by pharmaceutical companies for ongoing R&D projects. Information from 2008, published October 2009 from Scrip's Pharmaceutical Company League Tables – 2009, raw data in Appendix D.

1.7. Engineering characterisation of conventional cell culture bioreactors

It is important to characterise any cell culture system in terms of key engineering parameters that are known to have a significant effect on process performance. Knowledge of the qualitative values of these parameters, and the availability of correlations to predict them, aid process optimisation and allow for effective scale translation.

1.7.1. Stirred tank reactors

STRs are the most common format of cell culture bioreactor, and are the predominant format used for large scale cell culture (10L+). Power input into the system is via a centrally rotated shaft; equipped with one or more impellers. Power input is required to

create a homogeneous environment for cell culture by: minimising local concentration gradients of toxins or feeds; dispersing gas bubbles; aiding cell suspension and dispersion; and by increasing mass, heat and gas transfer. The number and type of impellers used is dependent on the scale of the bioreactor and also the nature of the cells grown in the bioreactor. The geometry, number and location of the impellers used, as well as the geometry of the bioreactor itself, will significantly affect the fluid flow. Fluid flow perpendicular to the impeller shaft is termed radial flow, whilst parallel to the shaft is axial flow. Impellers which create predominantly radial fluid flow include Rushton or concave impellers. This type of impeller has the potential for hydrodynamic shear, due to the flat, sharp-edged impeller paddles; although the impact of such shear forces is now known to be significantly less than previously thought (Godoy-Silva et al., 2009; Heath and Kiss, 2007; Nienow, 2006). Rushton impellers also provide excellent gas dispersion into the fluid and have high impeller power numbers. Radial flow impellers include marine impellers, which are regarded as low shear, have lower power numbers and provide good liquid mixing within the system.

Air is sparged into the culture to provide oxygen for metabolism and to strip CO_2 from the liquid. Gas sparging also affects fluid flow; gassing decreases the density of the culture medium thus decreasing the power requirement. Baffles are thin plates fixed perpendicular to the tank wall at regular intervals. These fixtures help to prevent liquid vortexing and aid the formation of a turbulent fluid flow regime within the system. Typically operating at medium to large scales, STRs can accommodate multiple probes to allow for online monitoring of key parameters, e.g. pH, DO and temperature, as well as control systems that can automatically adjust the operating conditions to maintain the process within certain set parameters, i.e. pumps attached to base to adjust pH upwards.

The nature of the fluid flow within a stirred tank reactor can be described by the dimensionless impeller Reynolds number, Re_i; values greater than 1×10^4 describe turbulent flow regimes for stirred tank systems:

$$Re_i = \frac{\rho N D_i^2}{\mu} \quad (1.1)$$

where ρ is the liquid density, N is the agitation rate, D_i is the impeller diameter and μ is the liquid viscosity (Doran, 1999). The power input, P imparted by the impeller is given by:

$$P = P_o \rho N^3 D_i^5 \quad (1.2)$$

where P_o is the impeller power number (Doran, 1999). Subsequently, the gassed power requirement, P_g can be determined on the basis of the ungassed power requirement by, for example, the Michel-Miller (1962) correlation:

$$P_g = c\left[\frac{P^2 N D_i^3}{Q^{0.56}}\right]^{0.45} \quad (1.3)$$

where c is a constant and Q is the volumetric airflow rate (Michel and Miller, 1962). The constant, c is based on the geometry of the impeller, with the most common value being 0.72. However, this original correlation has become widely questioned and therefore Amanullah et al. (2004) compares experimental data with a series of correlations in order to try and select one such equation for further use. They conclude that despite a lot of research in the field, no satisfactory correlation exists for accurately predicting the gassed power consumption (Amanullah et al., 2004). Further to this, Amanullah et al. (2004) and Nienow (2006) report that as agitation rates and sparged air flow are both relatively low for mammalian cell cultures, P_g can effectively be assumed equal to P_{ug}. The mean energy dissipation rate, $\bar{\varepsilon}$ can be determined given the power requirement of the system:

$$\bar{e} = \frac{\mathrm{P}}{r\mathrm{V_L}} \tag{1.4}$$

where V_L is the liquid volume (Nienow, 2006). Note that equation 1.4 calculates energy dissipation in W kg^{-1}. Energy dissipation in W m^{-3} can be calculated by P/V_L. An indication of the impact of the energy dissipation on cells cultured in an STR can be obtained using Kolmogorov's microscale of turbulence, λ_K. This method predicts the smallest eddy size generated in the fluid, and if on a relative level of magnitude to the cell size, may result in cell damage:

$$l_K = \left(\frac{n^3}{e}\right)^{\frac{1}{4}} \tag{1.5}$$

where ε is the local energy dissipation rate and n is the kinematic viscosity (n = μ/ρ) (Patterson et al., 2004; Tennekes and Lumley 1972). Local energy dissipation rates will vary depending on location in the bioreactor, i.e. the local energy dissipation rate will be highest in the impeller discharge zone. The bulk liquid and the impeller discharge zone energy dissipation rates, ε_b and ε_i respectively, can be estimated from the mean energy dissipation rate (Patterson et al., 2004). From such values the Kolmogorov microscale of turbulence can be determined for different regions in the STR. Another important characteristic is k_La, the volumetric oxygen mass transfer coefficient, a measure of the aeration capacity of a cell culture reactor (Stanbury and Whitaker, 1984). The following equation is typically used to determine the k_La for a given system operating under a given set of process conditions:

$$k_{\mathrm{L}}a = \mathrm{A}\left(e_{\mathrm{T}_g}\right)^{\alpha}\left(v_s\right)^{\beta} \tag{1.6}$$

where v_s is the superficial gas velocity, ε_{T_g} is the total energy dissipation rate in a gassed bioreactor and A, α and β are all constants. ε_{T_g} is the sum of the gassed energy dissipation rate imposed by the impeller, ε_{i_g} and that caused by air sparging, ε_{s_g}. Whilst

$\varepsilon_{s_g} = v_s g \rho$, Nienow (2006) proposes that ε_{s_g} can be ignored due to the low gas flow rates used in mammalian cell cultures. In addition, whilst $\varepsilon_{i_g} = P_{o_g} N^3 D_i^5 / V$ (where P_{o_g} is the gassed power number) due to the fact that air flow into a bioreactor is relatively low for mammalian systems, $P_{o_g} \approx P_o$, therefore $\varepsilon_{i_g} \approx \varepsilon_i$, and as such it can be assumed that $\varepsilon_{T_g} \approx \varepsilon_i$. Nienow (2006) proposes that both α and β values should always be 0.5 ± 0.1, whilst van't Riet (1979) states values of $A = 2 \times 10^{-3}$, $\alpha = 0.7$ and $\beta = 0.2$ for salt solutions (non-coalescing) and values of $A = 2.6 \times 10^{-2}$, $\alpha = 0.4$ and $\beta = 0.5$ for coalescing fluids. Stanbury and Whitaker (1984) state the same values as the second van't Riet correlation, with the exception of $\alpha = 0.6$. Mammalian cell culture media is a coalescing fluid (Betts and Baganz, 2006) therefore it is likely that Nienow's proposal (2006) will be suited to this work. Typical $k_L a$ values for mammalian cell culture media are in the range 1 - 15 hr^{-1} (Nienow 1996; Nienow, 2006)

Mixing time, t_m is a value used to describe the length of time required in order for the fluid in the STR to become homogenous following addition of a tracer compound. Whilst this value varies greatly depending on the vessel geometry, Nienow (1998) proposes the following equation, in circumstances where the tank height, H_T is equal to the tank diameter, D_T:

$$t_m = 5.9\left(e_{T_g}\right)^{-0.33}\left(\frac{D_i}{D_T}\right)^{-0.33} D_T^{\,0.67} \qquad (1.7)$$

Osman (2001) reports mixing time values of less than 60s for a 2L working volume (wv) STR.

1.8. Technologies for accelerating upstream process development

As described in Section 1.5, small scale, high throughput models are now required to improve process development timelines. Creation of such small scale models allows for faster development prior to product launch and subsequent process optimisation parallel to manufacturing. Such a system is beneficial to a pharmaceutical company as: material can be generated quicker for clinical trials; further experimentation may provide a better understanding of the cell line and process; it will provide increased throughput therefore leading to quicker process development cycles, thus reducing development times and costs and, crucially, decrease time to clinical trials and product launch. Reducing timescales and development costs in this manner could mean that products are faster to market, cheaper and more readily available.

Typically, a cell culture process can be scaled down from manufacturing size equipment (500L+ format) to varying degrees: pilot plant scale (large, 10L+ format), laboratory scale STR (medium, 0.5L+ format), shake flask systems, miniature bioreactors (small, >0.5L format), microwell plate formats and microfluidic bioreactors (micro, >1mL format). With decreasing scale, less process materials are required and therefore each run becomes cheaper. This allows for the throughput to be increased; however, it also becomes more difficult to recreate the engineering environment of the largest scale system. In addition, the ability to monitor and control the system also becomes harder. Therefore there is an apparent trade off between the degree of information that can be obtained from each run and the number of runs that can be performed in parallel (Figure 1.9).

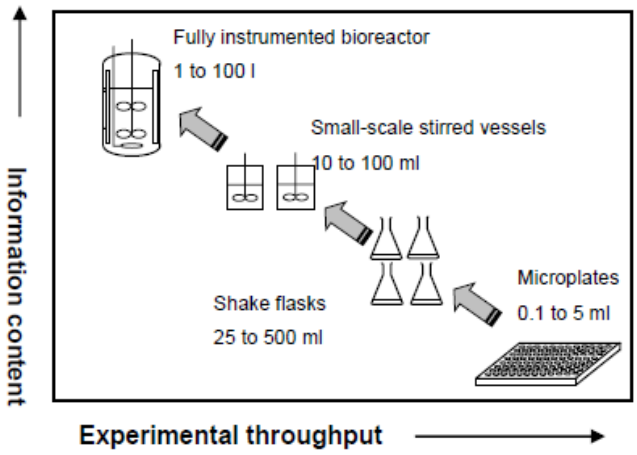

Figure 1.9. Apparent trade off between experimental throughput and the information that can be obtained from each experiment (Doig et al., 2006).

In addition, how and where the system will be placed in the product development process will affect the type of system adopted, i.e. for initial cell line selection, a microwell plate format may be desired for highest throughput, however, for process optimisation studies this tool may not be appropriate; a system with greater potential for process monitoring and control may be required. Both the production scale and small scale systems will need to be fully characterised in terms of the engineering environment in order to try and predict how the cells will behave when scaling down. Following this characterisation work, suitable scaling parameters can be adopted in an attempt to recreate the environment of the production scale system in the small scale model. The following are typical scaling criteria used in industry when scaling down bioreactor systems (Flickinger and Drew, 1999; Hemrajani and Tatterson, 2003):

- Equivalent power input per unit volume
- Maintaining geometric similarity
- Equal impeller tip speed (U)
- Constant mixing times
- Maintain constant $k_L a$
- Constant volumetric gas flow rate per unit volume
- Constant superficial gas velocity

In addition the following combinations of criteria have been proposed for stirred vessels and are typically used with animal cell cultures (Ju and Chase, 1992; Xing et al., 2009):

- Maintain geometric similarity, constant k_La, and constant specific impeller pumping rate (Qs)
- Maintain geometric similarity, constant k_La, and constant maximum shear, defined by impeller tip speed
- Constant k_La, constant impeller tip speed, and constant specific impeller pumping rate

Ultimately, the scaling criteria must be based on the cell culture environment at the production scale. For example, if hydrodynamic shear is identified as a greater issue at large scale than oxygen transfer, this will affect the scaling mechanism adopted, i.e. scale-down with equivalent tip speed might be appropriate. Furthermore, it is necessary to fully characterise the production scale environment in order to understand the unique set of scale-down challenges that the system presents. With regard to this, Nienow (2006) highlights some of the engineering challenges with cell culture operations carried out at very large scale. In such systems mixing time becomes a critical parameter; with poor mixing leading to non-homogeneous culture conditions in which physical and chemical concentration gradients can develop. Another critical parameter is that of CO_2 removal. Often at large scale pure oxygen is used to try and support the high cell density without increasing the overall gas flow through the system, thus CO_2 is generated faster than it is removed and can accumulate in the bioreactor over time (Nienow, 2006) which can be toxic to the cells at high concentrations.

In this manner there are inherent problems working with small scale systems. Due to the small liquid volume, process analysis can be more difficult, accuracy can be an issue and physical forces including surface tension become more significant, thus greatly

affecting orbital shaking, for example. However, one of the main problems is that caused by evaporation, which affects osmolality, cell growth and productivity (Ho et al., 2006). It is important to try and recreate the environment which the cells will experience at production scale when working with a scale-down device. One example of such a procedure is that employed by Godoy-Silva et al (2009). Attempting to recreate the maximum energy dissipation rate of a large scale bioreactor in a scaled down model, the group implemented a 'torture chamber' into which cells were routinely fed through in order to exert different degrees of physical pressure. The necessity is to first characterise the small and large scale formats, before scaling the cell culture operation with sound justification of the scaling criteria adopted. By doing so, greater understanding of the cells growing in the different scales will be achieved thus leading to greater ability to predict how the cells will behave in the large scale culture format, consequently improving process scale up and shortening development times.

1.8.1 Overview of high throughput systems for cell culture

Many commercially available systems have been employed to scale down cell culture processes for a wide variety of cell lines, each presenting a different set of engineering challenges at small scale. Some of these different formats are presented in Table 1.3.

Table 1.3. Examples of different commercial High Throughput Systems (HTS's) for cell culture. DOT = Dissolved Oxygen Tension, ISFET = Ion-sensitive field-effect transistor, MTP = microtitre plate, N/A = not applicable, NR = not reprted and OD = Optical Density (Modified from Betts and Baganz, 2006).

Device	Format	Volume (mL)	Agitation / Aeration	pH, DOT and OD Instrumentation	K_La (hr^{-1})	K_La Prediction Method	Multiplexing	Manufacturer / Reference
Fedbatch-Pro	Based upon Shake Flask	50-500	Orbital / Surface	pH (sterilisable probe)	NR	N/A	16	Dasgip (www.dasgip.com)
µ24	MTP with Microfabrication	3-5	Orbital / Gas Sparging	pH and DOT (optical probes)	NR	N/A	24	MicroReactor (www.Pall.com)
SimCell	Microfluidic Chip	0.3-0.7	Rotation of MBR chips / Surface via membrane	pH, DOT and OD (at-line via cell-reading station)	Up to 500	CFD estimation	1500	Seahorse Bioprocessors (www.seahorsebio.com)
MBR Array	MTP with Microfabrication	0.25	Orbital / Electrochemical O_2 Generation	pH;OD (ISFET;optically)	NR	N/A	8	Maharbiz et al., 2004
Polymer MBR	Microfabrication	0.15	Magnetic Stirrer Bar / Surface via membrane	pH, DOT and OD (optical probes)	20-75	Static Gassing Out	8	Szita et al., 2005; Zhang et al., 2006
Stirrer-Pro Flask	STR	200-275	Magnetic Stirrer Bar / Sparger	pH and DOT (sterilisable probe)	NR	N/A	8	Dasgip (www.dasgip.com)
Xplorer	STR	Up to 100	Single Turbine Impeller / Sparger	pH, DOT and OD	400	Static Gassing Out	16	BioXplore (www.bioxplore.net)
Cellstation	STR	Up to 35	Dual Paddle Impeller / Sparger	pH, DOT and OD (optical probes)	NR	N/A	12	Fluorometrix (www.fluorometrix.com)
MSBR	STR	18	Triple Turbine Impeller / Sparger	pH, DOT and OD (optical probes)	Up to 480	Dynamic Gassing Out	NR	Betts et al., 2005
Bioreactor Block	STR	8-12	Gas-inducing Single Impeller	DOT; pH and OD (optically; plate reader)	700-1600	Dynamic Gassing Out	48	Puskeiler et al., 2005
Parallel BCR	Bubble Column	200	Gas sparging	pH and DOT	Up to 540	Dynamic Gassing Out	16	Weuster-Botz et al., 2001
MBCR	Bubble Column	2	Gas sparging	pH and DOT (optical probes)	Up to 220	Dynamic Gassing Out	48	Doig et al., 2005
Ambr	STR	10-15	Single Marine Impeller / Sparger	pH and DOT (optical probes)	2-13	Static Gassing Out	24-48	TAP Biosystems (www.tapbiosystems.com); Nienow et al., 2003
Micro-Matrix	MTP with Microfabrication	1-7	Orbital / Gas Sparging	pH and DOT (optical probes)	NR	N/A	24	Applikon Biotechnology (www.applikon-bio.com)

As can be seen from Table 1.3, various systems offer different features: the number of experiments that can be performed in parallel; the degree of monitoring and subsequent control; and actual culture conditions that can be generated, i.e. working volumes and type of agitation/aeration employed. In terms of the scaling parameters that are used, P/V is the most commonly adopted scaling criterion for microbial fermentations (Junker, 2004). In a recent scale-up study with *E. coli* in a miniature bioreactor, 100 mL working volume, and a laboratory scale 3 L bioreactor, 1.5 L working volume, very similar growth kinetics were observed at matched k_La values (Gill et al., 2008a). Constant k_La is also used as a scaling parameter for an *E. coli* fermentation overexpressing transketolase in a microwell plate format with working volume of 1000 μL, and is successfully scaled to a 1.4 L bioreactor (Micheletti et al., 2006).

1.9. High throughput experimentation and mammalian cell culture

There are a different set of challenges that need to be addressed when devising small scale high throughput experimentation (HTE) models for mammalian cell culture. There are many different systems on the market, which offer varying degrees of throughput, process control, and automation. However, there are a limited number of research papers on this particular topic, and in general there is a lack of detail regarding any engineering characterisation performed and subsequently the scaling criteria adopted. Table 1.4 summarises some of the recent scale-down work with regard to using mammalian cell hosts. In some cases, computational fluid dynamics (CFD) and particle tracking velocimetry (PTV) have been adopted to theoretically and

experimentally characterise the culture environment in terms of power input and energy dissipation within the system.

A device called the SimCell (Seahorse Bioscience, SimCell website) has been evaluated for use in HT cell line characterisation experiments (Legmann et al., 2009). This cell culture chamber is rotated, allowing an internal gas bubble to provide mixing. The system was used to culture antibody producing CHO cells at a working volume of 700 μL and a Design of Experiments (DoE) approach was used to select the optimum cell line which was then cultured in a 1 L working volume bioreactor to verify the successful selection of an optimum cell line and matched growth kinetics (Legmann et al., 2009). In other work, a VPM8 hybridoma cell line expressing antibody was found to exhibit similar growth kinetics and productivity when scaling from 800 μL microwell plate to 100 mL shake flask on the basis of constant mean energy dissipation (P/V), and these results were also indicative of those expected from a 3.5 L working volume bioreactor (Micheletti et al., 2006).

Table 1.4. Summary of selected scale-down work that has been performed with industrially relevant cell processes or theoretically determined engineering characterisation.

Cell Line	Reactor Type	Scale Up Analysis	Notes	Reference
CHO	Applikon μ24: 24 Deep Well MTP - pH, DO and Temperature sensors - Thermal heat conductor - 0.2 μm sparge membrane	μ24 (5 mL wv) and 2 L wv Bioreactor Matched parameters: • VCD, Viability, Titre, Offline pH and Metabolites: - Matched Lactate, Glutamine, Glutamate and Ammonia - Glucose utilisation profile did not match	*Scale up criteria not specified* Problems with foaming and uneven gas distribution	Chen et al., 2008 (Genentech)
SP 2/0 Mouse Myeloma	3 L STR (Rushton, no baffles) with 75 L, 300 L, 2500 L (2 x pitched blade) - Formats not geometrically equivalent	Step-wise prediction, with constant: 1. impeller tip speed, 2. shear rate at tip, 3. circulation time 4. overall mixing time	Predictions used to estimate conditions where variables are most similar - i.e. 1 and 4 impracticable at largest scale *End up scaling with constant rpm*	Yang et al., 2007 (Immunomedics)
CHO	5000 L bioreactor scaled from 5 and 20 L bioreactors - Geometrically similar	Address particular issues at very large scale: 1.Bulk Mixing 2.Oxygen Transfer 3.CO_2 Removal Rate *Developed specific equations for CHO cell line*	Outcomes: 1. T_m more dependent on volume than agitation rate *Try to reduce overall feeding volume* 2. k_La more dependent on air flow rate than P/V *Configuration only capable of supporting 7 x 10^6 cells mL^{-1}* 3. Increased headspace airflow rate 200% with no effect *Consider changing configuration to allow higher sparge flow rates*	Xing et al., 2009 (Bristol-Myers Squibb)
N/A	a) Volumetric mass transfer coefficient (k_La) determination from 20mL wv to 1000L wv b) CFD Analysis of free-surface from 20mL wv to 13.4L wv	a) Correlated k_La values against shaking speed b) Matched experimentally and by CFD simulation the free-surface shapes	*Dominant effect of free-surface turbulence on gas transfer in orbitally shaken bioreactors* Proposed feasibility of orbital shaken systems for mammalian cell culture up to 1000L wv	Zhang et al., 2009 (ExcellGene)
N/A	Used energy dissipation rate (ε) values to quantify shear PTV to determine ε distribution within the impeller discharge zone	ε_{max} in the impeller region can be approximated: $E = \frac{e_{\max}}{N^3 D^2 r}$ With geometric equivalency, E does not alter significantly over a large range of impeller speeds	ε high in the impeller discharge stream - 43.5% and 70.5% of mechanical energy is dissipated in the impeller region for RT and PBT respectively *This work does not account for gas-liquid interfaces*	Mollet et al., 2004 (Genentech)

Both Zhang et al. (2008) and Barrett et al. (2010) preformed detailed theoretical and experimental engineering characterisation of the microwell plate cell culture format. Subsequently, Barrett et al. (2010) utilised a matched energy dissipation rate as a suitable scaling parameter and obtained similar growth and productivity results in a 24 well microtitre plate and shake flask using a VPM8 hybridoma cell line. Other work has utilised matched mixing times as a scaling parameter when scaling up from 800 μL working volume microwell plates to 50 mL shake flasks using an antibody producing CHO cell line achieving comparable cell growth kinetics and productivity (Silk et al., 2010). Utilising a diluted bolus, fed-batch culture mode, in conjunction with a sandwich lid style microwell plate covering, the issue of evaporation at small scale was overcome (Silk et al., 2010). At medium to large scale, Lonza Biologics have shown comparable growth kinetics and productivity data using constant P/V and v_s as a scaling parameter for their stainless steel reactors, but also in 50L, 250L and 1000L disposable single use bioreactors (SUBs) (Valentine, 2009).

Thus it is crucial to create a small scale model that accurately mimics the large scale equipment by employing a suitable scale translation criteria, based on theoretical and experimental characterisation of the cell culture system.

1.9.1 Engineering characterisation of shaken cell culture bioreactors

Shaken bioreactors are often used as small scale cell culture tools, for example, shaken flasks, and more recently, microwell plates. Such formats exploit smaller volumes of culture medium therefore allowing for higher throughput. The use of microwell plates also lends itself to automation. Whilst shaken systems are currently used at small to medium scales, Zhang et al. (2009) proposes that such a system could be used at up to

1000 L industrial scales. Due to the different mechanism for energy input, i.e. shaken not stirred, different engineering characterisation equations must be employed in order to define the cell culture environment. In contrast to the stirred systems described in Section 1.7 these geometries are less well defined in engineering terms and the available correlations tend to be more limited in their scope, i.e. to particular geometries and operating ranges. Büchs et al. (2000) propose the following modified power equation in order to determine the power requirements for a shaken culture system, in particular to shake flasks:

$$P_o^{'} = C\,Re^{-0.2} \tag{1.8}$$

where $P_o^{'}$ is the modified power number which takes the form:

$$P_o^{'} = \frac{P}{r N^3 d_f^4 V^{1/3}} \tag{1.9}$$

Leading to an overall expression for power input into a shaken system:

$$\frac{P}{V} = C.r\,\frac{N^3 d_f^4}{V^{2/3}}\,Re^{-0.2} \tag{1.10}$$

Here the Reynold's number, as defined in equation 1.1, is calculated using the maximum inner flask diameter, d_f as the characteristic length scale and C is a constant found to equal 1.94.

For shaken formats, Büchs et al. (2001) also discovered a phenomenon specific to shaken systems described as the phase number, Ph. This characterises two flow regimes observed in shaken systems. The 'in-phase' flow regime describes that which is seen when the majority of the fluid circulates around the edge of the shaken flask,

synchronized with that of the orbital motion of the shaker. On the other hand, an ‘out of phase’ fluid flow regime occurs when a minority of the fluid circulates along with the shaker platform, and a larger proportion of the fluid remains stationary in the centre of the flask. Thus, in an ‘out of phase’ flow regime the mixing and oxygen transfer are greatly reduced (Büchs et al., 2001). The following equation can be used to determine Ph:

$$\mathrm{Ph} = \frac{\mathrm{d}_s}{\mathrm{d}_f}\left\{1 + 3\log_{10}\left[\frac{r\left(2p\mathrm{N}\right)\mathrm{d}_f^{\,2}}{4p}\left(1 - \sqrt{1 - \frac{4}{p}\left(\frac{\mathrm{V}^{\frac{1}{3}}}{\mathrm{d}_f}\right)^2}\right)^2\right]\right\} \qquad (1.11)$$

where d_s is the shaker diameter (Buchs et al., 2001). This group state that for Ph > 1.26 the shaken fluid will be ‘in-phase’ and that for Ph < 1.26 the fluid will be ‘out of phase’ and thus poorly mixed and aerated. Barrett et al. (2010) use this correlation to predict the phase number for 24-standard round well (SRW) microtitre plates, at a shaking diameter of 20 mm, fill volumes from 800 µL to 2000 µL and agitation rates from 120 rpm to 300 rpm. Under all conditions the fluid flow was found to be in-phase.

Work carried out using microwell plates by Hermann et al. (2003) showed the presence of a critical shaking speed, N_{crit}. It was shown that at shaking speeds below N_{crit} there was little fluid movement within the well, and therefore there would be relatively little mass or oxygen transfer. However, at shaking speeds greater than N_{crit}, there is a much greater degree of fluid movement. A correlation to predict N_{crit} in 96 well microtitre plates was derived as follows:

$$N_{crit} = \sqrt{\frac{s d_w}{4 p V r d_s}} \quad (1.12)$$

where σ is the liquid surface tension (Hermann et al., 2003). Hermann et al. (2003) propose that the predominant influence on the hydrodynamic flow is that of surface tension. Therefore the correlation is based on the justification that the critical shaking frequency is reached when the labour delivered by the centrifugal force is equal to the surface tension of the liquid in the microtitre plate well (Hermann et al., 2003). Barrett et al. (2010) determined that N_{crit} was 230 rpm for 24 SRW at 800 µL fill volume.

With regards to mixing times within shaken systems, Barrett (2008) determined the mixing times in 24 SRW microtitre plates when Re = 1,830. In this case the mean mixing time was estimated at 1.7 ± 0.06 s for both 800 µL and 1000 µL fill volumes. Hydrodynamic shear can be determined using an equation that relates the power input per unit volume to the average shear rate, $\dot{\gamma}$ (Barrett et al., 2010):

$$\dot{\gamma} = \left(\frac{P}{V m} \right)^{\frac{1}{2}} \quad (1.13)$$

In addition, due to the different mechanism of agitation and the fact that microwell systems are not sparged; previous work has developed an equation from 24 SRW systems that can be used to determine the $k_L a$ for a non-sparged microwell system:

$$k_L a = c_1 \frac{D_{O_2}}{d_w} a_i Re^{0.68} Sc^{0.36} Fr^x Bo^y \quad (1.14)$$

where D_{O_2} is the oxygen diffusion coefficient, c_1 is a constant, Fr is the Froude number ($= d_s(2\pi N)^2/2g$), g is the gravitational acceleration, Bo is the Bond number ($= \rho g d_w^2/W$), d_w is the shaken microwell diameter, W is the wetting tension and Sc is the Schmidt number ($=\mu/\rho D_{O_2}$) (Doig et al., 2005). With reference to equation 1.10 it is expected that increasing the shaking frequency or throw will increase the power input into the system. Similarly, with reference to equation 1.14 and the work carried out by Barrett (2008) on mixing times within microwells, it is expected that increasing the well diameter and decreasing the liquid fill volume will have the effect of increasing the k_La and decreasing the mixing time within the fluid of the shaken system.

CFD has previously been implemented as a tool to estimate the fluid mixing, energy dissipation rates and mass transfer in orbitally shaken 250 mL shake flask, 24 SRW, deep square 24 and 96 well microtitre plates (Barrett et al., 2010; Zhang et al., 2005; Zhang et al., 2008). It was reported that the numerical calculations fitted well with experimental data. Liquid motion was determined to be more dependent on the shaking throw than that of the agitation frequency (Zhang et al., 2008). Average power consumptions between 70 – 100 Wm^{-3} and 500 – 1000 Wm^{-3}, and k_La values between 18 - 100 hr^{-1} and 200 - 360 hr^{-1} were obtained for 24 well and 96 well microtitre plates respectively at an orbital shaking amplitude of 3 mm and shaking frequencies ranging from 500 rpm to 1500 rpm (Zhang et al., 2008).

1.9.2. Analytical tools for high throughput experimentation

An intrinsic problem working with small scale cell culture devices is that there is less volume for traditionally designed probes to fit into and there is a further limitation on the volume of sample that can be removed for offline analysis. Therefore, to fully utilise a small scale device effectively, alternative analytical tools must be employed to allow for online monitoring without affecting the culture environment. In addition, as the number of cell culture experiments that can be performed in parallel increases, there is an ever-increasing need for faster analytical techniques that can match the potential throughput of the cell culture system. As described earlier with regard to the choice of different small scale cell culture systems that might be used at different stages in process development, the same argument can be applied to analytical tools employed. For example, it may not be necessary to monitor or control process conditions if the high throughput device is used in an initial cell line screening stage; however, for process optimisation experiments it would be more appropriate to implement a device with some degree of online monitoring and control of process conditions.

Instruments such as the Vi-Cell (Beckman Coulter) or the CASY (Innovatis) are able to measure cell number and viability using the trypan blue exclusion method and electronic pulse area analysis respectively (Beckman Coulter website; CASY website). Both systems offer significant advantages in terms of speed and consistency of analysis, analytical throughput and accuracy over the traditional manual haemocytometer method. In addition, these systems can be validated for process monitoring as well as being able to provide additional data on average cell size and cell size distribution. Cell size is itself a parameter that can be monitored to assess the culture environment. The cell size can indicate the process of cell death, either apoptosis or necrosis, programmed

cell death or accidental cell death as a result of cell injury, respectively. With respect to changes in cell size, the process of apoptosis causes cell shrinkage and 'blebbing,' the release of small apoptotic bodies; whilst necrosis leads to cell swelling (Lodish et al., 2004). Cell size can also be interpreted in relation to specific recombinant protein productivity, Q_P. Recent articles have determined that cells do not necessarily express recombinant protein only in specific phases of the cell cycle, but instead that cell size is a major determinant of Q_P (Dinnis and James, 2005; Lloyd et al., 2000).

Cell cycle distribution analysis can be determined by flow cytometry (Carroll et al., 2007). Metabolites and byproducts such as glucose, glutamine, lactate, ammonium and also osmolality can be assayed in a high throughput manner using equipment like the Nova Bioprofile (Nova Biomedical) or the YSI system (YSI Life Sciences). Antibody productivity can be qualitatively measured using ELISA techniques, involving detection of the product by staining with fluorophore molecules attached to secondary antibodies. However, a more rapid and less labour intensive method is the use of Protein A/G affinity High Performance Liquid Chromatography (HPLC) that can utilise microwell plates to increase throughput and also provides a quantitative measurement of the level of product. Near-infrared (NIR) spectroscopy has also been used to measure levels of recombinant protein produced (Harthun et al., 1997; Henriques et al., 2009) as well as for metabolite levels including glucose, glutamine, lactate and ammonia; though currently only at conventional cell culture scales (Yeung et al., 1999).

Optical sensors generally offer the advantage of noninvasive, nondestructive, and continuous process monitoring. This helps with the small working volume issue, often experienced in scaled down models, as culture volume is not removed for offline measurement. PreSens GmbH offer a range of non-invasive sensor spots for pH and O_2,

which are fixed to the inside of the culture vessel and a transmitter is directed at the probe to determine the levels of the respective components. Microwell plates are commercially available with such PreSens sensors integrated into the plate format. The μ24 MicroReactor system utilises single-use culture cassettes with integrated sensor spots for monitoring of both pH and dissolved oxygen for each well of the bioreactor cassette (MicroReactor Technologies website). The main issue with use of this system is that the integrated analytical sensor probes are relatively expensive and thus this adds to development costs and limits the adoption of such online sensor systems in HTE, especially in early round cell screening experiments.

It is important to not only monitor process conditions, but also examine the cells at the physiological and molecular levels. Recent work has utilised surface-enhanced laser desorption/ionization (SELDI) in conjunction with time-of-flight (TOF) mass spectrometry in an attempt to screen, and subsequently characterise, cell culture supernatant material for secreted 'biomarkers' that may be indicative of process performance. Woolley and Al-Rubeai (2009) showed that a protein fragment of galnectin-1 was actively secreted in response to physiological stress in CHO cell culture. Such a technique could be further employed to identify biomarkers indicative of certain secondary characteristics, i.e. response to feed, and used in a high throughput format to rapidly examine cell culture supernatants and select for such characteristics.

In addition to the amount of recombinant protein produced, the quality of the expressed product is crucial, especially when considering that the selection procedure will aim to create and select highly productive cell clones, but high productivity itself might compromise post-translational modification machinery and result in low product quality (Jefferis, 2009). Thus it is essential to examine for critical product quality attributes,

which can include: protein charge heterogeneity; glycosylation profile; low molecular weight and aggregate species; and deamidation. Protein glycosylation can, for example, be determined by first treating the glycoprotein with enzymes to liberate the glycan residues and then analyse the sample using matrix-assisted laser desorption/ionization (MALDI) mass spectrometry (Colangelo and Orlando, 2001). To prevent protein aggregation in mammalian cells, misfolded proteins are 'sensed' in the Endoplasmic Reticulum (ER) and the unfolded protein response (UPR) is activated. This response attempts to either refold the protein or degrade the misfolded protein, but also slows protein production mechanisms thus allowing the misfolded proteins to be dealt with before they have a chance to accumulate (Schröder and Kaufman, 2005). Prolonged activation of the UPR can lead to cellular apoptosis (Schröder and Kaufman, 2005). For this reason there have been attempts to engineer ER-resident protein folding machinery to be able to process more recombinant proteins without activating the UPR; however results have been varied (Schröder, 2008). In a similar manner however, cell lines may be screened for characteristics such as elevated ER-resident chaperone levels or other signaling proteins involved in the UPR, i.e. XBP1 or eIF2α, if they do in fact prove to be indicative of recombinant protein quantity or quality.

1.9.3. High throughput experimentation and automation

Automated systems can be invaluable both in cell culture processes and for analytical purposes. As well as increasing throughput, automation can be more accurate and consistent in comparison to a human performing the same manipulation repeatedly. With regard to implementing high throughput cell line characterisation or cell culture optimisation, without automated capacity, costs will increase rapidly on increased staff requirements, and also human error will most likely increase with greater number of

operations, particularly when dealing with small, intricate devices. In comparison, with automation, personnel numbers can be reduced, thus reducing development costs, or alternatively can release personnel for more complex tasks such as data analysis and interpretation. The key to making full use of high throughput cell culture systems will be if the culture is automated and can be integrated with high throughput automated analytical tools to examine online process performance alongside collated offline data, thus while increasing speed and throughput, precision and reliability do not deteriorate.

There are a variety of systems commercially available that could be employed to assist in high throughput automation of cell culture operation and analysis. Liquid handling robotic platforms, e.g. Tecan systems, might be employed for cell culture, feed additions during culture and sample removal for analysis in a microwell plate format. Similarly, TAP Biosystems offer a variety of automated cell culture robotic units, varying from the SelecT for T-175 flasks, the Cellmate for roller bottle culture to the new advanced microbioreactor (ambr) that cultures cells in a sparged, 24 vessel STR microbioreactor format (10-15mL) (TAP website). MicroReactor Technologies offer a similar product to the ambr (TAP) called the μ24 MicroReactor, operating in a 24 well microplate format (3-7mL working volume) (MicroReactor Technologies website).

1.10. Critical evaluation of the published literature

One of the main issues in the published literature regarding the scale-down of mammalian cell culture process development experimentation has been a lack of definition around suitable scale translation parameters. Primarily, there is a lack of fundamental engineering characterisation for the majority of the available small scale

bioreactor systems (Table 1.4). The key issue is a failure to critically evaluate the scale-down environment and subsequently devise suitable scaling parameters that may then be used to establish HTE in conditions that accurately replicate the production scale system. In practice, there have been numerous studies displaying seemingly matched growth kinetics (e.g. Chen et al., 2008; Yang et al., 2007) with limited explanation as to how this has been achieved or on what basis the authors believe this method to be successful in achieving such scaled down cell culture. Failing to perform basic bioreactor characterisation leads to a lack of fundamental information regarding the cell culture system and therefore uncertainty over how scale translation has been achieved in published papers.

In this area of research, mammalian cell culture in small scale systems will be most successful, and yield the most valuable data, if the culture format has firstly been thoroughly characterised both experimentally and theoretically. Further work is required to develop small scale systems in which process conditions can be monitored, and preferably also controlled online. The adoption of small scale devices that allow for such monitoring and subsequently a more precise control of environmental parameters will help establish the critical factors that are affecting cell culture performance or experimental outcomes. With respect to this, whilst it is undoubtedly key to provide small scale bioreactors with appropriate analytical tools to assay for basic process variables, e.g. pH and DOT, it remains unclear what other analytical tools, e.g. metabolite or product measurement, can be successfully applied at such a scale and at what cost this can be achieved. On the basis of understanding the device in terms of mixing, oxygen transfer, etc., suitable scaling criteria may then be implemented in order to replicate cell growth and productivity kinetics at small scale. Further effort is

required in this field to create a truly representative scaled down system that can easily be used for HTE.

It is also crucial to better understand how cells and the products they make respond to the environment in which they are cultured. Further work is required in evaluating large scale cell culture performance, in understanding why some cells are better able to grow or express heterologous proteins to the desired product quality and in defining biomarkers that can identify cells suitable for large scale culture. It is also crucial to appreciate what are the correct indicators for successful cell culture scale translation; whilst it may generally be perceived that cell growth, metabolite concentrations and product titre are the key indicators of successful scale translation, product quality may actually represent a more accurate marker with regard to replicating the cell's metabolome between culture scales. With regard to this, greater data and insight of the nature of large scale cell culture is required from industry in order to provide a benchmark for researchers to work towards. This work aims to address such issues and investigate the novel relationship between scale translation and the introduction of a specific engineering characteristic, namely the presence of a dispersed gas phase.

1.11. Aim and objectives

Based on the current limitations described in Section 1.10, the aim of this project is to establish a small scale cell culture platform for the rapid selection of robust and scalable cell lines. The miniature bioreactor platform investigated is the μ24 microbioreactor system (MicroReactor Technologies, owned by Pall Life Sciences), given the scale of operation, the degree of parallel operation and the ability to monitor and control pH,

temperature and DOT in individual wells (Table 1.3). The industrial relevance of the work will be ensured by use of a fed-batch culture process with two GlaxoSmithKline (GSK) CHO cell lines expressing mAb products.

Given this overall aim, the specific project objectives are as follows:

- To perform a detailed engineering characterisation of the novel, shaken miniature bioreactor system and the conventional stirred bioreactors used as scale-down mimics of pilot scale GSK cell culture processes. This work is described in Chapter 3 and will inform the criteria used for scale comparison between miniature and stirred bioreactor formats.
- To establish a fundamental understanding of how changes in the engineering environment in the miniature bioreactor affect cell culture kinetics. This work is described in Chapter 4 and will inform how best to use the miniature bioreactor system as a tool for clone ranking and selection.
- To evaluate cell culture performance in miniature and scale-down bioreactor formats and establish an engineering methodology for predictive scale translation. This work is described in Chapter 5 and will rigorously assess scale translation in terms of culture kinetics, product titre and quality as well as the downstream processing characteristics of the culture broth.

Finally, the conclusions arising from this work and suggestions for further investigations are covered in Chapter 6. The wider issues regarding industrial adoption and validation of the miniature bioreactor technology are discussed in Appendix A as part of the requirements for award of the UCL EngD degree in Biochemical Engineering.

Chapter 2. Materials and methods

2.1. Bioreactor formats and engineering characterisation

In order to accurately recreate the STR engineering environment in the small scale bioreactor, both systems were fully characterised so that the small scale system could be operated in a manner to reflect the STR environment as closely as possible. In this work all experimental characterisation experiments were performed in triplicate.

2.1.1. Stirred tank reactor

For this work a standard GSK bench scale STR was used as the model system. This format is itself a scale-down model of GSK pilot scale bioreactors.

2.1.2. Description of the STR

The STR (Applikon, Tewkesbury, UK) used was an unbaffled vessel of 3 L total volume and 2 L working volume. The bioreactor internal tank diameter is 0.13 m. The impeller shaft was equipped with a Rushton impeller, with a power number of 5 (data provided by GSK, Stevenage). This impeller has a diameter of 0.045 m, thus resulting in a D_i/D_t ratio of 0.35.

2.1.3. Experimental determination of mixing time

Liquid phase mixing times for the 3 L Applikon STR were measured experimentally using the iodine decolourisation method as described by Barrett (2008) with all experiments carried out at 25°C. The brown 5 mM iodine solution (Sigma, Cat No. 35089) turns colourless upon addition of a 1% v/v 1.8 M sodium thiosulphate solution (Sigma, Cat No. S8503). The iodine solution was transferred into the STR and the test conditions set. The sodium thiosulphate addition was made rapidly using a serological pipette positioned 2-3 cm under the liquid surface. Dye decolourisation was measured using a digital stopwatch and followed by eye where approximately 95% decolourisation was defined as the mixing time.

2.1.4. Theoretical determination of the power input

For gassed power correlations a value of 0.014 m was used for the blade width of the pitched blade impeller. Volumetric gas flow rates can be converted to superficial gas velocities by dividing volumetric values by the area of the vessel. For theoretical calculations, the test liquid was assumed to be very close to water and therefore have a density of 998.2 kg m^{-3}, a viscosity of 1.003×10^{-3} Nm^{-2} s and a liquid-air surface tension of 0.072 N m^{-1}.

Various equations have been proposed to predict the gassed power consumption rate from the ungassed power values (Table 2.1). Van't Riet (1975) noted that the presence of gas-filled cavities that occupied the space behind the blade of the impeller; and defined three cavity forms dependent on impeller speed and gas flow rate: vortex,

clinging and large cavities. Subsequently, Warmoeskerken (1986) identified flow regimes that relate the formation of these cavities to the power consumption of Rushton impellers and proposed the following correlations, which also take into account gas recirculation, to calculate the gassed power input for each type of cavity structure.

Table 2.1. Literature gassed power correlations.

Author	Equation	No.	Notes	Abbreviation
Mockel et al. (1990)	$\frac{P_g}{P} = \frac{1}{\sqrt{1 + Z\frac{v_s}{\sqrt{gD_t}}}}$	2.1		Z is the number of impellers used: 1 (Z = 750) 2 (Z = 490) 3 (Z = 375)
Calderbank (1958)	$\frac{P_g}{P} = 1 - 12.6\left(\frac{Q}{ND_i^3}\right)$	2.2	Apply equation when Fl < 0.035	Fl is the flow number (=Q/NDi^3)
Calderbank (1958)	$\frac{P_g}{P} = 0.62 - 1.85\frac{Q}{ND_i^3}$	2.3	Apply equation when Fl > 0.035	
Cui et al. (1996)	$1 - \frac{P_g}{P} = 9.9\left(\frac{QN^{0.25}}{D_i^2}\right)$	2.4	Apply equation when $\frac{QN^{0.25}}{D_i^2} \le 0.055$	
Cui et al. (1996)	$1 - \frac{P_g}{P} = 0.52 + 0.62\left(\frac{QN^{0.25}}{D_i^2}\right)$	2.5	Apply equation when $\frac{QN^{0.25}}{D_i^2} > 0.055$	
Nagata (1975)	$\log\frac{P_g}{P} = -192\left(\frac{D_i}{D_t}\right)^{4.38}\left(\frac{rD_i^2N}{s}\right)^{0.115} Fr^{1.96\left(\frac{D_i}{D_t}\right)} Fl$	2.6		
Warmoeskerken (1986)	$\frac{P_g}{P} = 1 - 16.7\,(Fl)(Fr)^{0.35}$	2.7	For vortex and clinging cavities; 0 < Fl < $Fl_{3\text{-}3}$	$Fl_{3\text{-}3}$ is the flow number at which small 3-3 cavities appear
Warmoeskerken (1986)	$\frac{P_g}{P} = b - \left[\frac{0.1(a-b)}{Fl_{3\text{-}3} - 0.1}\right] + \frac{(a-b)\,Fl}{Fl_{3\text{-}3} - 0.1}$	2.8	For small 3-3 cavities; $Fl_{3\text{-}3}$ < Fl < 0.1	a = 1–17$Fl_{3\text{-}3}$(Fr)$^{0.35}$ b = 0.27 + 0.022Fr^{-1}
Warmoeskerken (1986)	$\frac{P_g}{P} = 0.27 + 0.022Fr^{-1}$	2.9	For large 3-3 cavities; 0.1 < Fl < Fl_F	

2.1.5. Experimental determination of k_La values

The k_La for the 3 L Applikon STR was measured experimentally using the static gassing out method as described by Barrett (2008) and Betts et al. (2005), with all experiments carried out at 37°C. The dissolved oxygen (DO) probe was first calibrated to 0% DO using 100% N_2 gas and then to 100% DO saturation with air. Probe calibration was performed using the test fluid and temperature used for the experiment. k_La studies used water supplemented with 0.5 g L^{-1} Pluronic-F68 (Sigma Aldrich, P1300), to match standard bioreactor setup. Test fluid was sparged with N_2 gas until the measured DO saturation was below 5%. The bioreactor was then set to the test conditions for agitation rate and N_2 sparging was switched off. The test gas was then sparged at the desired flow rate and run until the probe reading reached greater than 55% DO. The k_La was determined from this raw data by first calculating the natural log of 100% DOT – the DOT at each data point (Appendix E, Figure E.1). These calculated results are then plotted against time and the negative value of the slope is equal to the k_La at a given test condition.

The probe response time was determined as described by Barrett (2008). The probe was first positioned inside a cap into which was sparged the air supply. Once at 100% DO saturation the gas supply was switched to N_2. The probe response time is determined as the time taken for the probe DO reading to drop below 37%. If $1/k_La >>$ than the probe response time, then the response time is insignificant and can be ignored. In determining the k_La it is necessary to also take into account the probe response time. The probe response time is determined using Equation 2.10 (Dunn and Einsele, 1975):

$$C_p = \frac{1}{t_m - t_p}\left[t_m \exp\left(\frac{-t}{t_m}\right) - t_p \exp\left(\frac{-t}{t_p}\right)\right] \qquad (2.10)$$

where C_P is the normalised dissolved oxygen concentration measured by the probe at time t, t_m is $1/k_La$ and τ_P is the probe response time.

2.1.6. Theoretical determination of k_La values

Various equations have been proposed to predict the k_La for a bioreactor under given process conditions. These equations all follow the form of Equation 1.6 with various values proposed for the constant A and exponents α and β as shown in Table 2.2.

Table 2.2 Literature values for k_La equation constant and exponents.

Reference	Value		
	A	a	b
Gill et al. (2008b)	0.224	0.35	0.52
van't Riet [non-coalescing] (1979)	0.002	0.7	0.2
van't Riet [coalescing] (1979)	0.026	0.4	0.5
Stanbury and Whitaker (1984)	0.026	0.6	0.5
Vilaca et al. (2000)	0.00676	0.94	0.65
Linek et al. (2004)	0.01	0.699	0.581
Smith et al. (1977)	0.01	0.475	0.4
Zhu et al. (2001)	0.031	0.4	0.5

2.2.1. µ24 bioreactor system

For this work the µ24 bioreactor system (MicroReactor Technologies, Pall, Port Washington, USA) was investigated for potential use as an industrial scale-down model of bench scale STR's.

2.2.2. Description of µ24 bioreactor platform

The µ24 bioreactor platform (MicroReactor Technologies) has previously been

described by Isett et al. (2007) and Chen et al. (2009). Briefly, the μ24 consists of a single shaking base plate, with an adjustable shaking frequency from 0 to 800 rpm at a fixed 2.5 mm orbital diameter. The cell culture cassette comprises a pre-sterilised 24 deep well microtitre plate, available in PERC (headspace gas sparging) or REG (direct gas sparging) designs as shown in Figure 2.1. Each well has a working volume (wv) of 3 to 7 mL. Individual wells are equipped with two thermistors that correspond to equivalent temperature monitoring and heating elements on the μ24 base plate. In addition, each well also has fluorescent pH and DO patches to allow optical monitoring via LED's and detectors on the base plate. During shaking a vacuum is applied to seal the cell culture cassette to the base plate. Individual gas injection ports from the base plate feed into 0.2 μm hydrophobic membranes within each of the wells. For the PERC plate design gas enters the vessel via a sparge tube which is above the liquid surface, and therefore passes into the head space of the well to provide surface aeration only. For the REG plate design, gas is sparged directly into the base of each well creating a dispersed gas phase. Up to three different gases can be used at any one time; for mammalian cell culture purposes these will typically include an oxygen source for DO control and a carbon dioxide containing gas for pH control.

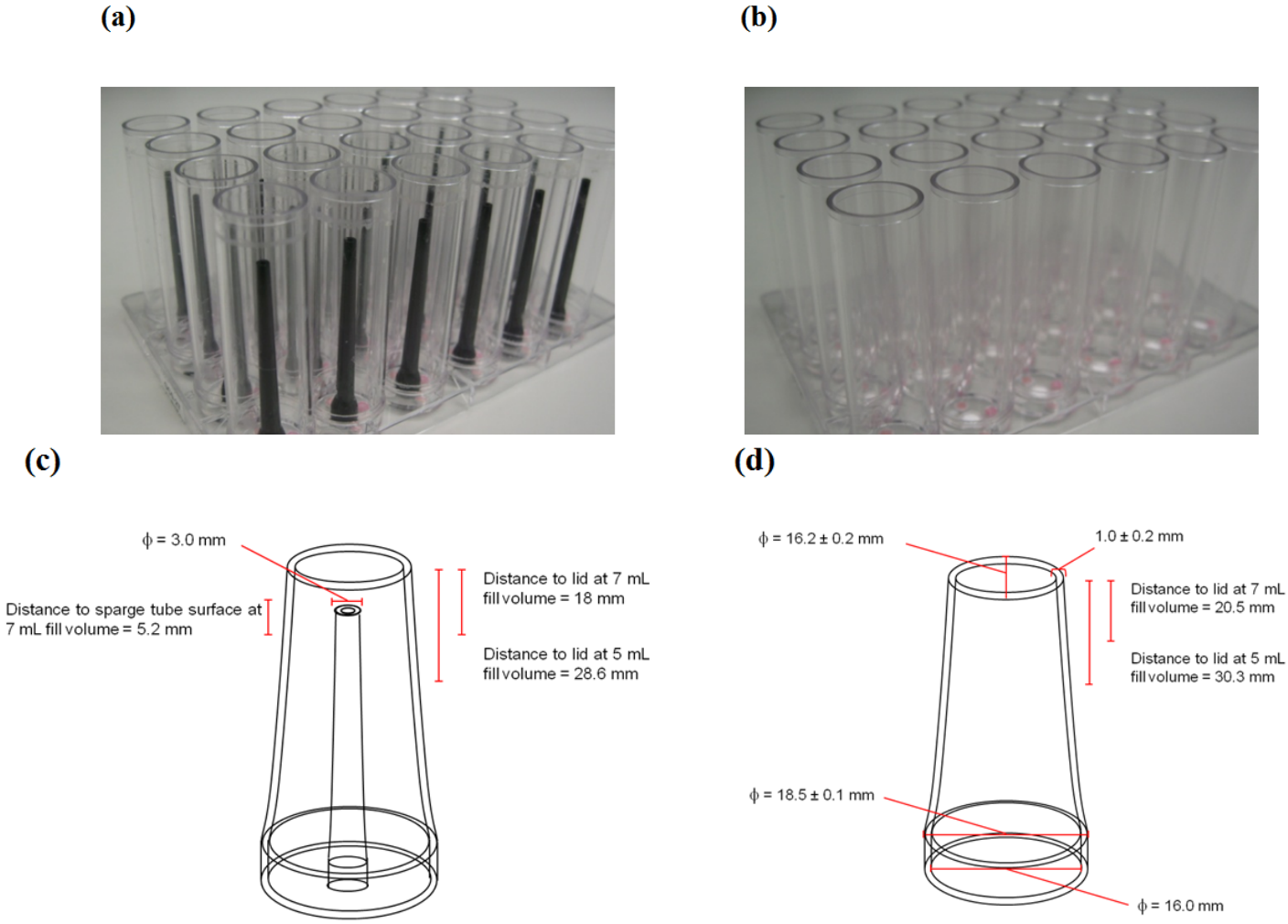

Figure 2.1. Images of the (a) PERC and (b) REG plate designs for use with the µ24 bioreactor system and (c, d) details of individual wells, respectively.

2.2.3. Mixing time determination

Liquid phase mixing times were measured experimentally using the iodine decolourisation method as described by Bujalski et al. (1999). The brown 5 mM iodine solution (Sigma-Aldrich, Cat No. 35089) turns colourless upon addition of an equimolar sodium thiosulphate solution (1.8 M) (Sigma-Aldrich, Cat No. S8503). Experiments were performed from either a static start with sodium thiosulphate added directly to the base of the well or with a dynamic start where sodium thiosulphate addition was made

down the side of the well at a fixed position 2 cm above the liquid surface. Mixing times were quantified as described in Section 2.3 from analysis of video images as described previously (Nealon et al. 2006).

2.2.4. k_La determination

The k_La values were determined experimentally using the static gassing out method as described by van't Riet (1979). All experiments were carried out at 37°C. The fluorescent DO sensor of an individual well from a μ24 cassette (PERC or REG design) was pre-calibrated to 100% oxygen saturation in air at 37°C. The system was operated in 'constant flow' mode, with oxygen control turned on to enable DO logging but operated such that there was no active oxygen sparging. The purge line was used to sparge test gases at defined flow rates. The test fluid was then sparged with N_2 until the DO reached zero. The required bioreactor operating conditions (shaking frequency, aeration rate, etc.) were then set and the air sparged until the probe reading reached approximately 100%. The k_La was determined taking into account the probe response time using Equation 2.10. The response time of the optical probe, 18 s, was calculated by determining the time required for the DO reading to drop from 100% to below 33% by sparging the probe directly, firstly with air and then rapidly switching to N_2. Since the μ24 software contains a proprietary algorithm for averaging DO readings over time all k_La values reported here are represented as apparent, k_La_{app}, values, which will slightly under predict the true k_La values.

2.2.5. Determination of evaporation levels

Specific evaporation levels from individual wells were determined based on measured changes in the concentration of a blue dye (Super Cook, Leeds, UK; at an initial concentration of 0.002% v/v) over time. Control experiments showed that the measured increase in optical density (OD) at 630 nm was directly proportional to the reduction in liquid volume. To determine the specific well evaporation rate, a PERC plate was filled with dye stock solution (7 mL fill volume) and set in the μ24 bioreactor system at 37°C for 9 days. Standard culture conditions were simulated by using a shaking frequency of 650 rpm and a constant purge gas flow rate of 10 mL min^{-1}. The OD was determined for each well by transferring 100 μL of sample to a standard microtitre plate and measuring the absorbance in a plate reader (Safire, Tecan, Männedorf, Switzerland). Measurements were blanked against 100 μL reverse osmosis (RO) water. The fold evaporation per well could then be calculated using Equation 2.11:

$$\text{Fold Evaporation} = \frac{\left(A_{630,\text{final}} - A_{630,\text{blank}}\right)}{\left(A_{630,\text{initial}} - A_{630,\text{blank}}\right)} \qquad (2.11)$$

2.2.6. Visualisation of liquid phase hydrodynamics and gas-liquid dispersion

A high speed camera was used to study the liquid phase hydrodynamics, the motion and deformation of the gas-liquid surface and for bubble size and size distribution measurements. The camera used was a DVR Fastcam (Photron, California, USA). The resolution was set to 640 x 480 pixels for all experiments. For mixing time experiments

the camera was set to record at 125 frames per second with a shutter speed of 1/frame rate. For the bubble size and distribution experiments and the surface deformation experiments the camera was set at 500 frames per second with a 1/1000 second shutter speed and twice normal gain. Image analysis was performed using ImageJ software (http://rsbweb.nih.gov/ij/). For these experiments individual wells from PERC and REG cassettes were cut from a cassette to aid visualisation and subsequent image analysis. A small Perspex box was constructed around each individual well and this was filled with glycerol so as to prevent image distortion. A chemically defined CHO cell media (CD-CHO) was used to provide a comparison to the proprietary production growth media (PPG media) used for cell culture. Pluronic-F68 (Sigma-Aldrich, P1300) was added to RO water at 0.5 g L^{-1} to determine the effect of this component on bubble size and distribution.

For both the PERC and REG plate designs image analysis of the wells at varying shaking frequencies was performed using ImageJ to determine the displaced liquid height (h_L) and thus the area of the gas-liquid surface (a). The displaced liquid height values were determined for both plate designs at a 7 mL fill volume assuming an oval geometry. The gas sparging mechanism in the μ24 bioreactor delivers 'pulses' of gas, opening valves for 22 ms an appropriate number of times to equal the programmed gas flow rate. As such, discrete gas pulses were analysed and compared to determine reproducibility of pulses with variation of gas bubble size and number. From these values the relative gas-liquid surface area per pulse was determined. From the pulse beginning and ending frame number, and known frame rate, the average gas bubble residence time was determined. The measurement of the bubble diameter and displaced liquid height assumed that all the bubbles were spherical in order to calculate the surface area.

2.2. Cell lines and culture

Multiple clones from two model CHO DG44 (*dhfr* $^{-/-}$) cell lines were provided by GSK, Stevenage, and used for cell culture experiments in this thesis (Sections 4.2; and Sections 4.3, 4.4 and Chapter 5 respectively). These cell lines differ in that they express two different whole IgG1 mAb products and were developed for a non-chemically defined (CHO-A) and a chemically defined process respectively (CHO-B).

2.2.1. Cell line banking

CHO *dhfr*$^{-/-}$ cell line clones were laid down in banks using a standard GSK CHO cell line banking procedure. Samples were removed from the cell culture vessel for viable cell density analysis as described in Section 2.3.1. Using this value, the appropriate volume of cell culture was removed and centrifuged at 1000 rpm for 5 minutes using a Sorvall Legend RT centrifuge. The supernatant was removed and the pellet gently resuspended in the remaining media by tapping. A proprietary freezing media solution was added to resuspend the pellet and mixed by gentle aspiration using a serological pipette to break up any clumps. Cells were aliquoted into Cryotube vials (Nunc, ThermoFisher, Massachusetts, USA, Cat No. 363401) of 1 mL volume at a concentration of 1.8×10^7 cells mL^{-1} and frozen using an EF600 Control Rate Freezer (Asymptote, Cambridge, UK). Cell banks were stored in liquid nitrogen.

2.2.2. Cell line revival

CHO *dhfr*$^{-/-}$ cell line clones were revived using a standard GSK CHO cell line revival procedure. All cell culture work in this thesis was undertaken in a Class 2 Biological Safety Cabinet (BSC) and employed standard tissue culture techniques throughout. Vials taken from liquid nitrogen storage were transferred to a BSC and gently thawed by holding in sterile, pre-warmed media, taking care not to immerse the vial past the lip of the lid. Vial contents were next transferred into a 30 mL universal tube containing 18 mL pre-warmed media specific for each cell line. The universal tube was centrifuged at 1000 rpm for 5 minutes using a Sorvall Legend RT centrifuge (Thermo Scientific). The supernatant was discarded and the pellet gently resuspended in the remaining media by tapping. A 125 mL shake flask was filled with 20 mL pre-warmed media. 5 mL media from the shake flask was transferred to the pellet and mixed by gentle aspiration using a serological pipette to break up any clumps. The cell suspension was added to the shake flask, and a further 5 mL media was taken from the same flask to wash the contents of the universal tube before replacing in the flask. A sample was removed for viable cell density analysis and the shake flask culture adjusted to 0.6×10^6 cells mL^{-1}. The shake flask was incubated in a Multitron incubator (Infors HT) at 140 rpm, 37°C, 5% CO_2 for 4 days before passaging and routine subculture.

2.2.3. Cell subculture

CHO-A cells were routinely passaged in a proprietary, non-chemically defined growth media (Gibco, Cat No. 041-96214V) supplemented with methotrexate (MTX) (Hanna Pharmaceutical Supply Company, Delaware, USA, Cat No. 55390-033-10) at a final

concentration of 50 nM. CHO-B cells were routinely passaged in a proprietary, chemically defined medium (Gibco, Cat No. 041-96330V) supplemented with MTX and Glutamax (Gibco, Cat No. 35050-038) at final concentrations of 50 nM and 0.02 M respectively.

Cultures were maintained in disposable vented cap shake flasks in a Galaxy S incubator (Wolf Laboratories, York, UK) at 37°C and 5% CO_2, on an orbital shaker (Certomat MO II, Sartorius Stedim, Aubagne, France) at a shaking frequency of 150 rpm with a 25 mm orbital shaking diameter. Both CHO *dhfr*$^{-/-}$ cell lines were repeatedly subcultured by dilution at 3 to 4 day intervals using a seeding density of 6×10^5 cells mL^{-1}. Cultures were maintained in disposable vented cap shake flasks in a Multitron incubator (Infors HT, Bottmingen, Switzerland) at 37°C and 5% CO_2, on an orbital shaker at a shaking frequency of 140 rpm with a 25 mm orbital shaking diameter.

2.2.4. Fed-batch cell culture experiments

For fed-batch experiments, CHO-A cells were seeded at 8×10^5 cells mL^{-1} into a non-chemically defined proprietary, production growth media (PPG media) supplemented with MTX, at a final concentration of 50 nM, and an additional proprietary amino acid solution. A standard GSK fed-batch culture protocol was followed using a single 5% v/v proprietary feed solution added on day 7. The CHO-B cells were seeded into chemically defined passage media but again at a concentration of 8×10^5 cells mL^{-1}. A standard GSK chemically defined fed-batch cell culture protocol was followed with 10% v/v Feed 6 AGT solution (Gibco, Cat No. 041-96360A), supplemented with an additional proprietary amino acid solution, added on days 3, 6, 8, 10, 13. Cells were cultured at 35°C for CD fed-batch processes. Cells were not used for fed-batch cell culture experiments past passage 50.

Shake flask fed-batch experiments utilised disposable, vented cap 125 mL or 250 mL Erlenmeyer shake flasks (Corning Life Sciences, Amsterdam, Netherlands) with working volumes of 20 to 60 mL and 100 to 140 mL respectively.

For PERC and REG plate cultures in the μ24 system, the temperature set point of all wells was 35°C, with an environment temperature set point of 33°C. In addition, each well used a pH set point of 6.95 and a DO set point of 30%. All wells were sealed with a cap which has a central gas permeable filter and a check valve to limit evaporation from the culture. For cell culture with the PERC plate design enough stock inoculum was made to fill an entire plate using a 7 mL fill volume per well, in order to minimise well to well variability. Similarly, for cell culture using the REG plate design the required volume of media with Antifoam C emulsion (0.003% v/v) (Sigma-Aldrich, Cat No. A8011) was aliquoted per well, the plate was placed into the μ24 so that the desired control set points could be reached before inoculation from one inoculum suspension. The antifoam was added in REG plate cultures due to the presence of the sparged gas phase. The μ24 bioreactor allows for ‘active’ gas flow to control pH and DO set points. There is also the ability to use a ‘constant’ gas flow mode which sparges a purge or background gas at a desired flow rate as well as having gases for ‘active’ control. PERC plates were operated using a ‘constant flow’ mode only whereas REG plate cultures were operated either in the ‘constant flow’ or ‘active flow’ modes. The μ24 operating conditions for these different cultures are shown in Table 2.3. The cassettes were weighed at regular stages to determine the dilution factors required for the stock base feed (1 M sodium bicarbonate, 1 M sodium hydrogen carbonate) additions. Large volume inoculum additions were made using a Rainin AutoRep E (Mettler Toledo,

Greifensee, Switzerland). Plate agitation was provided by an orbital microplate shaker (MS3 Digital, IKA, Staufen, Germany; agitation rate set equivalent to bioreactor operating frequency) in between individual well sampling.

For the STR cultures, 3 L bioreactors (Applikon Biotechnology, Tewkesbury, UK) were run at a 1.5 L working volume. These reactors have a single rushton impeller operated at 350 rpm, an open pipe sparger using a 40% oxygen/air supply for DO control at a 200 mL min^{-1} flow rate, CO_2 for downwards pH control at a 100 mL min^{-1} flow rate and a 1M sodium carbonate base supply for upwards pH control. The DO set point was 30% and the pH set point was 6.95.

2.2.5. Scaling criteria between different bioreactor geometries

The shaking frequencies for the μ24 plate formats, shake flasks and the stirrer speed for the STR's were selected in order to provide a matched mixing time, $t_m \approx 7s$ (Sections 4.2 to 4.4 and Section 5.2) This scaling criterion was chosen as it had previously been shown to be successful in scaling a mammalian cell culture process from the microwell to shake flask scale (Silk, 2014). A summary of the operating conditions used is shown in Table 5.1.

Table 2.3. Details of μ24 cell culture operating conditions using the PERC plate design, under 'constant flow' gassing mode, or the REG plate design, in either 'constant flow' or 'active flow' modes.

	PERC (No dispersed gas phase)	REG (Dispersed gas phase)	
		'Constant Flow'	'Active Flow'
Shaking frequency (rpm)	650	550	550
Fill volume (mL)	7	7	7
Constant flow gas	5% CO_2	Air	N/A
Constant flow rate (mL min^{-1})	0.5	0.05	N/A
Oxygen control	40% O_2	40% O_2	40% O_2
pH control	20% CO_2	100% CO_2	100% CO_2
Active gas flow limit (mL min^{-1})	10	0.5	0.5

N/A Not Applicable

2.3. Analytical techniques

2.3.1. Viable cell density

Viable cell density (VCD) and cell viability values were determined using the Trypan Blue exclusion method using a Vi-Cell XR (Beckman Coulter, High Wycombe, UK). Samples were diluted as appropriate with TryplExpress (Gibco, Invitrogen, Cat No. 12605) and incubated at 37°C for 10 minutes whilst being agitated at 175 rpm using an Innova 4000 benchtop incubator shaker (New Brunswick Scientific, Eppendorf, Connecticut, USA) before analysis to break up any cell clumps. Offline pH was measured using a Rapidlab 1240 blood gas analyser (Siemens AG, Munich, Germany).

2.3.2. Metabolite analysis

Supernatant samples were generated by spinning cell culture broth at 13,000 rpm using a microcentrifuge (Centrifuge 5424, Eppendorf) for 10 minutes. Metabolite analysis was performed using a 7100 Multiparameter Bioanalytical System (YSI, Ohio, USA) or a CEDEX BioHT (Roche, Indianapolis, USA). In both cases supernatant samples were diluted with PBS as appropriate for analysis. These systems utilise immobilised enzymes in biosensor patches which enable measurement of specific dissolved metabolite levels in solution (Büntemeyer, 2007).

2.3.3. Antibody titre

Product titre from the CHO *dhfr*$^{-/-}$ cell lines was determined from supernatant samples using an IMMAGE nephelometer (Beckman Coulter, High Wycombe, UK) in conjunction with the IMMAGE immunoglobulin G reagent (Beckman Coulter, Cat No. 446400). End-point supernatant samples were stored in a -80°C freezer (Eco VIP Freezer, Panasonic, Leicestershire, UK) for subsequent product quality analysis.

Statistical analysis of the data displayed in Figure 5.5 used two sets of statistical testing. An ANOVA was used to determine whether there was a statistical difference between the groups in each sample set, i.e. between the culture formats for each clone. Secondly, an unpaired student's t-test was used to determine two-tailed p values, performed such that each cell culture format was evaluated against the relevant bioreactor data for that particular clone.

2.4. Product quality analysis

Cell culture broth samples for product quality evaluation were analysed for aggregate content using Size Exclusion Chromatography (SEC), the glycosylation profile was measured using Quantitative Time of Flight (Q-TOF) Liquid Chromatography Mass Spectrometry (LC/MS) and for Non-Glycosylated Heavy Chain (NGHC) levels using the Agilent Bioanalyser. Samples were Protein A purified prior to analysis.

2.4.1. Protein A purification

The purification method used here is a mimic of the in-house Protein A purification process for mAbs (GSK, Stevenage, UK) and is scaled down so that the purification process can use small volume chromatography columns in combination with a TECAN Freedom EVO robotic platform (TECAN, Männedorf, Switzerland) for automated liquid handling. Supernatant samples were filtered to remove any particulates using a syringe driven 0.22 μm Polyethersulfone (PES) filter unit (Millex GP PES filter unit, Millipore, Cork, Ireland) prior to loading on to the Protein A chromatography columns. The small scale, automated TECAN Protein A chromatography protocol loads 2 mL of supernatant onto a 200 μL ATOLL column (MediaScout RoboColumn, ATOLL, Weingarten, Germany) that is pre-packed with MabSelect SuRe Protein A resin (GE Healthcare, Uppsala, Sweden). The protocol uses a pH 7.50 55 mM Tris base 45 mM acetic acid buffer to equilibrate the column, a 55 mM Tris base 45 mM acetic acid 300 mM sodium acetate 100 mM sodium capryolate wash buffer and a 1.8 mM sodium acetate 28.2 mM acetic acid elution buffer at pH 3.6. The column is cleaned using a 0.1 M sodium hydroxide solution and stored in a 20% v/v ethanol solution.

Samples are eluted in to 10 100 μL fractions that are collected directly into a 96 well plate and can be chilled in the TECAN Freedom Evo if required. Pathlength corrected absorbance readings measured at 280 nm, taken on the Infinite plate reader (TECAN) are used to identify and pool fractions over 1 g L^{-1} antibody concentration. 10 μL of 3 M Tris base is added to the pooled fractions to neutralise the acidic pH. Antibody concentration is then measured at a wavelength of 280 nm using an ND-1000 spectrometer (Nanodrop, Wilmington, USA) and samples diluted to 1 g L^{-1} with

equilibration buffer to make a stock solution. This stock solution is diluted 50% v/v with a 200 mM DTT solution and incubated at 37°C for 20 minutes in order to reduce the antibody product for glycosylation or NGHC analysis.

2.4.2. Aggregates

Sample aggregate levels were determined using a standard GSK HPLC-SEC method. 10 µL sample was injected onto a TSKgel G3000SWxl column (Tosoh Bioscience, Stuttgart, Germany. 7.8 mm i.d. x 30 cm column length, 5 µm particle size with 250 Å pore size). A 100 mM sodium phosphate monobasic, 400 mM sodium chloride mobile phase was used at pH 6.8 and a 1 mL min^{-1} flowrate. Protein was detected at a wavelength of 214 nm. Samples were maintained on an autosampler prior to analysis at 5°C ± 3°C.

2.4.3. Glycosylation profile

Antibody glycosylation profiles were determined using a standard GSK LC-MS Q-TOF method. Samples were injected onto a Zorbax Poroshell 300SB-C8 guard column (2.1mm x 12.5mm, Agilent Technologies, Stockport, UK), desalted by washing with 0.1% v/v formate in 5% acetonitrile, and then eluted with 0.1% v/v formate in 90% acetonitrile at a flow rate of 0.5 mL min^{-1}. The eluate was split such that a flow of 0.2 mL min^{-1} was directed to the electrospray ionization interface via a standard Z-spray source fitted with an electrospray probe, of a Micromass Q-TOF API-US mass spectrometer (Waters, Massachusetts, USA) controlled from a PC running MassLynx (version 4.1, Waters) software. The source temperature and desolvation temperature

were set to 100°C and 150°C respectively. The capillary voltage was 3.0 kV and the sample cone voltage was 35 V. The mass spectrometer was routinely calibrated against myoglobin or sodium iodide to ensure that peaks in the mass/charge spectrum accurately represent the samples. Raw data were externally mass corrected and deconvoluted to the parent mass spectrum using the MaxEnt 1 algorithm of MassLynx.

2.4.4. Non-glycosylated heavy chain

NGHC levels were determined using an Agilent 2100 Bioanalyzer (Agilent Technologies) in which the NGHC can be separated and quantified under reduced condition by SDS electrophoresis. Samples were reduced using a ß-mercaptoethanol containing reducing buffer. Samples were prepared using the Agilent Protein 230 kit (Agilent Technologies, Cat No. 5067-1517) and samples analysed according to running conditions recommended by the manufacturer (Agilent Protein 230 Kit Guide, Agilent Technologies). Relative NGHC levels were determined compared to the amount of antibody heavy chain present in the sample. Peak areas were calculated using the Bioanalyzer software.

2.5. Derived growth parameters

2.5.1. Integral viable cell concentration

The integral of viable cell concentration (IVC) is a measure of the number of viable cells in the culture with time; an approximation of the area underneath a graph plotting

viable cell density with culture duration between two time points. The following equation was used to determine the IVC:

$$\mathrm{IVC}_{i+1} = \left(\frac{x_i + x_{i+1}}{2} \right) \times \left(t_i - t_{i+1} \right) \qquad (2.12)$$

where IVC is the integral of viable cell concentration, *x* is the viable cell density and *t* is the time point. The sum of the IVC values gives the cumulative IVC (cIVC).

2.5.2. Instantaneous specific productivity

The instantaneous specific productivity, Q_P is a measure of the cell specific rate of antibody produced between two time points. The following equation was used to determine Q_P:

$$\mathrm{Q_{P}}_{i+1} = \left(\frac{\mathrm{Ab}_{i+1} - \mathrm{Ab}_i}{\mathrm{IVC}_{i+1}} \right) \qquad (2.13)$$

where Q_P is the instantaneous specific productivity and Ab is the antibody titre. The average specific productivity over the cell culture period is given by the total antibody titre at the end of the culture divided by the cumulative IVC value.

2.5.3. Average specific glucose consumption rate

The average specific glucose consumption rate, $Q_{gluc\ (avg)}$ is a measure of the rate at which cells utilised glucose from the culture media over the culture period. The following equation is used to determine $Q_{gluc\ (avg)}$:

$$Q_{gluc\,(avg)} = \left(\frac{[glucose]_{final} - [glucose]_{initial}}{cIVC_{final}} \right) \quad (2.14)$$

where $Q_{gluc\ (avg)}$ is the average specific glucose consumption rate and [glucose] is the glucose concentration in the cell culture.

2.6. Cell culture broth characterisation and processing

2.6.1. Ultra scale-down primary recovery

For the Ultra scale-down (USD) depth filtration studies, 05SP grade filters (CUNO Zeta Plus 05SP grade, 3M Purification Inc, Meriden, USA) were cut to an effective filter area of 0.28 cm^2. These discs were used in conjunction with a USD depth filtration rig (originally developed by Jackson (2011) and adapted for depth filtration studies by Kong et al (2010)) (Figure 2.2) (constructed in-house by the UCL Mechanical Workshop). The depth filtration rig is designed to fit on the vacuum filtration manifold on the TECAN Freedom Evo robotic platform where all samples were run at a constant pressure of 300 mbar. Between each experiment water flux tests were performed to ensure that filters were of a constant and reproducible standard. The cell culture feed material for the experiments described in this work were harvested at approximately 50 – 60% viability.

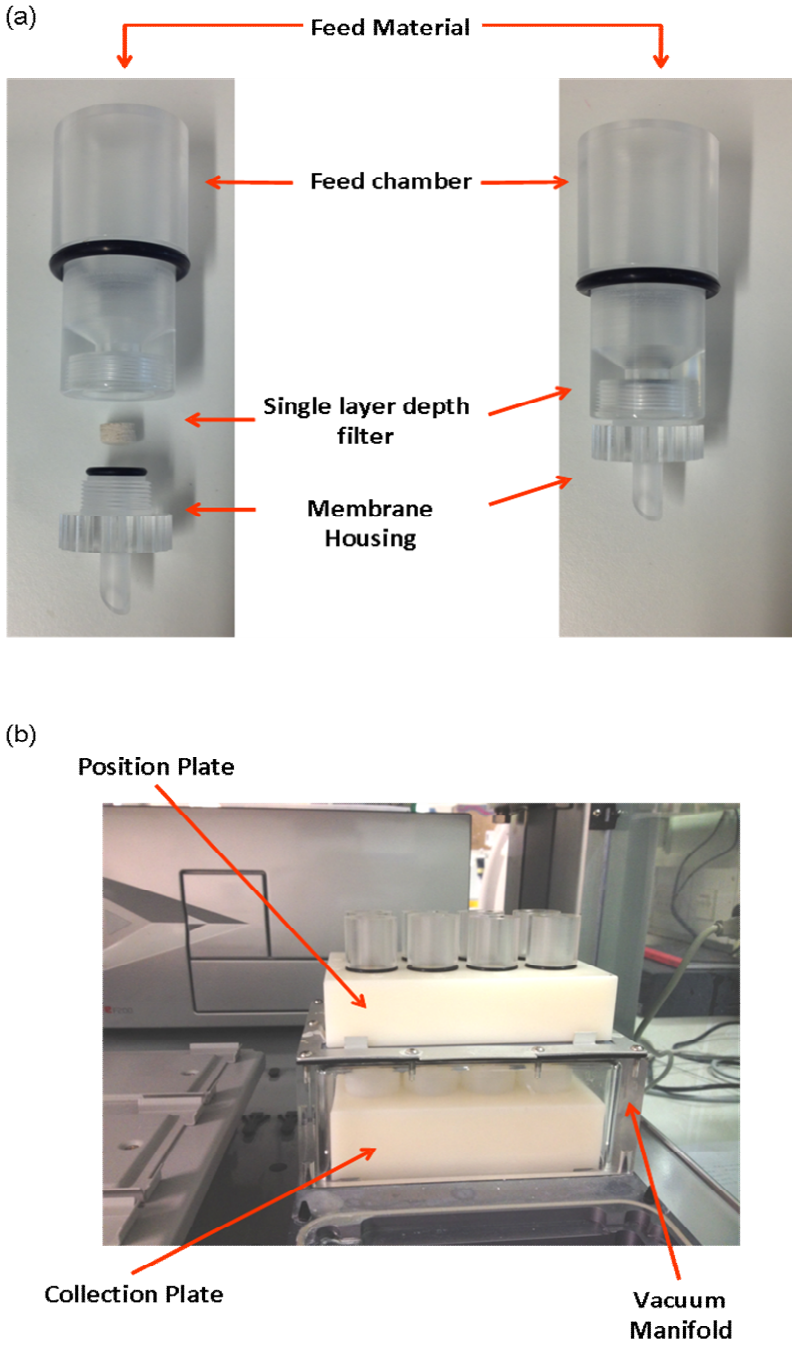

Figure 2.2. Image of (a) a single USD depth filter membrane housing and (b) the set up of the USD filter housings placed on the vacuum manifold situated in the TECAN platform.

2.6.2. Broth quality analysis

To determine the efficiency of the primary recovery step two different analyses were performed: percentage solids remaining and filter capacity (L m^{-2}). The relative

performance in terms of amount of solids remaining is calculated as described in Equation 2.15:

$$S(\%) = \left(\frac{OD_s - OD_o}{OD_f - OD_o} \right) \times 100 \qquad (2.15)$$

where S (%) is the percentage solids remaining in the filtrate, OD_s is the OD_{600} value of the filtrate sample, OD_o is the OD_{600} value of the well spun sample material and OD_f is the OD_{600} value of the feed material. With regard to membrane sizing, the gradual pore constriction model was applied to the filtration data (Zydney and Ho, 2002). The linearised version of the equation is described in Equation 2.16:

$$\frac{t}{V^*} = \frac{1}{Q_0^*} + \left(\frac{1}{V_{max}^*} \right) t \qquad (2.16)$$

where V* is the total volume of filtrate per unit filter area collected over time, t, Q^*_{max} is the initial specific volumetric filtrate flow rate per unit filter area and V^*_{max} is the predicted maximum volume of fluid per unit filter area that can be filtered before the filter is completely plugged by fouling, calculated directly from the flux decay data as the inverse of the slope of a plot of t/V.

Chapter 3. Engineering characterisation of scale-down and miniature bioreactor formats*

3.1. Introduction and aim

Biopharmaceuticals are ultimately manufactured at large scale; however, at this size there is limited opportunity to perform process development and optimisation. Consequently, most companies have validated scale-down models of their pilot and manufacturing scale bioreactors (Doig et al. 2006). These usually take the form of 0.5 to 10 L scale stirred tank bioreactors (Nienow, 2006; Szita et al. 2005) and are used for cell culture process development. Nevertheless, there is a need for more efficient, high throughput and miniaturised biorecactors that can be used earlier during process development to further reduce time and costs.

The need to bring new biopharmaceutical products to market more quickly and to reduce final manufacturing costs is driving early stage, small scale bioprocess development. Large scale bioreactors are inefficient clone ranking or process development tools due to the limited number of clones or conditions that can be investigated. Small scale, high throughput bioreactors are required to help resolve this bottleneck, as discussed in Section 1.8.

The aim of this chapter is to fully characterise the cell culture formats that will be investigated in this thesis. The bench scale STR system (described in Section 2.1.2) is

* The work presented in Section 3.3 of this chapter has been published as: Betts et al. (2014) Impact of aeration strategies on fed-batch cell culture kinetics in a single-use 24-well miniature bioreactor. *Biochemical Engineering Journal*, **82**, 105 - 116.

itself a scale-down model of GSK pilot scale bioreactors. This STR format will be used as a reference in the scale translation of a novel, single-use 24-well parallel miniature bioreactor system (described in Section 2.2.2 and illustrated in Figure 2.1). Thus, a detailed engineering characterisation of this large scale bioreactor is performed in order to benchmark a set of operating parameters that can be replicated at small scale yielding analogous engineering conditions.

The specific objectives are as follows:

- To characterise the scale-down STR format including investigating the liquid mixing times and gas transfer capacity.
- To apply existing engineering correlations available for STRs in order to be able to predict key engineering parameters such as power input and verify experimental measurements.
- To investigate two distinct plate types with the small scale bioreactor format, allowing for either headspace or direct gas sparging.
- To characterise the miniature bioreactor format including an evaluation of the fluid mixing, gas transfer capacity, dispersed gas phase and evaporation across the 24 well plate cell culture format.

3.2. Engineering characterisation of the 3 L stirred scale-down bioreactors

The 3 L bench scale STR is the standard scale-down bioreactor format currently used for cell culture process development at GSK, Stevenage. By characterising this system

over the range of typical operating parameters, it is possible to set a benchmark for the engineering parameters that will be used to characterise miniature shaken bioreactor performance (Section 3.3). The power consumption, volumetric oxygen mass transfer coefficient, k_La and the mixing time, t_m are all key engineering parameters (Section 1.7.1) that can be experimentally determined in STRs and which are commonly used as a basis for fermentation and cell culture scale up (Section 1.8).

3.2.1. Power consumption prediction

For standard STR geometries the ungassed power consumption can readily be calculated using Equation 1.2 and knowledge of the particular STR design and operating conditions (Section 2.1.2). Values calculated for the GSK STRs fitted with either Rushton turbine (P_o = 5) or pitched-blade turbine (PBT) (P_o = 1.7) impellers over a range of agitation rates are presented in Table 3.1. As expected from Equation 1.2, the power consumption is greater for the Rushton impeller than the PBT, as both the power number and the impeller diameter are greater. The corresponding impeller Reynold's numbers calculated for the various conditions studies can be determined using Equation 1.1, and values are shown in Table 3.2. Again, as expected the Reynolds numbers are greater for the Rushton impeller due to the fact that the impeller diameter is greater than the PBT diameter. In both cases, however, the Re values would indicate turbulent flow at all but the lowest agitation rate.

Various correlations have been proposed to correlate the ungassed power consumption to the gassed power consumption during bioreactor operation (Section 1.7.1, Table 2.1). However, no single correlation has been shown to satisfactorily predict the gassed power consumption in smaller scale bioreactors, primarily because most of them do not

take into account the flow regime, which can significantly affect the power consumption (Amanullah et al. 2004). For this reason, multiple correlations from literature (Section 2.1.4) have been considered here to estimate typical gassed power consumption values that might be expected. Figure 3.1 shows the gassed to ungassed power ratio as a function of the flow number (Table 2.1). In accordance with Amanullah et al. (2004) and Nienow (2006), the majority of the correlations predict gassed power consumption to be approximately equal to the ungassed power, with all but one correlation predicting less than 15% decrease in power consumption even at the highest flow number investigated. Thus, in agreement with Nienow (2006), for mammalian cell culture systems, as the gas flow rates used are relatively low, P_g can effectively be assumed equal to P. Values calculated range from 1 – 500 x 10^{-3} W (0.6 – 260 W m^{-3}) (Table 3.1) agree with those found in the literature for similar systems (Heath and Kiss, 2007; Nienow, 2006) which refer to values ranging from 10 - 1000 W m^{-3}.

Table 3.1 Calculated ungassed power consumption as a function of agitation rate and impeller design in the 3 L scale-down STR. Values were determined using Equation 1.2 and STR dimensions and operating ranges (Section 2.1.2).

Ungassed Power Input (x10^{-3} W)	**N (rpm)**				
	100	**200**	**300**	**400**	**500**
Rushton turbine	4.3	34.1	115.1	272.9	533.0
Pitched blade turbine	1.2	9.2	31.2	73.9	144.4

Table 3.2 Calculated impeller Reynolds number values as a function of agitation rate and impeller design in the 3 L scale-down STR. Values were determined using Equation 1.1 and STR dimensions and operating ranges (Section 2.1.2).

Reynolds Number	**N (rpm)**				
	100	**200**	**300**	**400**	**500**
Rushton turbine	3359	6718	10077	13435	16794
Pitched blade turbine	3067	6133	9201	12268	15335

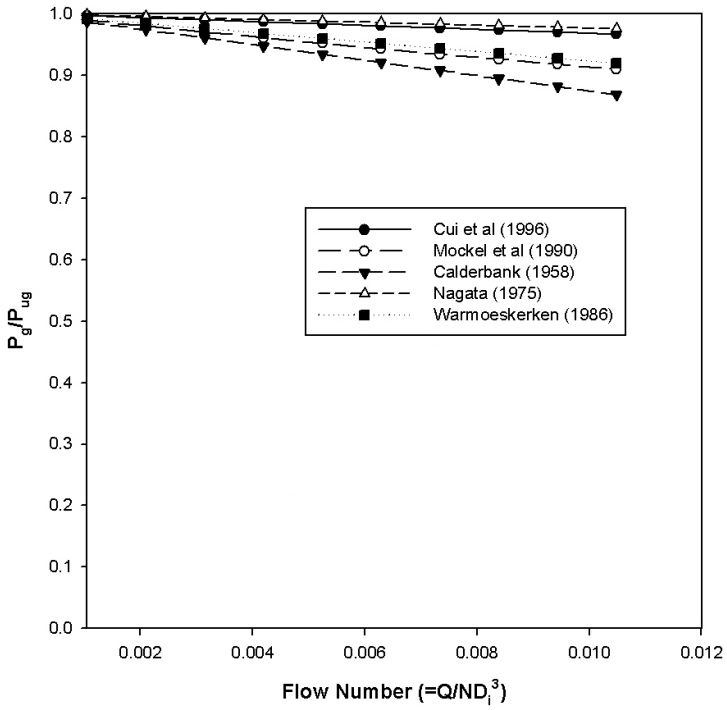

Figure 3.1 Gassed-ungassed power consumption ratio as a function of the flow number. Values were determined using equations described in Section 2.1.4 and STR parameters described in Section 2.1.2.

3.2.2. k_La prediction and measurement

As mentioned in Section 3.2, k_La is an important scale translation parameter and so was investigated here as a function of the impeller agitation rate and the gas flow rate of air sparged into the test fluid. In this case water was used to replicate the culture media and was supplemented with the shear protectant, Pluronic-F68 which is typically used in mammalian cell culture media since this has been shown to significantly lower k_La (Nienow, 2006). Experiments were carried out at 37°C as this is the typical operating temperature for mammalian cell culture and test conditions were chosen to span the typical operating values for an STR for mammalian cell culture.

As highlighted by Equation 1.6 it is expected that k_La will increase with both power input and gas flow rate. Increasing gas flow rate will provide a higher quantity of oxygen carrying gas bubbles however it is also important that the agitation rate is able

to effectively break up larger bubbles and distribute these bubbles around the system and therefore aid oxygen transfer. Calculated k_La values are presented in Table 3.3.

As expected, experimental data shows that increasing either the gas flow rate or the agitation rate will increase the k_La value. However, there is an observed decrease in k_La from 175 to 250 mL min^{-1} at 300 rpm. It is possible that the increased gas flow rate causes the impeller to flood with gas, thus reducing power input and hence k_La. In addition, the k_La values at 500 rpm are lower than those at 300 rpm. This effect may be as a result of liquid vortexing around the impeller, reducing the liquid height between the sparger and liquid surface therefore bubbles may be entrained for a shorter period of time and thus effectively reducing the gas transfer area.

Subsequently, the experimentally determined k_La values were compared with equations from the literature (Section 1.7.1; Section 2.1.6) and shown in Figure 3.2. Theoretically determined k_La values were calculated using Equation 1.6. ε_{T_g} is calculated as the sum of ε_{s_g} and ε_{i_g}, which is estimated by assuming that Pg = P, as reported by Amanullah (2004), Nienow (2006) and results of the theoretical gassed power correlations investigated in Section 3.2.1. Whilst no single literature correlation is able to satisfactorily predict k_La values and their variation with impeller agitation rate and gas flow rate in the STR, typically, required k_La values for mammalian cell culture processes are 1 – 15 hr^{-1} (Nienow, 2006) therefore experimentally determined values presented here are comparable to the values expected from literature correlations and should be sufficient to meet the oxygen requirements of a typical mammalian cell culture process.

Table 3.3 Calculated k_La values in the 3L scale-down STR as a function of agitation rate and volumetric gas flow rate. Values determined using Equation 1.6 and STR parameters as described in Section 2.1.2. Values in brackets represent r^2 values linearised experimental data.

k_La (hr^{-1})		Volumetric Airflow Rate (mL min^{-1})			
		25	**100**	**175**	**250**
Agitation Rate (rpm)	**100**	1.6 (0.99)	4.4 (0.99)	6.4 (1.00)	12.3 (0.80)
	300	5.0 (1.00)	34.2 (0.99)	47.4 (0.99)	45.8 (0.99)
	500	5.5 (1.00)	27.0 (0.98)	35.4 (0.98)	39.9 (0.99)

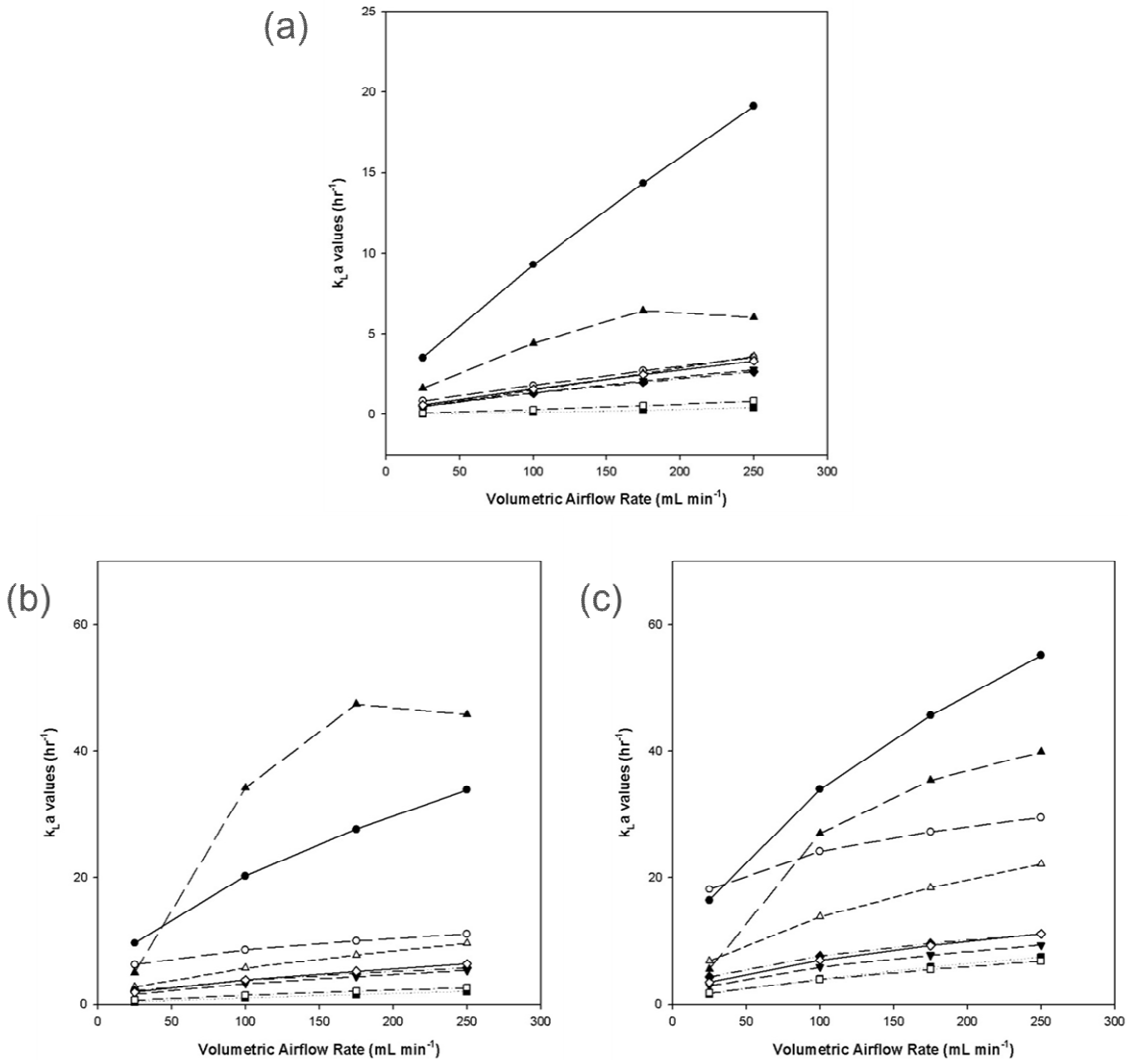

Figure 3.2 Comparison of experimentally determined k_La values (described in Section 2.1.5) at 100, 300 and 500 rpm (a, b, and c respectively) compared with literature correlations as described in Section 2.1.6. Gill et al. (2008) (*closed circles*), van't Riet [non-coalescing] (1979) (*open circles*), van't Riet [coalescing] (1979) (*closed downward triangles*), Stanbury and Whitaker (1984) (*open triangles*), Vilaca et al. (2000) (*closed squares*), Linek et al. (2004) (*open squares*), Smith et al. (1977) (*closed diamonds*), Zhu et al. (2001) (*open diamonds*) and experimental results (*dashed line, closed upward triangles*).

3.2.3. Mixing time measurement

Given the importance of maintaining a homogeneous culture environment for process monitoring and control (Birch, 1999) mixing time, as defined in Section 1.7.1, was measured as a function of operating conditions in the scale-down STR. Referring to Equation 1.7 it can be seen that mixing time is inversely proportional to the total energy dissipation rate in a gassed bioreactor. Therefore, it is expected that increasing either the power input or the gas flow rate will decrease the mixing time.

As shown in Table 3.4, it is clear that the measured mixing time values rapidly decrease with increased agitation rate. The effect of the gas flow rate is only observable at 100 rpm, the lowest agitation rate tested. At this condition, there is an observable decrease in the mixing time with increasing gas flow rate, indicating that gas flow from the sparger does indeed impact on the overall mass transfer. Mixing time values were calculated and are plotted alongside experimentally determined values in Figure 3.3. It is clear that Equation 1.7 provides an accurate prediction of the liquid phase mixing time, although the correlation provides less accurate values below an agitation rate of 200 rpm. Osman (2001) reports mixing time values of less than 60 s for a 2 L working volume (wv) STR, therefore values presented here agree with the literature.

Table 3.4 Mean mixing time values measured in the 3L scale-down STR. Values were determined using the iodine decolourisation method as described in Section 2.1.3. A working volume of 2 L was used for all experiments, and carried out at 25°C. Error represent one standard deviation about the mean (n = 3).

Mixing Time (s)		**Volumetric Airflow Rate (mL min^{-1})**			
		25	**100**	**175**	**250**
Agitation Rate (rpm)	**100**	52 ± 3	38 ± 1	21 ± 1	19 ± 1
	200	14 ± 1	13 ± 0	13 ± 1	13 ± 1
	300	6 ± 1	7 ± 1	6 ± 1	7 ± 1
	400	6 ± 1	5 ± 1	5 ± 0	5 ± 0
	500	5 ± 1	4 ± 1	4 ± 0	4 ± 0

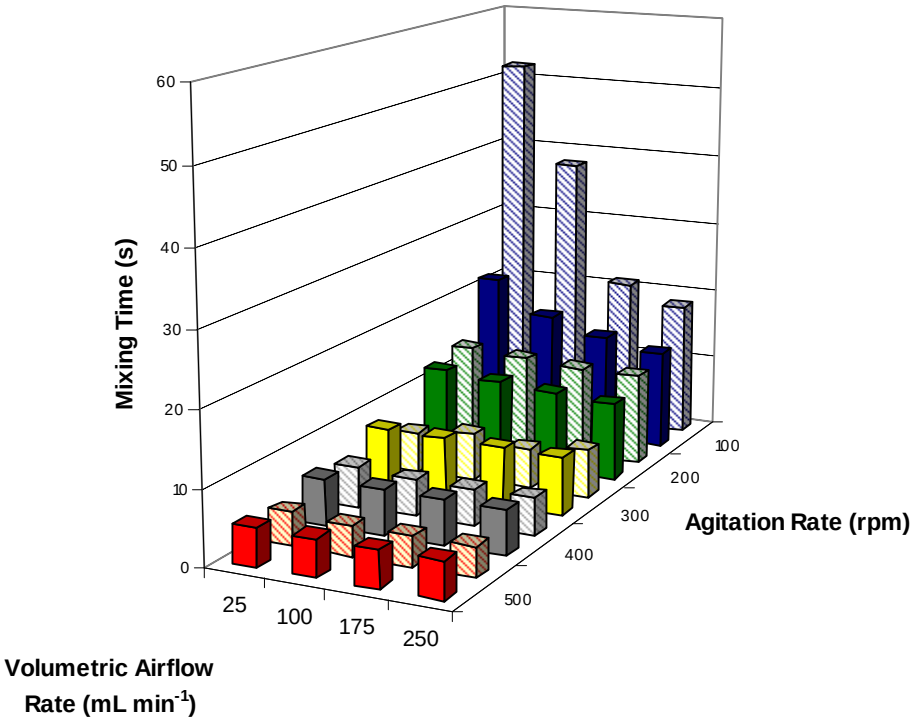

Figure 3.3 Experimental and theoretical mixing time values in the 3 L scale-down STR as a function of agitation and gas flow rates. Dashed bars represent experimental measurements while solid bars represent correlation predictions. Experimental values determined using the iodine decolourisation method as described in Section 2.1.3. Theoretical values determined using Equation 1.7 and STR parameters as described in Section 2.1.2.

3.3. Engineering characterisation of the shaken miniature bioreactor

3.3.1. Liquid phase hydrodynamics and mixing times

Initial experiments in the novel miniature bioreactor format aimed to characterise the fluid flow in individual wells from each of the two plate designs (described in section 2.2.2) and to quantify the liquid phase mixing times. As shown in Figure 3.4, for all the shaking frequencies studied orbital shaking induced deformation of the liquid surface which then moved in an orbital motion around the walls of the well. Visually there was no difference in the nature of the fluid flow between the two plate designs.

Büchs et al. (2001) discovered a phenomenon specific to shaken systems depicted by the Phase number, Ph. The 'in-phase' flow regime describes conditions where the bulk liquid circulates around the edge of the shaken vessel, synchronized with the orbital motion of the shaking platform. 'Out of phase' fluid flow occurs when only a small portion of the fluid circulates around the walls of the well with the majority of the fluid remaining stationary in the centre of the vessel (Büchs et al. 2001). The Phase number can be calculated according to Equation 3.1:

$$\mathrm{Ph} = \frac{\mathrm{d}_s}{\mathrm{d}_f}\left\{1 + 3\log_{10}\left[\frac{r\,(2p\mathrm{N})\mathrm{d}_f^2}{4p}\left(1 - \sqrt{1 - \frac{4}{p}\left(\frac{\mathrm{V}^{\frac{1}{3}}}{\mathrm{d}_f}\right)^2}\right)^2\right]\right\} \qquad (3.1)$$

where d_f is the inner diameter of the shaken vessel, d_s is the shaker diameter, N is the shaking frequency and V is the liquid volume (Büchs et al. 2001). For Ph > 1.26 the shaken fluid will be 'in-phase' while for Ph < 1.26 the fluid will be 'out of phase' (Buchs et al. 2001). Barrett et al. (2010) have applied this correlation to calculate Ph for standard 24-round well plates (24 SRW), at a shaking diameter of 20 mm, fill volumes from 800 – 2000 µL and shaking frequencies from 120 – 300 rpm. Under all conditions the flow of fluid was found to be 'in-phase' (Ph 8.2 - 12). For the µ24 system used here, assuming the liquid properties of water, Equation 3.1 predicts flow conditions to be 'in-phase' for fill volumes between 3 – 7 mL and shaking frequencies above 100 rpm. This is in agreement with video image observations at all conditions investigated.

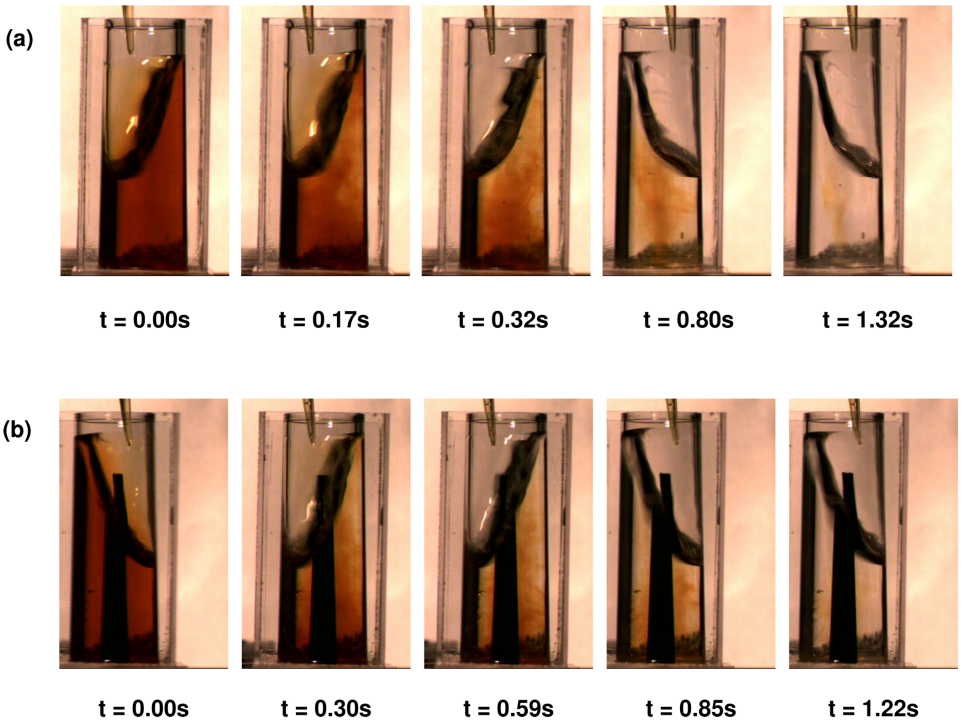

Figure 3.4. Visualisation of fluid flow during iodine decolourisation mixing time experiments for (a) PERC plate and (b) REG plate designs. Images show minimum time required to achieve complete decolourisation in each case from a dynamic start. Experimental conditions: 5 mM iodine solution; 7 mL fill volume; 800 rpm shaking frequency; d_o 2.5 mm; 25°C. Video images captured as described in Section 2.2.6.

Liquid phase mixing times were subsequently determined under non-aerated conditions. Mixing times were determined from a dynamic start, i.e. shaking platform is in operation, which is important with regards to bioreactor monitoring and control; and also from a stationary start which is unique to this bioreactor system due to the fact that the plate is removed from the shaker platform for liquid handling operations and is therefore important for initial set up, sampling, and nutrient or base feeds.

Representative time courses of these experiments for each plate design are illustrated in Figure 3.4. Mean values of the calculated mixing times over all the conditions investigated are given in Table 3.5. Increasing the shaking frequency and decreasing the fill volume is seen to decrease the mixing time. This is in line with results for

conventional 24 SRW plates (Barrett et al. 2010) where t_m values ranged from 2 – 12,900 s with fill volumes ranging from 800 – 2000 µL. Tissot et al. (2011) reported t_m values below 30 s for a 1.5 L STR fitted with a single 45 mm pitched blade impeller at agitation rates between 80 – 150 rpm and Nienow reports all values below 40 s for a range of different STR configurations (Nienow, 1997). Thus, the t_m values reported in Table 3.5 are within the ranges previously reported for conventional microwell plates and at shaking frequencies above 500 rpm, are of a comparable magnitude to those seen in laboratory scale bioreactors under cell culture conditions. Specifically with the PERC plate, the central sparge tube appears to retard mixing at low shaking frequencies, however, at higher shaking frequencies differences between the two well designs are not significant.

In conventional stirred tank cell culture reactors the presence of a dispersed gas phase is known to decrease liquid phase mixing times (Nienow, 2006). Similarly, the presence of a dispersed gas phase in the REG plate designs is seen to improve mixing as indicated in Table 3.6. Increasing gas flow rate leads to an almost 20-fold decrease in the mixing time. The influence of the dispersed gas phase on liquid mixing in shaken systems is particularly pronounced since the bubbles add an additional axial component to the fluid flow. In Table 3.6, the gas flow rates are also shown as the volumetric gas flow per unit liquid volume per minute, or VVM. This is a useful term to consider when scaling up cell culture systems. Catapano et al. (2009) reports that for mammalian cell culture in stirred bioreactors the VVM should be lower than 0.1.

Table 3.5. Measured liquid phase mixing times for PERC and REG plate designs from either a stationary or dynamic start. Experiments performed at 25°C over a range of shaking frequencies and fill volumes with d_o 2.5mm. Errors represent one standard deviation about the mean (n = 3). Mixing time measurements made as described in Section 2.2.3.

Mixing Time (s)			Shaking Frequency (rpm)					
			500		650		800	
			REG	PERC	REG	PERC	REG	PERC
Fill Volume (mL)	Static Start	3	11 ± 1	14 ± 4	4.3 ± 0.6	4.3 ± 0.6	3.3 ± 0.6	3.0 ± 0.1
		5	31 ± 2	190 ± 34	5.0 ± 0.1	5.0 ± 0.1	4.3 ± 0.6	3.7 ± 0.6
		7	210 ± 78	3700 ± 1000	6.0 ± 0.1	6.7 ± 0.6	4.0 ± 0.1	4.0 ± 0.1
	Dynamic Start	5	ND	ND	1.4 ± 0.2	1.0 ± 0.2	0.8 ± 0.1	0.8 ± 0.2
		7	13 ± 1	ND	2.0 ± 0.1	2.0 ± 0.2	1.5 ± 0.2	1.3 ± 0.2

ND: not determined

Table 3.6. Measured liquid phase mixing times for the REG plate design as a function of gas flow rate. Experimental conditions: stationary start; shaking frequency 500 rpm; d_o 2.5mm; 7 mL fill volume; 25°C. Errors represent one standard deviation about the mean (n = 3). Mixing time measurements made as described in Section 2.2.3.

Gas Flow Rate (mL min^{-1})	Normalised Gas Flow Rate (VVM)	Mixing Time (s)
0	0.00	210 ± 78
0.2	0.03	59 ± 18
2	0.29	31 ± 7
4	0.57	26 ± 5
6	0.86	20 ± 5
8	1.14	12 ± 2
10	1.43	11 ± 2

3.3.2. k_La_{app} determination and gas-liquid interfacial area

Apparent k_La values (k_La_{app}) for both the PERC and REG plate designs are shown in Figure 3.5. These were determined as described in Section 2.2.4 and are reported as 'apparent' values since the µ24 software contains a proprietary algorithm for averaging DO readings over time. It is important to understand how these k_La values vary with bioreactor operating conditions as they will influence oxygen transfer and CO_2 removal

(Nienow, 2006). Overall, increasing shaking frequency or increasing gas flow rate increases k_La. In general k_La_{app} values in the REG plate are higher and show a stronger dependency on gas flow rate than in the PERC plate. This is expected given the presence of the dispersed gas phase. For the REG plate at high shaking frequencies however, i.e. 800 rpm, k_La_{app} values seem to decrease, rather than increasing. This is likely due to fluid vortexing, thus decreasing the height of liquid above the sparger and reducing the bubble residence time. Pluronic is a non-ionic surfactant that stabilises bubble formation which will therefore cause the bubbles to separate, thus increasing a and hence k_La. However, the water-pluronic solution values, shown in Figure 3.5, are most likely lower than values in actual culture media due to the presence of additional salts. Increasing salt concentration will decrease the mean bubble size (Villadsen et al. 2011), thus increasing a, hence leading to increased k_La values.

Various methods have been used to assess k_La values in shaken microwells. Doig et al. (2006) used a dynamic gassing out method to measure k_La values and compared these to calculated values from the mass transfer limited growth rate of a strict aerobic microorganism. For a 24-well plate, fill volume of 1182 µL, orbital diameter from 3 – 8 mm and shaking frequencies from 200 – 900 rpm, k_La values were reported between 36 – 180 hr^{-1}. Furthermore these authors established a correlation in order to predict k_La values in microwell systems as a function of fluid properties, shaking frequency and well geometry (Doig et al 2006). Hermann et al. (2003) utilised the sulphite oxidation method to determine k_La values for a 96 well plate design, with reported values ranging from approximately 25 – 150 hr^{-1}. For mammalian cell cultures, however, the oxygen demand is less severe (Nienow, 2006). Barrett et al. (2010) reported values ranging from 1.1 – 29 hr^{-1} for 24 SRW plates at shaking frequencies from 120 – 300 rpm. In comparison to stirred bioreactors Micheletti et al. (2006) reports a value of 61.2 hr^{-1} for

a 3.5 L STR equipped with a 70 mm three-blade segment impeller at an agitation rate of 150 rpm and 0.1 VVM gas flow rate; whilst Tissot et al. (2011) reports a value of 4 hr^{-1} for a 1.5 L STR employing a 45 mm pitched blade impeller and a gas flow rate of 0.3 mL min^{-1} and agitation rates up to 150 rpm. Therefore, k_La_{app} values reported here ranging from 4 – 22 hr^{-1} and 4 – 53 hr^{-1} for media; and from 4 – 24 hr^{-1} and 4 – 46 hr^{-1} for water with 0.5 g L^{-1} Pluronic solution for the PERC and REG plate designs respectively are within the ranges reported for similar systems. In terms of cell culture, specific oxygen uptake rates (qO_2) range from 2.3×10^{-17} – 1.7×10^{-16} mol oxygen $cell^{-1}$ s^{-1} (Godoy-Silva et al. 2010) and so k_La_{app} values of this magnitude would appear adequate to satisfy the oxygen transfer demands of most mammalian cell culture processes.

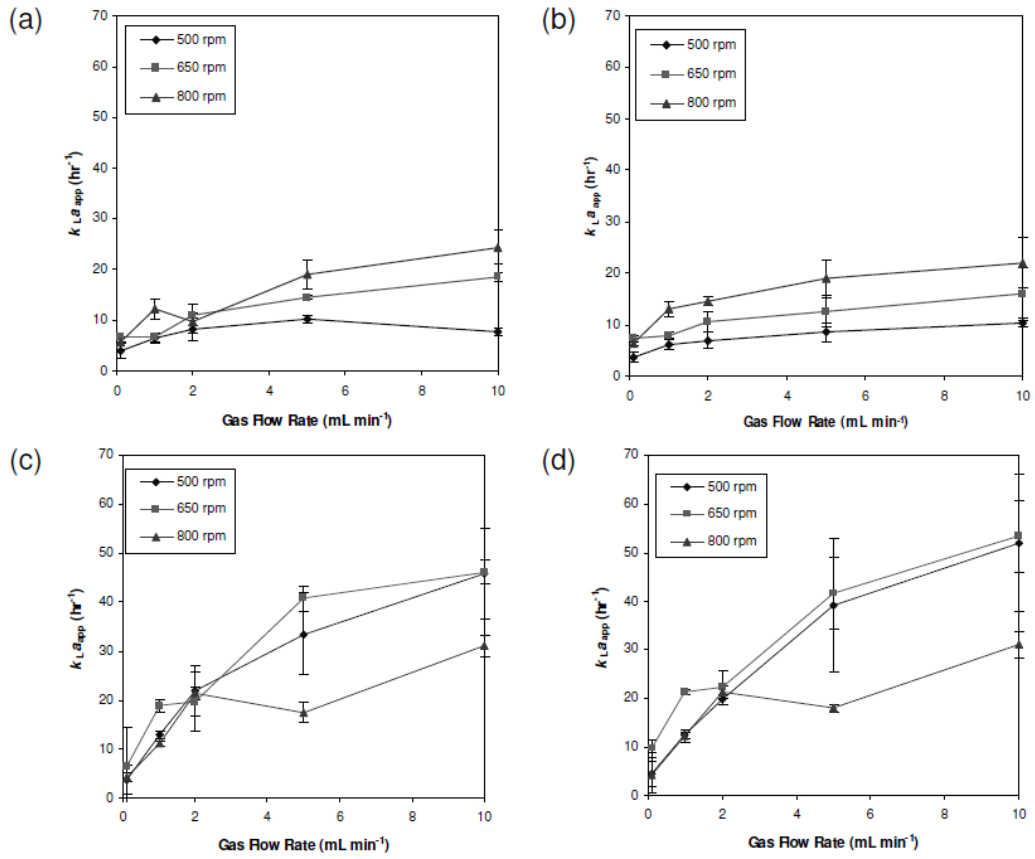

Figure 3.5. Apparent k_La values determined using the static gassing out method for (a, b) PERC and (c, d) REG plate designs with RO water containing 0.5 g L^{-1} Pluronic F-68 and PPG media respectively. Experimental conditions: 7 mL fill volume; d_o 2.5 mm; 0.1 – 10 mL min^{-1} gas flow rates; shaking frequencies 500 (♦), 650 (■) and 800 rpm (▲). Error bars represent one standard deviation about the mean (n = 3). k_La values determined as described in Section 2.2.4.

In order to understand how the available gas-liquid interfacial area impacts on the measured $k_L a_{app}$ values, the displaced liquid height was quantified by analysis of high speed camera images (Section 2.2.6). For either plate design, the displaced liquid height increases by 17, 23 and 32 mm at agitation frequencies of 500, 650 and 800 rpm with gas-liquid interfacial areas of 220, 310 and 410 mm^2 respectively. Subsequently, the gas-liquid transfer area at the surface of the liquid was calculated based on these values. As expected, increasing the shaking frequency increases the displaced liquid height for both plate designs and thus the calculated liquid area in contact with the gas at the liquid surface. This reinforces the trends seen in $k_L a_{app}$ values indicating that increasing the shaking frequency increases the available gas-liquid transfer area and thus $k_L a_{app}$. For the PERC plate, where there is no dispersed gas phase, the relationship between a and $k_L a_{app}$ is almost linear over the range of shaking frequencies tested. An increase in shaking frequency from 500 to 800 rpm is seen to approximately double the gas-liquid transfer area; leading to an approximate doubling in $k_L a_{app}$ (Figure 3.5 a, b). This indicates that the increases in $k_L a_{app}$ and hence oxygen transfer are primarily due to the increase in a while the fluid hydrodynamics have little influence on k_L. As seen in Figure 3.4 the plate design also has little impact on the displaced liquid height and the available gas-liquid transfer area at the surface.

Table 3.7. Analysis of gas bubble size, size distribution and volumetric gas hold up in the REG plate design for RO water (with/without 0.5 g L^{-1} Pluronic F-68), PPG and CD-CHO media. Experimental conditions: 7 mL fill volume; d_o 2.5 mm; 0.5 mL min^{-1} gas flow rate; shaking frequency 650 rpm. Values based on image analysis of high speed video images as shown in Figure 3.6. Errors represent one standard deviation about the mean (n = 3).

Fluid	Bubbles Per Pulse	Mean Bubble Diameter, d (mm)	a (mm^2) Per Pulse	Bubble Residence Time (s)	Gas Holdup Per Pulse (% v/v)
Water	5.0 ± 0.1	4.8 ± 0.2	370	0.21 ± 0.06	4.4
Water + 0.5 g L^{-1} Pluronic F-68	22 ± 2	2.4 ± 1.1	410	0.11 ± 0.04	2.4
CD-CHO	56 ± 2	1.8 ± 0.5	560	0.15 ± 0.02	2.4
PPG	34 ± 4	2.9 ± 0.6	930	0.14 ± 0.02	6.5

When the REG plate is aerated, Figure 3.6 shows the nature of the gas-liquid dispersion produced. Visually this varies greatly between water (coalescing) or the water-pluronic solution and the two types of cell culture media (non-coalescing) studied. In all cases, there is no significant entrainment of the gas bubbles, but rather an 'imperfect bubbly' (Kantarci et al. 2005) flow regime. Bubble packing is also observed resulting in a 'foam' layer appearing at the surface of the well, a phenomenon which is less likely to occur in a traditional STR under cell culture conditions. This foam layer was observed to persist for up to 4 minutes and hence antifoam was used during all REG plate cell culture experiments.

Analysis of the number and size distribution of the dispersed gas bubbles produced is presented in Table 3.7. This indicates a complex series of interactions between media composition and the resultant gas phase characteristics in the bioreactor, which can be attributed to the presence of electrolytes in solution (Sideman et al. 1966). For example, in contrast to water, for the water-pluronic solution or either media, the mean bubble diameter d is smaller, therefore there are an increased number of bubbles and surface area, a, available for oxygen transfer with each gas pulse. The bubble size will also be affected by the orifice diameter and the gas flow rate; in this case the high gas flow rate will dominate this relationship as observed by the relatively small gas bubbles produced (Kantarci et al. 2005). The gas bubble size has a dramatic impact on energy dissipation as a result of gas bubble disengagement at the liquid surface (Al-Rubeai et al. 1990). Similarly, there is a progression to a decrease in average bubble residence time per pulse. For the different fluids tested, as residence times change, the gas-liquid surface area changes inversely. Accordingly, there is relatively little difference between the media in terms of the total gas-liquid surface area available per gas pulse when averaged out over the pulse duration. It is worth noting that the gas bubble distribution and

dynamics observed here will be rather different in an STR, due to impeller-induced bubble break-up and their subsequent interaction and coalescence (Nienow, 2006).

Figure 3.6. Visualisation of gas bubble number and size distribution in the REG plate design for (a) water (b) water with 0.5 g L^{-1} Pluronic-F68, (c) CD-CHO media and (d) PPG. Experimental conditions: 7 mL fill volume; 650 rpm shaking frequency; d_o 2.5 mm; 5 mL min^{-1} gas flow rate. Images taken as described in Section 2.2.6.

3.3.3. Evaporation studies

Due to the extended culture periods required for cell culture, evaporation, particularly from small scale systems with low working volumes can be problematic leading to uncontrolled changes in metabolite levels and culture osmolality (Silk et al. 2010). It has been reported that high osmolality conditions increase cell specific productivity (Oh et al. 1989) therefore evaporation effects need to be minimised to overcome these non-specific influences on culture performance.

In the μ24 system, the cassette is positioned such that column 1 is closest to the fans that control the environmental temperature and 6 is furthest away whilst rows A and D are at the outside of the plate. Each well on the μ24 plate has a cap (Section 2.2.2.) with a plastic check valve and sterile membrane barrier to help reduce evaporation. The specific fold evaporation values over 9 days of a simulated batch culture are shown in Figure 3.7. These were measured as described in Section 2.2.5. It can be seen that not only is there very little culture volume reduction by evaporation over this time (average of 0.6% per day over the whole plate) but evaporation rates are generally consistent across the plate and less than 10% v/v overall.

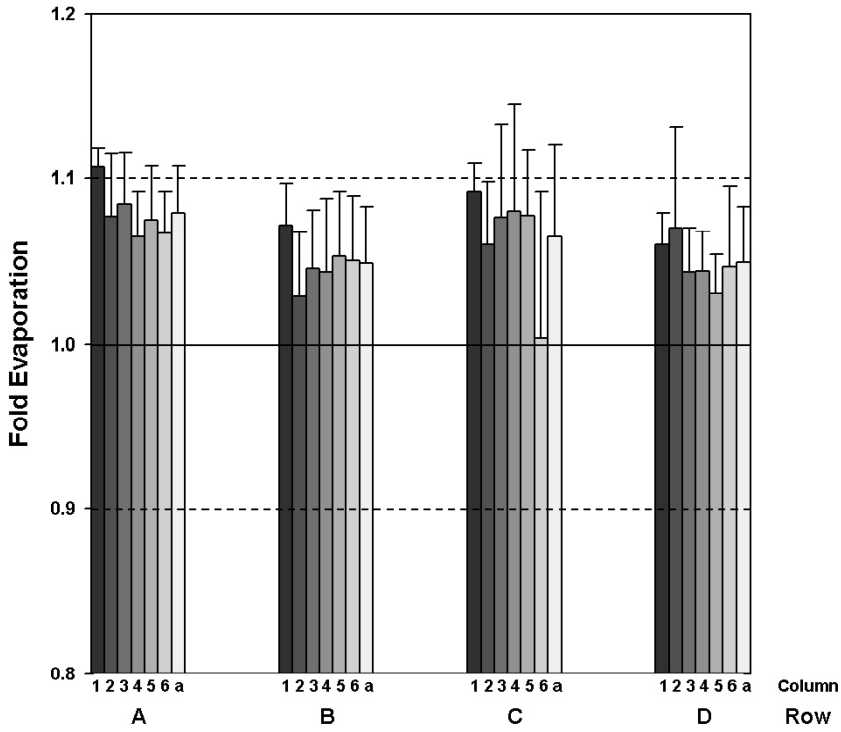

Figure 3.7. Variation of evaporation per well across a µ24 PERC cassette during a typical batch culture period. Evaporation was measured as described in Section 2.2.5. Experimental conditions: Initial 0.002% v/v blue dye in RO water; 37°C; 9 days duration; shaking frequency 650 rpm; d_o 2.5 mm; purge gas flow rate of 10 mL min^{-1}. Average (a) represents the mean with error bars indicating one standard deviation. Dashed lines represent ± 10% variation about the mean. Evaporation rates measured as described in Section 2.2.5.

3.4. Summary

This chapter aimed to characterise the cell culture systems that are used in this thesis; delivering an essential set of engineering parameters across a range of typical operating conditions for mammalian cell culture.

For the characterisation of the scale-down, 3L stirred bioreactor the basic engineering parameters were first quantified and compared to existing literature correlations. Under typical operating conditions mixing times were in the range 4 – 52 s (Figure 3.3; Table 3.4), k_La values in the range 2 – 40 hr^{-1} (Table 3.3) and 1 – 500 x 10^{-3} W (0.6 – 260 W m^{-3}) (Table 3.1). As discussed previously, in comparison to literature data for similar 3 L STR systems these experimental and calculated values fit well with reported values.

In the case of the miniature shaken bioreactor a fundamental engineering characterisation of this cell culture platform had not previously been reported. The critical difference between the two plate designs investigated is the absence (headspace sparging; PERC plate) or presence of a dispersed gas phase (sparging directly into the fluid phase; REG plate). Under typical operating conditions, dynamic mixing times were in the range 0.8 – 13 s (Table 3.5) and apparent $k_L a$ values in the range 5 – 50 hr^{-1} (Figure 3.5). Little work has been done to characterise such small scale bioreactors; a full engineering characterisation of the μ24 bioreactor system was necessary to aid our fundamental understanding of the engineering environment in such a system.

Comparing the two different bioreactor formats, the work completed in this chapter emphasises the fact that it is possible to operate systems at different scales in a manner which will generate comparable engineering environments. Overlapping ranges of key engineering characteristics illustrate that it is possible to match the fundamental engineering parameters despite the different scales of operation and mechanism of energy input to the two systems (mechanical agitation as opposed to orbital shaking).

This chapter underlines the fact that the small scale bioreactor system is capable of achieving comparable physical conditions to that of the existing scale-down stirred bioreactor. This is crucial for any future cell culture experiments in order to establish comparable physical environments in which the cells will grow. Significant differences in such engineering parameters are likely to cause distinct cellular metabolism effects and result in altered cell culture kinetics. In the next chapter the impact of the different μ24 plate formats on cell culture performance will be determined.

Chapter 4. Miniature bioreactor cell culture kinetics and clone ranking*

4.1. Introduction and aim

Typically in industry, large numbers of cell line clones are screened in simple static microwell or small scale shake flask cultures in order to select high productivity lines (Markusen and Robinson, 2013). A small sub-set of high producers subsequently enter process development studies and before selecting the 'best' cell line for final large scale manufacture of a biopharmaceutical product. Crucially however, the engineering environment in such simple cell line selection systems may not yield the optimum lines for cultivation in bench scale, scale-down bioreactors (10 - 200 L) and ultimately at manufacturing scale. At the bench scale and above virtually all bioreactors will involve suspension culture of cells in the presence of a dispersed gas phase in fully instrumented and controlled mechanically stirred bioreactors (Nienow, 2006). Therefore, cell culture systems used for initial cell line selection might not identify the 'best' or most robust cell lines for large scale culture.

This chapter investigates the fundamental impact that the distinct physical environments found in the different microbioreactor plate formats, described in Section 3.3, have on cell growth and antibody productivity. Particular emphasis is placed on the aeration strategies adopted at this small scale (7 mL) either by headspace sparging alone or by direct gas sparging into the culture medium. It is hypothesised that the absence of a dispersed gas phase will provide a good mimic for existing clone ranking tools, and the

* The work presented in Section 4.2 of this chapter has been published as: Betts et al. (2014) Impact of aeration strategies on fed-batch cell culture kinetics in a single-use 24-well miniature bioreactor. *Biochemical Engineering Journal*, **82**, 105 - 116.

presence of a dispersed gas phase will provide a better prediction of larger scale STR formats. This will be a novel set of experiments attempting to prove that the presence of a dispersed gas phase is critical to cell culture performance. In this chapter, the strength of the hypothesis is also tested across a range of cell clones. Given these differences, the aim in this chapter is to investigate use of the single-use 24-well parallel miniature bioreactor system for use as a clone ranking tool in a cell line selection scenario.

The specific objectives are as follows:

- To establish the basic methodologies for reproducible culture performance in the microbioreactor system to minimises well-to-well variation.
- To investigate cell culture in the miniature bioreactor system using a model CHO DG44 cell line expressing a whole IgG1 mAb in a non-chemically defined media.
- To examine the impact of aeration, and the gassing strategy adopted, on cell growth kinetics and antibody productivity.
- To establish the miniature bioreactor as a platform system by replicating cell culture results using a model CHO *dhfr*$^{-/-}$ cell line expressing an IgG1 mAb in a chemically defined media.
- To evaluate a range of clones in the two plate formats against traditional shake flask screening tools.

4.2. m24 cell culture kinetics

4.2.1. Achievement of consistent well-to-well performance

As shown in Figure 4.1 (a) initial parallel batch cultures (n = 24) of the CHO *dhfr*$^{-/-}$ cell line in PERC plates showed considerable well-to-well variation even though all wells were controlled at the same set points. By day 8 the maximum VCD was 10.5×10^6 cells mL^{-1} and there was a maximum difference of 6.4×10^6 cells mL^{-1} equivalent to an 88% difference in final maximum and minimum VCD values. Subsequent experiments investigated ways to reduce this variability. Initial experiments identified inconsistent cell growth in some wells, either due to variation in the inoculum added or due to cell settling whilst sampling.

To counter these issues a microplate shaker was used to gently agitate the culture cassette when removed to a biological safety cabinet for sampling. In addition, a large volume, automated electronic pipette was employed to inoculate the wells in parallel. Using the optimised methodology cell culture kinetics across all wells were virtually identical as shown in Figure 4.1 (b) and the final VCD increased to 19.3×10^6 cells mL^{-1}. There was no apparent systematic variation in performance across the plate with well-to-well variation in viable cell number reduced to less than 2.6×10^6 cells mL^{-1} at day 11, equivalent to a 14% difference in maximum and minimum VCD values.

4.2.2. Fed-batch cell culture kinetics in PERC plates

As shown in Section 3.3 the PERC plate design provides a homogeneous culture environment with adequate gas-liquid mass transfer for cell culture occurring solely via head space aeration. The detailed kinetic performance of 24 parallel fed-batch cultures of the CHO *dhfr*$^{-/-}$ cell line grown in PPG media under optimised conditions using the PERC plate is shown in Figure 4.2 (a). Under the conditions used the measured t_m

during shaking was 2.0 s (Table 3.5) while the maximum $k_L a_{app}$ was approximately 8 hr^{-1} (Figure 3.5 (b)). A standard fed-batch process was carried out for this cell line using a single 5 % v/v bolus feed addition on day 7 as described in Section 2.2.4.

As shown in Figure 4.2 (a) (i) reproducible performance is again seen across all 24 wells. In terms of cell growth the peak cell density was almost 20.4 $\times 10^6$ cells mL^{-1} at day 14 and viability remained above 60% for all wells. The on-line parameters (Figure 4.2 (a, ii)) demonstrate that the system was capable of maintaining all wells at their set points and that the control was reproducible across the culture cassette. DO was maintained at 57 ± 12% and pH at 6.95 ± 0.3. The spikes seen in the pH trace, for example at day 7, corresponds to manual sodium bicarbonate base feeding to readjust online pH. The metabolite data (Figure 4.2 (a) (iii)) and antibody titre (Figure 4.2 (a) (iv)) was shown to be consistent across the wells. The antibody titre reached a peak of approximately 1.6 g L^{-1} at day 14.

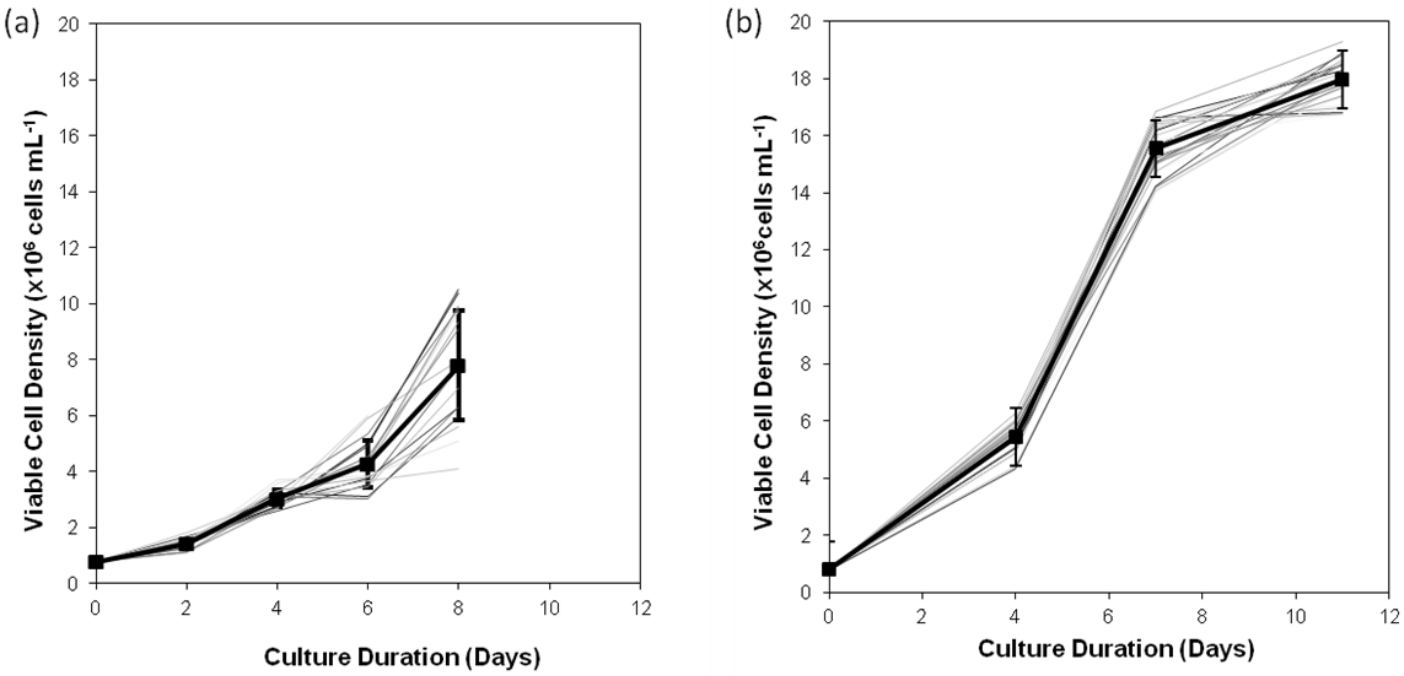

Figure 4.1. Parallel fed-batch culture kinetics of a *dhfr*$^{-/-}$ cell line grown in PERC plates using (a) initial and (b) optimised operating conditions. Bold line represents mean with error bars showing one standard deviation (n = 24). Experimental conditions: shaking frequency 650 rpm; d_o 2.5 mm; temperature set point 37°C; pH set point 6.95; DO set point 57%. Experiments performed as described in Section 2.2.4.

4.2.3. Fed-batch cell culture kinetics in REG plates

In contrast to the PERC plate, wells in the REG plate are individually aerated leading to the formation of a dispersed gas phase (Figure 3.6). Using the REG plate format different operating strategies for aeration were investigated. The presence of the dispersed gas phase was believed to affect cell growth and antibody production (Godoy-Silva et al. 2010) as described in Section 4.1.

In a traditional bioreactor a carrier gas is sparged through the culture in a continuous manner, and other control gases, i.e. oxygen or carbon dioxide, are actively blended in as appropriate in order to control the system pH and DO set points (Nienow, 2006). This aeration strategy was replicated in the µ24 'constant flow' protocol as reported in Section 2.2.4 and Table 2.3, whereby air is constantly sparged at a desired flow rate, interspersed by the appropriate active sparging of gases to control pH (CO_2) and DO (40% O_2). In order to evaluate the effect of gas sparging on the system an 'active flow' protocol was also investigated as described in Section 2.2.4 and Table 2.3. In this case no purge gas was used to constantly sparge the culture and therefore only 'active' sparging of gasses occurred in order to maintain pH and DO set points.

The performance of 24 parallel fed-batch cultures of the CHO *dhfr*$^{-/-}$ cell line in PPG media using the REG plate with either 'constant flow' or 'active flow' protocols is shown in Figures 4.2 (b) and (c) respectively. Under the operating conditions used the measured t_m values was approximately 7.0 s (Table 3.5) and the $k_L a_{app}$ was approximately 12 hr^{-1} (Figure 3.5 (d)). The mean bubble size was 2.9 mm and the gas phase hold-up was 6.5% v/v (Table 3.7).

As shown in Figure 4.2 (b) (i) the REG plate experiments operated using the ‘constant flow’ protocol again showed reproducible culture performance. The peak cell density was almost 12.9 $\times 10^6$ cells mL^{-1} at day 14 and viability remained above 70% for all wells. Gassing in this case appeared to retard cell growth at the beginning of the growth phase, but the cells maintained a higher percentage viability over this time when compared to the PERC experiments. DO was maintained at 57 ± 32% and pH at 6.95 ± 0.4 (Figure 4.2 (b) (ii)). Glucose and lactate concentrations were consistent across the parallel experiments (Figure 4.2 (b) (iii)) and antibody concentration is seen to peak at 1.15 g L^{-1} (Figure 4.2 (b) (iv)).

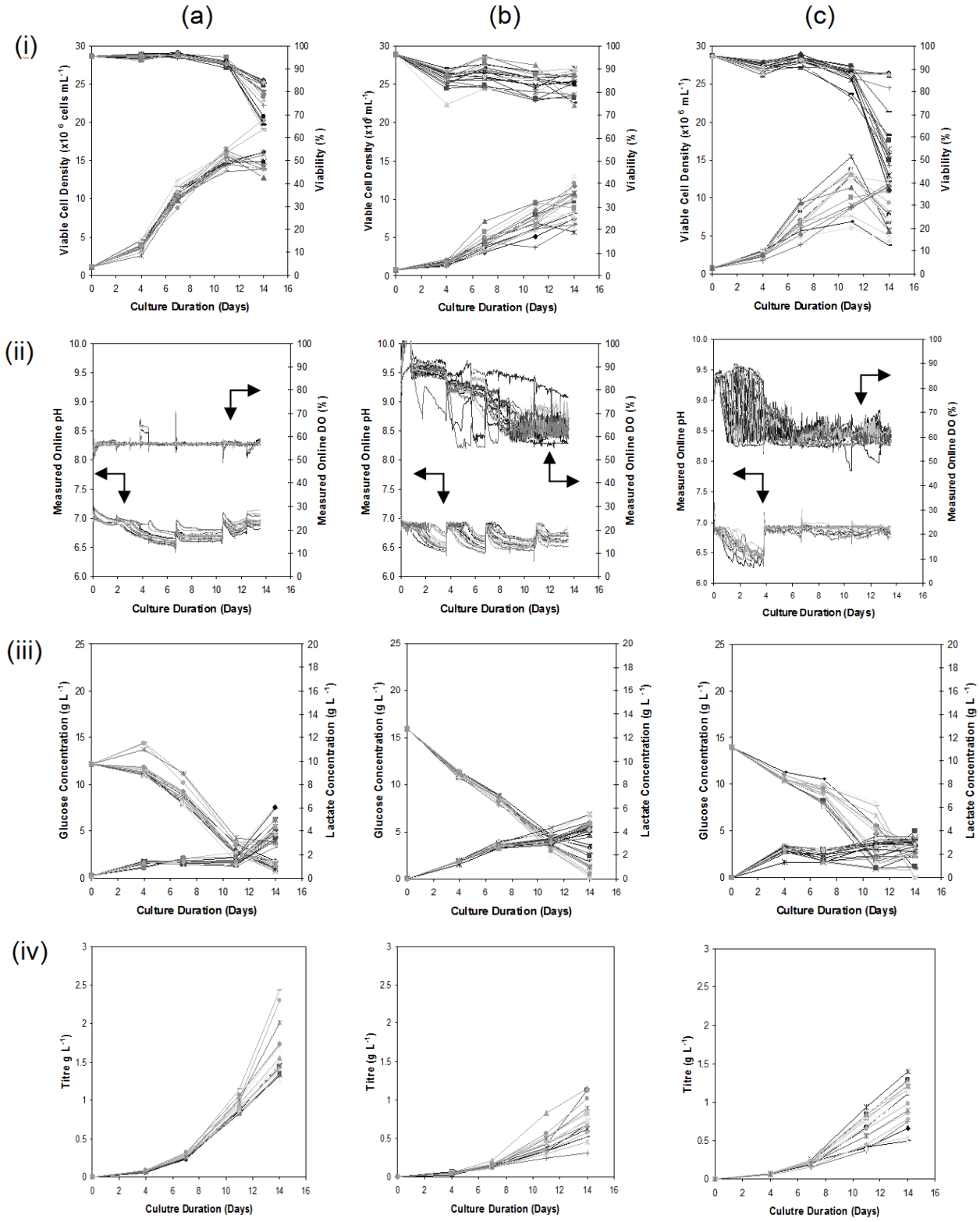

Figure 4.2. Influence of plate design on 24 parallel fed-batch culture kinetics of a *dhfr*$^{-/-}$ cell line for (a) PERC plate, (b) REG plates operated in 'constant flow' mode, and (c) REG plates operated in 'active flow' mode: (i) VCD and viability (ii) online pH and DO values, (iii) glucose and lactate concentrations and (iv) mAb titre. Experimental conditions: d_o 2.5 mm; shaking frequency 650 rpm for the PERC plate and 550 rpm for the REG plate design. Experimental set points as described in Figure 4.1 and feeding performed as described in Section 2.2.4.

In contrast, use of the 'active flow' protocol (Figure 4.2 (c) (i)) showed a greater degree of variability in growth profiles. However, in general, there is good consistency across the wells in the plates, and the effect of bubble damage on cell culture performance is clearly shown. In this case the cell growth follows a pattern resembling that shown for the PERC plate, with a visible exponential growth phase, reaching a peak VCD of 15.5 $\times 10^6$ cells mL^{-1} at day 11. However, after this point there is a more rapid decline in cell viability, leading to a final average viability below 60% at day 14. This can be explained due to the increased frequency in active gassing, at the higher cell densities, in order to control bioreactor set points. Online parameters are maintained with DO at 57 ± 24% and pH at 6.95 ± 0.2 (Figure 4.2 (c) (ii)). Glucose and lactate concentrations follow cell growth, but with increased glucose utilisation and lactate production (Figure 4.2 (c) (iii)). This is assumed to be because the cells are undergoing a greater degree of environmental stress, and are thus utilising more energy for cellular repair (Heath and Kiss, 2007; Ho et al. 2006). The peak antibody concentration was 1.40 g L^{-1} (Figure 4.2 (c) (iv)).

Taken together these results highlight the significant impact that gas sparging has in small scale cell culture formats like the µ24. Energy dissipation rate increases rapidly with decreasing bubble size, e.g. in pure water for a bubble diameter of 6.32 mm energy dissipation is 1 x 10^5 W m^{-3} which increases to 1 x 10^8 W m^{-3} for a bubble diameter of 1.7 mm (Godoy-Silva et al. 2010). In comparison, the energy dissipation generated by an impeller which will have an approximate 1 x 10^1 W m^{-3} volume average for a typical animal cell bioreactor (Godoy-Silva et al. 2010). The constant gassing protocol appears to significantly retard cell growth at the exponential growth phase. However, this appears to condition the cells to the stress as a result of bubble damage. This is seen in the active gassing strategy; after approximately day 11 when there is a significant

decrease in the viability of the cell population as a result of a significant increase in the frequency of gas sparging in order to control the bioreactor set points at these now high cell densities.

Another issue that could be affecting cellular metabolism with regard to the different gassing strategies is that of CO_2 toxicity. It is widely believed that CO_2 build up is primarily an issue in large scale bioreactors where the increased hydrostatic pressure increases CO_2 solubility, and the low VVM gas flow rates that use an enriched oxygen air supply are unable to sufficiently strip the CO_2 and hence lead to cellular toxicity (Nienow, 2006). However, this is not believed to be the cause of the lower VCD and titres exhibited by the REG plate cultures in 'constant flow' gas mode. Due to the low bioreactor volume and use of the 'constant flow' gassing regime, CO_2 stripping would be greater than that of the REG plate in the 'active flow' mode and thus the build-up of dissolved CO_2 to toxic levels is unlikely to occur. Thus the reduced growth kinetics under the 'constant flow' regime is most likely solely attributed to the increased gas sparging frequency.

4.2.4. Comparison of m24 and shake flask culture kinetics

In the previous section, comparison of PERC and REG plate designs under similar operating conditions (well mixed, i.e. low t_m, adequate $k_L a_{app}$) showed that differences in cell culture performance were primarily attributed to the presence of the dispersed gas phase in the REG plates. Here the performance of the two plate designs is compared to conventional shake flask fed-batch cultures also at a matched mixing time (~7 s) as shown in Figure 4.3.

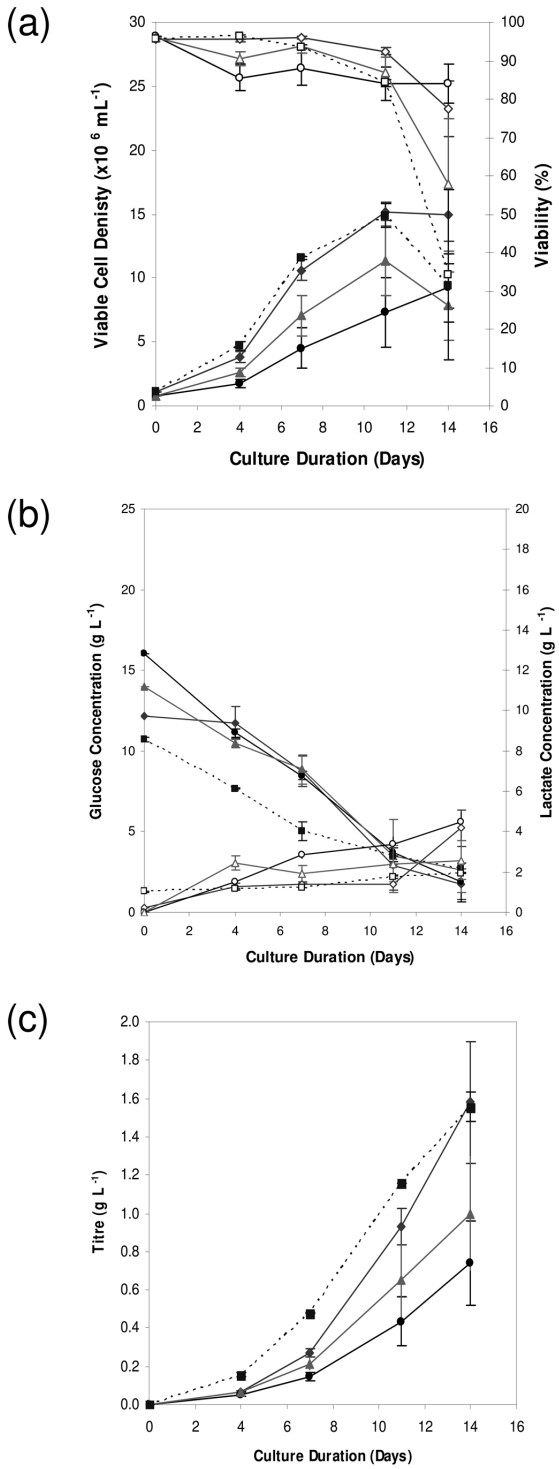

Figure 4.3. Comparison of fed-batch culture kinetics of a *dhfr*$^{-/-}$ cell line between PERC (♦, ◊) and REG plate designs operated in 'constant flow' mode (▲, Δ), and 'active flow' mode (●,○). Reference shake flask data (■, □) indicated with dashed line: (a) VCD (♦, ■, ▲, ●) and viability (◊, □, Δ, ○), (b) glucose (◊, □, Δ, ○) and lactate (♦, ■, ▲, ●) concentrations and (c) mAb titre. The PERC and REG cultures were performed as described in Figure 4.2 with shake flasks shaken at 250 rpm at a 25 mm orbital diameter. Error bars represent one standard deviation about the mean (n = 24 for μ24 data; n = 6 for shake flask data). Shake flask cultures performed as descried in Section 2.2.4

As shown in Figure 4.3 (a) the cell growth kinetics in the PERC plates outperform those measured in the shake flask systems due to better control of culture parameters in the μ24. The observed higher antibody titre in the shake flask (Figure 4.3 (c)) is in fact not significantly different from that observed in the PERC plate (P = 0.91 between the two data sets). The shake flask titre data is believed to be comparable to that of the PERC plate results due to the fact that the viability is lower and therefore incomplete antibody fragments will be released, thus over predicting the shake flask antibody titre value. Alternatively, as the pH is not controlled for the shake flask culture, the pH may drift towards a value that is favoured for cell growth and antibody production. The REG plate results are lower due to increased cellular stress as a result of gas sparging, and hence lower VCD values and lower product titre.

Derived growth parameters are calculated and presented in Table 4.1 for the four culture conditions. The Integral Viable Cell (IVC) count shows the measure of viable cells in the culture at a given time point. The PERC plate has the highest maximum IVC, thus illustrating the capacity for this system to support the highest number of viable cells. Similarly, the PERC plate has the highest instantaneous cell specific productivity (Qp) value. This highlights that the system is able to support a high number of cells, and also because of the monitoring and control capabilities, the cells also express a greater amount of product. The maximum specific growth rate reflects the cell growth data, with the growth rates in the REG plate lower than that of the PERC format. This also highlights the fact that the negative impact due to the cellular damage caused by the bubbles in the REG cultures has a greater impact than the positive impact of monitoring and controlling culture conditions.

Monitoring and control of culture parameters, pH and DO, in the µ24 as in conventional bench and production bioreactors, means that more representative data is obtained as opposed to other scale-down formats, e.g. shake flasks, normal microtitre plates. The PERC plate design appears most suited to identifying very high VCD/producing cell lines, i.e. in the context of early stage clone screening and selection. However, for the REG plate, whilst relative culture performance was not as good, this design introduces a dispersed gas phase and so is expected to be more similar to conventional bioreactors. Therefore, when looking to devise a scale-down mimic of a conventional STR the REG plate design may be preferable. Conditions in bench and production scale bioreactors are not uniform or constant engineering environments and do challenge cells to grow, therefore early screening of cells by introducing demanding processing conditions may actually be beneficial to aid early stage cell culture process development and identification of scalable cell lines.

Table 4.1. Derived growth parameters calculated from average cell culture data for shake flask, µ24 bioreactor using a PERC plate, and REG plate designs operated in a 'constant flow' or 'active flow' mode respectively, as described in Section 2.2.4 and Table 2.3. Values calculated from Figure 4.3.

System	Maximum IVC ($\times 10^6$ cells day mL^{-1})	Cumulative IVC ($\times 10^6$ cells day mL^{-1})	Instantaneous Qp (pg cell^{-1} day^{-1})	Maximum volumetric productivity (mg L^{-1} day^{-1})	Maximum specific growth rate (day^{-1})	Maximum doubling time (day^{-1})
Shake Flask	125	261	13.6	111	0.37	11.0
PERC 'constant flow'	128	253	14.4	113	0.34	7.7
REG 'constant flow'	62	119	12.2	53	0.32	8.7
REG 'active flow'	87	173	12.1	71	0.33	5.8

4.3. Validating the small scale bioreactor system as a platform process technology

As described in Section 4.2.4, the PERC plate design and controlled culture conditions in the μ24 provide an optimal engineering environment for the culture of mammalian cell lines. Improved growth and productivity in PERC plates compared to shake flasks was demonstrated for a cell line expressing a whole IgG1 mAb product, as illustrated in Figure 4.3 (a). This data was obtained for a model CHO DG44 (*dhfr*$^{-/-}$) cell line in a non-chemically defined, fed-batch process (CHO-A). It is possible to reproduce this effect for a different CHO DG44 (*dhfr*$^{-/-}$) cell line, expressing a different IgG1 mAb product (Figure 4.4). This second cell line operates under a chemically-defined, fed-batch process (CHO-B). Thus, it appears that the μ24 platform displays similar operational characteristics, including key cell culture outputs such as VCD and titre, in either case, and for very different product, cell lines and processes. Establishing technologies such as the μ24 as a platform cell culture technology is crucial in order to encourage the uptake of such products into the relevant companies, and therefore improve process development economics and timescales.

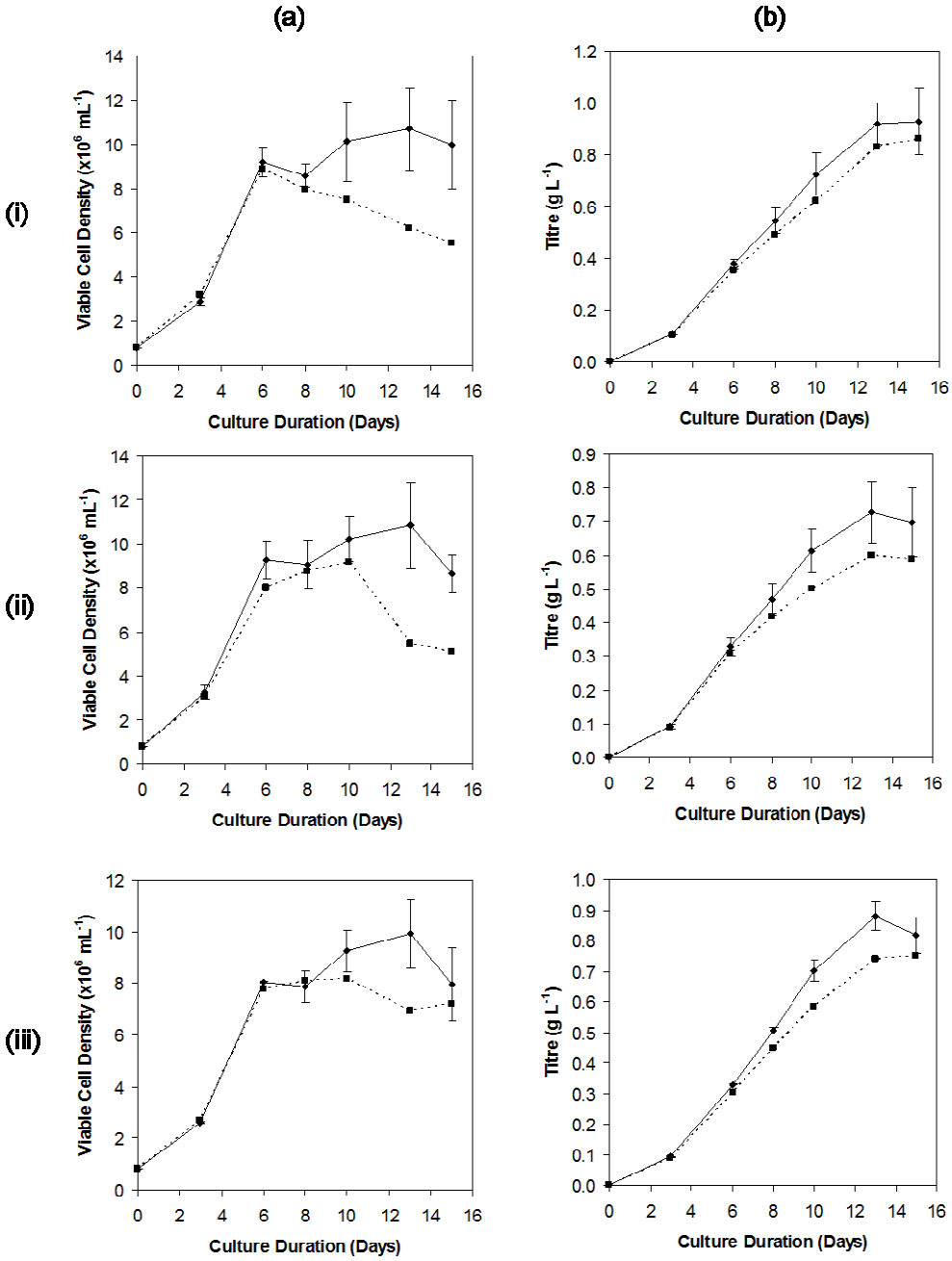

Figure 4.4. Comparison of fed-batch culture kinetics between PERC (♦) and reference shake flask (■) data: (a) VCD and (b) mAb titre for three CHO-B cell line clones (i) B5, (ii) B6 and (iii) L4. The PERC and shake flask cultures were performed as described in Section 2.2.4 Error bars represent one standard deviation about the mean (n = 3 for μ24 data).

4.4 Cell line selection under process relevant conditions

Having established the reproducibility of the miniature bioreactor system it was attractive to evaluate its use for early stage clone ranking experiments and in particular to evaluate clone ranking in unaerated (PERC) and aerated (REG) plate designs. In order to do this, a group of 24 cell clones expressing an IgG1 mAb were chosen. These clones represent an actual range of clones that were transfected and initially selected at GSK, Stevenage, before further refinement of clones prior to bioreactor screening and finally cell culture process development. The rationale for this experimental approach is to reduce the time and cost required for cell line selection and process development by recreating the engineering environment and, in particular, the presence of a dispersed gas phase comparable to that of the final cell line and process development tool earlier on in the cell line selection process and process development cycle. In addition, certain clones that may have previously been discarded by a shake flask screening process may actually have been incorrectly removed from this process due to the fact that the environment experienced in this cell culture format is so dissimilar to a bench, or production, scale bioreactor. Thus, whilst not only reducing time and costs in the development process, further gains in productivity may actually be realised because the right clones are being selected in the first place.

As shown in Figure 4.5, the 24 cell clones were initially screened based on antibody titre in the traditional manner, i.e. in shake flasks, and in parallel were also screened using the μ24 PERC plate format. In general, there was a positive correlation between the performance of clones in both formats. For the purpose of the subsequent experiments, clones of varying performance were selected from this screen. Selection criteria entailed picking clones of high performance in both formats (green), poor

performance in both formats (red) and finally clones that performed significantly better in one format as opposed to the other (purple), as illustrated in Figure 4.5.

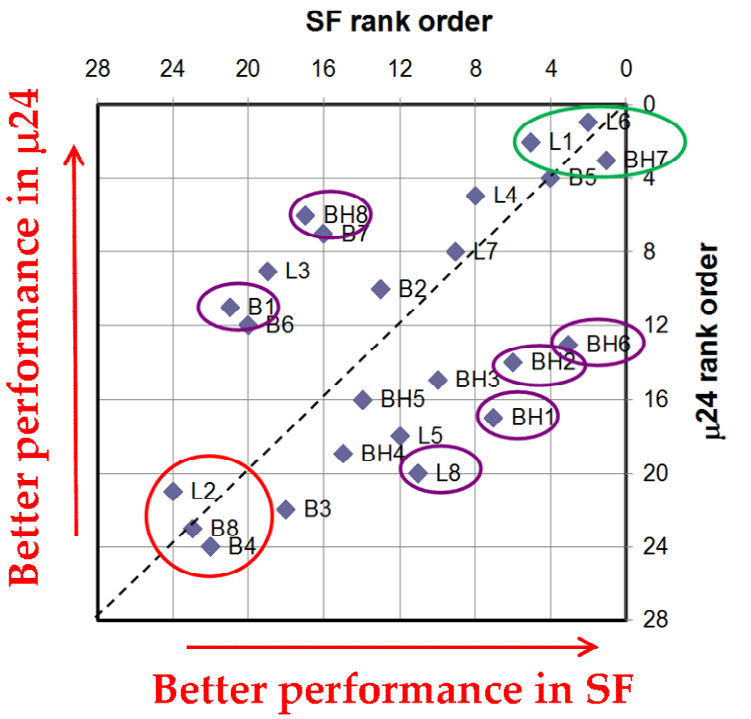

Figure 4.5. Parity plots comparing relative ranking of day 15 titres between the µ24 PERC plate cultures and shake flasks for 24 clones of a mAb expressing CHO cell line in a fed-batch process. Experimental conditions for µ24 PERC plates as described in Section 2.2.4: fill volume 6.5 mL; shaking frequency 650 rpm; d_o 2.5 mm; pH set point 6.95; DO set point 30%. Shake flask experimental conditions as described in Section 2.2.4: 50 mL wv; shaking frequency 140 rpm; d_o 25 mm. Cultures in either system were maintained at 35°C and fed on days 3, 6, 8, 10 and 13 with a 10% v/v Feed 6 AGT feed solution supplemented with additional proprietary amino acid solution.

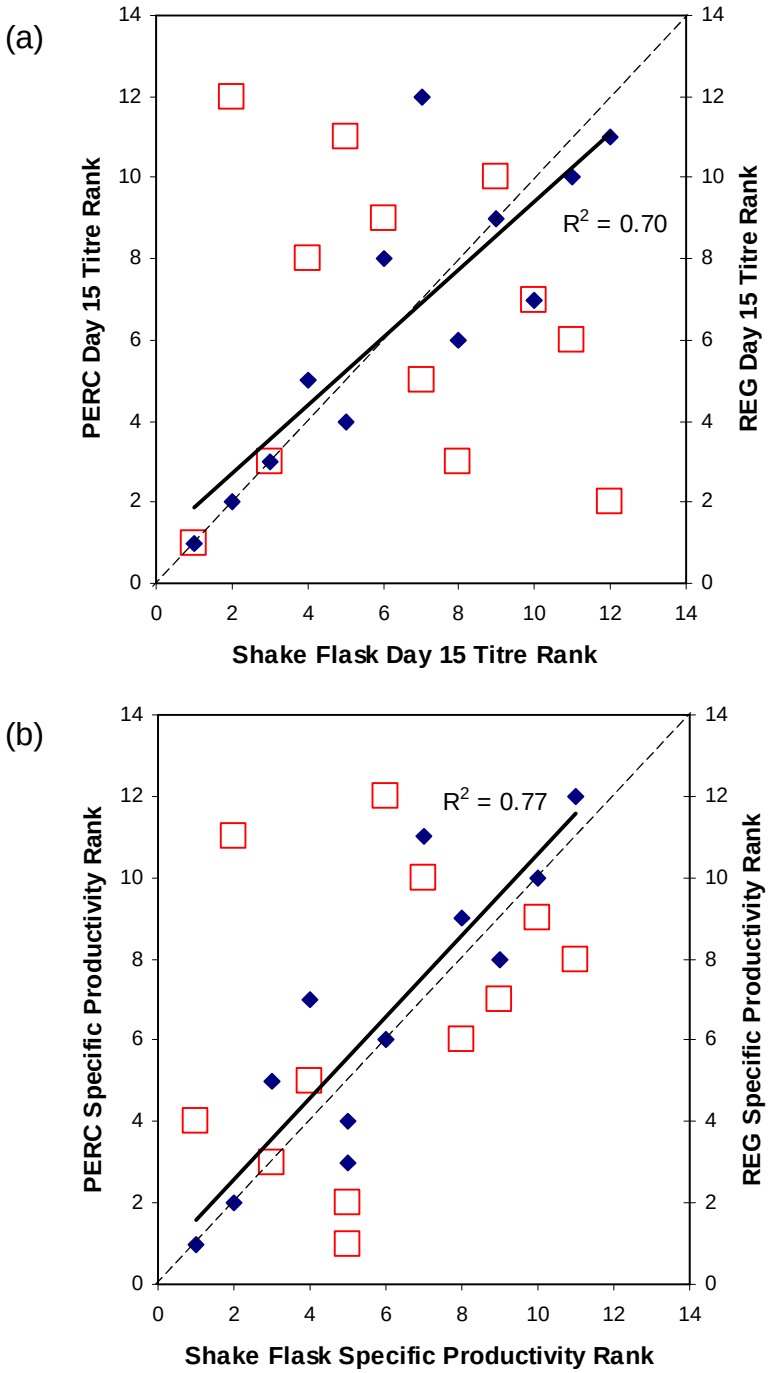

Figure 4.6. Graphs of relative ranking performance comparing PERC versus shake flask cultures (♦) and REG versus shake flask cultures (□). Graph (a) displaying day 15 titre data, g L^{-1}, with graph (b) displaying specific productivity, pg $cell^{-1}$ day^{-1}, data. PERC and shake flasks were performed as described in Figure 4.5. Experimental conditions for µ24 REG plates: fill volume 6.5 mL; shaking frequency 550 rpm; do 2.5 mm; pH set point 6.95; DO set point 30%. Trendline (solid line) in both graphs fitted by linear regression to the PERC and shake flask dataset. Dashed line represents line of parity.

Table 4.2. Correlation analysis between the shake flask and PERC data sets and the shake flask and REG plate data sets

Shake Flask : PERC		**Shake Flask : REG**	
Titre Rank	SPR Rank	Titre Rank	SPR Rank
0.84	0.88	-0.11	0.31

These 12 clones were subsequently screened in parallel, once again in shake flasks and μ24 PERC plates, but also the μ24 REG plates. Shake flask data is compared to μ24 PERC data (*solid diamonds*) in Figure 4.6, together with μ24 REG plate data compared to shake flask data (*open squares*). As expected, there is once again a good correlation between the PERC and shake flask data, for either (a) day 15 rank titres, or (b) specific productivity values, as illustrated by the R^2 values in both graphs and the highly positive correlation coefficients displayed in Table 4.2. This data confirms that the small scale μ24 bioreactor system operating with the PERC plates can be used as an early stage cell line selection tool in place of the traditional shake flask platform.

However, when considering the REG plate data there is a significant difference in the ranking of this plate format in comparison to the shake flask, and also therefore the PERC plate, cultures. Both the REG plate titre and SPR correlation coefficients (Table 4.2) are lower and the titre rank correlation is negative between the shake flask and REG plate titre ranking. The fact that there is a greater reduction in the titre correlation titre rather than the SPR ranking indicates that the SPR is less affected by the change in culture conditions, i.e. the presence of a dispersed gas phase, than the titre is. This indicates that the cell growth, and therefore the IVC, is the major factor affected by introducing a dispersed gas phase into the cell culture environment, as opposed to the SPR, or the amount of product made per cell. This data extends previous work to show that not only does the dispersed gas phase impact on cell line performance in the REG plate design it also impacts on clone ranking. This latter observation suggests that different cell clones may respond differently to larger scale bioreactor culture conditions.

The data illustrated in Figure 4.5 is expanded upon in Table 4.3. Here it is clear to see the significant differences in individual clone performance with an obvious correlation between the shake flask and μ24 PERC plate data. Again, the REG plate data generally do not following this same correlation. A further round of clone selection occurred at this stage in order to choose a small number of interesting clones for scale translation studies, as illustrated in Table 4.3; selected clones are shown with an asterisk and highlighted in the table in bold. The reasons for selecting these clones are as follows: BH1 due to the fact that this clone displays a high REG performance with average to poor shake flask and PERC results respectively; BH7, this is the lead clone in any of the cell culture formats; B1 as this exhibits the worst performance in any of the cell culture formats; and L6, in a converse manner to BH1, this clone shows poor REG performance but high PERC and shake flask results. As such a range of clone cell culture characteristics have been selected to test the robustness of the theory and the cell culture system that is being investigated.

Table 4.3. Ranking data for the 12 clones across the three cell culture formats. Experiments performed as described in Figures 4.5 and 4.6. Selected clones shown with an asterisk and highlighted in the table in bold. Selection reasons: BH1 – high REG performance with average to poor shake flask and PERC results; BH7 – high performance in all cell culture formats; B1 – poor performance in all cell culture formats; L6 – poor REG performance but high PERC and shake flask results.

		Shake Flask		REG		PERC	
		Titre Rank	SPR Rank	Titre Rank	SPR Rank	Titre Rank	SPR Rank
BH1*	**1**	**5**	**5**	**2**	**1**	**11**	**4**
BH2	2	8	12	5	8	12	12
BH6	3	2	7	12	12	2	6
BH7*	**4**	**1**	**1**	**1**	**4**	**1**	**1**
BH8	5	10	10	3	7	6	8
B1*	**6**	**12**	**8**	**6**	**10**	**10**	**11**
B4	7	11	11	7	9	7	10
B8	8	7	9	9	6	8	9
L1	9	3	6	3	2	3	3
L2	10	9	4	10	5	9	7
L6*	**11**	**6**	**2**	**11**	**11**	**4**	**2**
L8	12	4	3	8	3	5	5

4.5. Summary

This chapter aimed to establish the microbioreactor as a cell culture platform system. Initial work focussed on optimising the cell culture methodology in order to increase well-to-well consistency (Figure 4.1). Successful application of the μ24 bioreactor was demonstrated for a model cell line in terms of cell growth and productivity kinetics (Figure 4.2; Figure 4.3). Results in the REG plate were also reproducible but showed the impact that a dispersed gas phase can have on cell culture performance (Figure 4.2; Figure 4.3).

A second cell line, expressing a different product, was subsequently tested in order to validate the small scale bioreactor as a platform cell culture system (Figure 4.4). A selection of 12 clones from this second cell line were subsequently screened in the different cell culture systems investigated here. There is good correlation between the PERC and shake flask data (Figure 4.6), illustrating its use as an early stage cell line selection tool in place of the traditional shake flask platform. However, the same clones screened in the REG plate format differ significantly to either the PERC or shake flask cultures (Figure 4.6). This data highlights the fact that the presence of a dispersed gas phase can significantly alter cell culture kinetics; and potentially impact cell line selection. In the following Chapter the scale-up performance of the different cell clones selected in the distinctive microbioreactor plate designs is investigated.

Chapter 5. Scale translation between miniature and scale-down bioreactors: culture kinetics, broth harvesting and product quality

5.1. Introduction and aim

Complex biopharmaceutical products are manufactured at production scale in, generally, large stirred tank bioreactors. At such a scale it is not possible to perform extensive experimental studies; therefore, small scale models of such systems are required. With decreasing scale, less process materials are required and therefore each run becomes cheaper. This allows the throughput to be increased; however, it also becomes more difficult to recreate the engineering environment of the largest scale system. At such scales, fewer analytical methods can be employed, whether this is in terms of online monitoring tools or product quality and downstream processing analysis. Therefore there is an apparent trade off between the degree of information that can be obtained from each run and the number of runs that can be performed in parallel (Doig et al. 2006).

Work performed in Chapter 4 described the use of a 24-well parallel miniature bioreactor system for use as a clone ranking tool in early stage cell line selection. In this chapter, cell culture performance is investigated in order to establish the scalability of miniature bioreactor results (7 mL scale) to bench scale reactors (1.5 L scale), which are themselves scale-down models of pilot scale systems (50 L scale). The engineering characteristics of the different bioreactor formats were previously investigated in Chapter 3. In particular, this work will test the novel aim of this thesis whereby matched

cell culture performance requires comparable engineering parameters and, crucially, the presence of a dispersed gas phase. If successful, such a small scale device would prove invaluable in a process development setting; an accurate and high throughput miniature scale system to explore the process operating space would be ideal as a Quality by Design (QbD) tool; this will be further explored in Chapter 6.

Subsequently, work investigates whether material generated across the different scales exhibit similar Down Stream Processing attributes. Finally, a small scale preparative Protein A purification technique is used to generate material for detailed product quality analysis across the different cell culture scales. This will determine if not only the cell culture kinetics are similar across the systems investigated, but also the product quality attributes which are a critical factor in validating the microbioreactor format as a scale-down tool.

Specific objectives are therefore:

- To evaluate a subset of four clones, investigated in Chapter 4, in each of the miniature bioreactor formats against the standard bench scale STR model.
- To replicate bench scale STR performance in these clones using the miniature bioreactor system with matched engineering parameters and the presence of a dispersed gas phase.
- To implement an Ultra Scale-Down primary recovery technique to evaluate how material generated at different scales compares in terms of Down Stream Processing.
- To analyse mAb product generated across the range of scales for an array of product quality characteristics including aggregate level, non-glycosylated heavy chain content and glycosylation profile.

5.2. Scale translation of µ24 bioreactor cell culture kinetics

The selected four clones (as described in Section 4.4) were subsequently cultured in parallel in the four different cell culture systems: shake flask, µ24 PERC and REG plate formats and 1.5L wv bench scale STRs. Details of the operating conditions for these different formats are described in Section 2.1.2 and are summarised in Table 5.1. The cell culture formats were matched using mixing time as a scaling criterion ($t_m \approx 7s$) as previously suggested by Silk (2014) for culture of GS-CHO cells in miniature and stirred bioreactor formats. Under these conditions all $k_L a$ values were above 10 hr^{-1} (Section 3.2.2 and 3.3.2) and so oxygen transfer would not be considered a limiting regime. Representative data for one of the selected clones (BH1) is presented in Figure 5.1 while data for the other clones is presented in Figures 5.2 to 5.4. In general the µ24 data shows similar performance to that reported previously in Section 4.4. Comparing to the other bioreactor designs, however, there is a clear distinction in the cell culture performance between the shake flask and PERC plate formats (solid lines), and that of the REG plate format and the bench scale STR's (dashed lines). In this case it is evident that the reduced performance in the STR is reflected in the REG plate data. In contrast the shake flask and PERC plate data are well matched. The effect of the dispersed gas phase is reflected on cell growth and productivity which decreased by 24% and 27% (VCD) and equally by 40% and 36% (titre) respectively at their peak values.

This phenomenon has been described previously, whereby the presence of a dispersed gas phase causes cell damage thus diverting energy from cell growth and productivity to cellular repair mechanisms (Heath and Kiss, 2007; Ho et al. 2006). From the data shown here it can be clearly seen that in this case the REG plate format is a much better

indicator of stirred bioreactor performance. Matched mixing time was used as a scaling criterion to ensure that culture composition is homogenous in each case. Due to the fact that the REG and PERC plate formats are identical apart from the presence of this dispersed gas phase, differences in cell culture performance can be directly linked to this individual characteristic.

Identical sets of matched cell cultures in the different culture formats were performed for the further three selected clones (Figures 5.2 to 5.4). A similar picture emerges in that cell growth and antibody production kinetics in the μ24 REG plate format provides the closest match to the larger scale STR data for each of the clones. In particular, this work reveals the issue with using a cell line selection or process development tool that does not closely mimic an STR format. As can be seen in Figures 5.2 and 5.4 (clones BH7 and L6 respectively), there is a significant disparity between the cell culture profiles as seen in the shake flask and PERC plate, as compared with the STR. The μ24 REG plate provides the most comparable small scale cell culture data and therefore the most valuable data.

Table 5.1. Details of cell culture operating conditions for the four different culture formats investigated and associated engineering characteristics. Cell culture performed in these different systems as described in Section 2.2.4.

	Shake Flask	**PERC**	**REG**	**Bench Scale STR**
Shaking / stirring frequency (rpm)	140	650	550	350
Orbital shaking diameter (mm)	25	2.5	2.5	N/A
Fill volume (mL)	50	6.5	6.5	1500
Aeration Strategy	Headspace	Headspace	Dispersed	Dispersed
Constant flow gas	5% CO_2	5% CO_2	N/A	N/A
Constant flow rate (mL min^{-1})	N/A	0.5	N/A	N/A
Oxygen control	N/A	40% O_2	40% O_2	40% O_2
pH control	N/A	20% CO_2	100% CO_2	100% CO_2
Active gas flow limit (mL min^{-1})	N/A	10	0.5	O_2 at 200; CO_2 at 100

N/A Not applicable

(a)

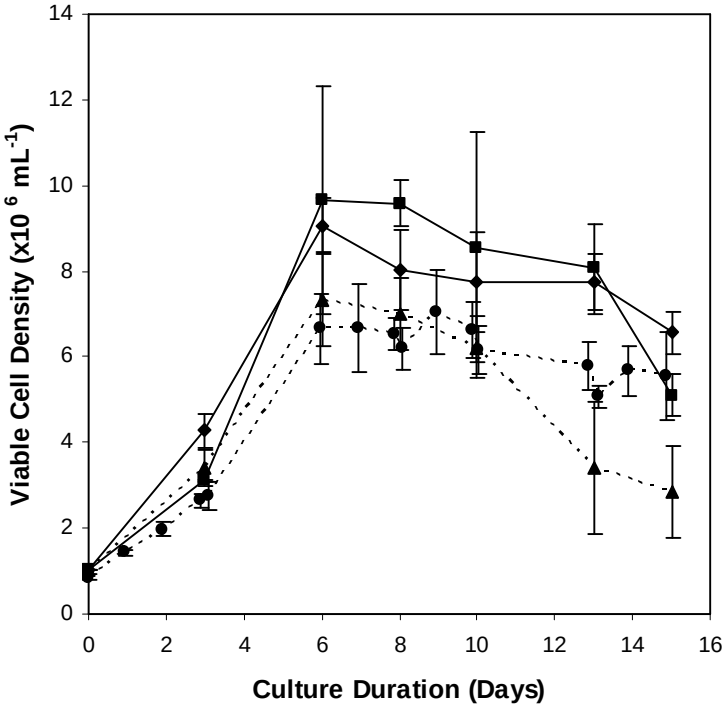

(b)

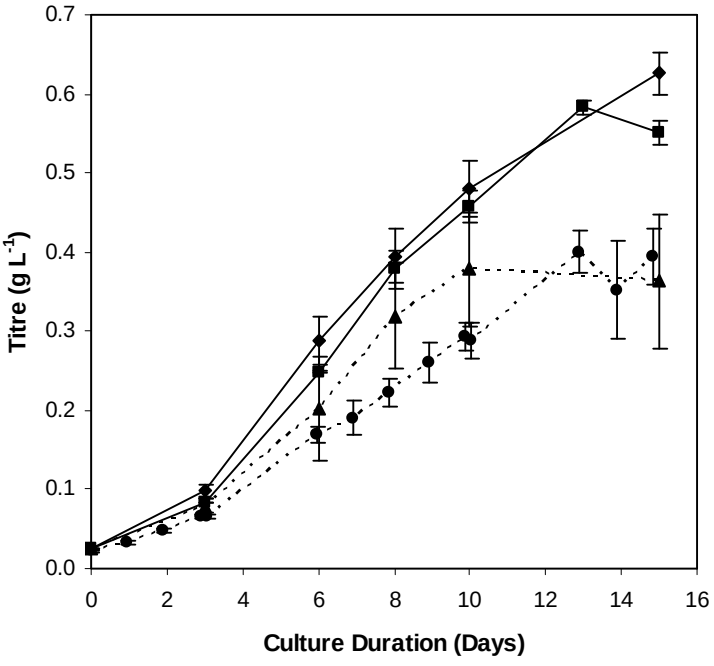

Figure 5.1. Cell culture kinetics for clone BH1 in shake flask (■), PERC (♦) and REG (▲) µ24 plate formats and 1.5L wv bioreactors (●). Cell cultures performed as per Figures 4.5 and 4.6. Bioreactor conditions: single rushton impeller at 350 rpm; horseshoe sparger at 200 mL min^{-1} 40% oxygen/air gassing, 100 mL min^{-1} CO_2; DO set point 30%; pH set point 6.95; temperature set point 35°C. Error bars represent one standard deviation about the mean (n = 6 for µ24 data; n = 3 for shake flask data, n = 3 for bench scale bioreactor data). Solid and dashed lines represent pairs of cell culture formats displaying the most similar performance. Experiments performed as described in Section 2.2.4.

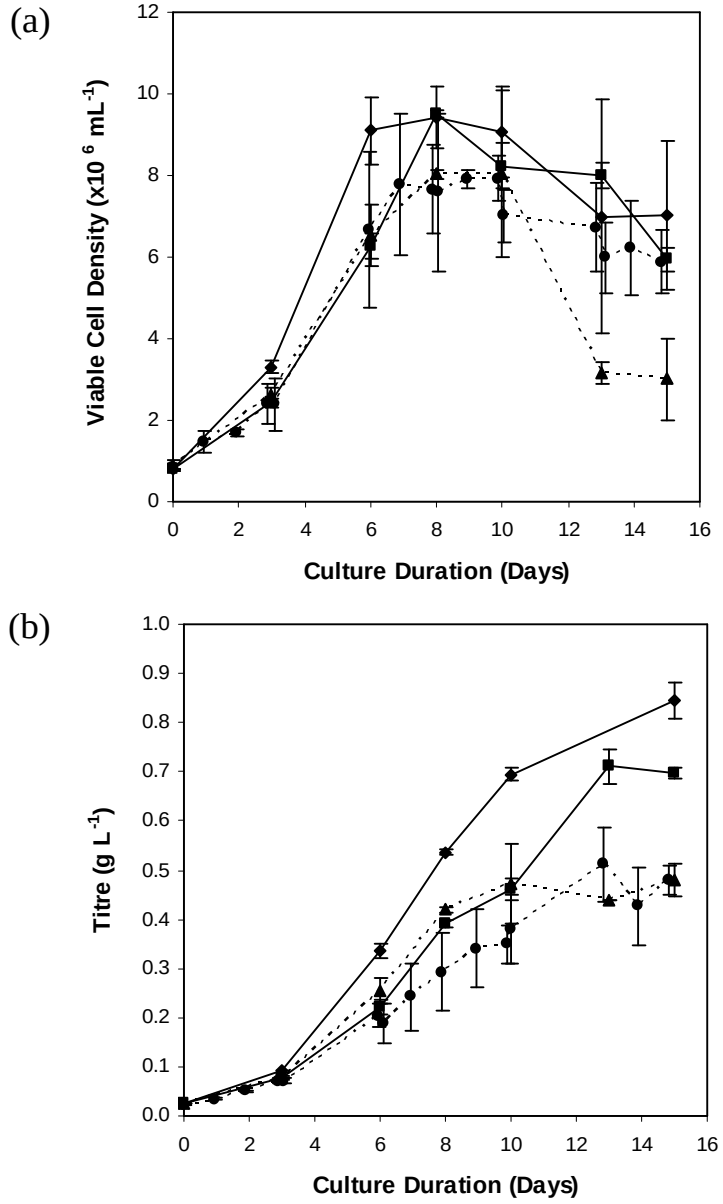

Figure 5.2. Cell culture kinetics for clone BH7 in shake flask (■), PERC (♦) and REG (▲) µ24 plate formats and 1.5L wv bioreactors (●). Cell cultures performed as per Figure 5.1 Error bars represent one standard deviation about the mean (n = 6 for µ24 data; n = 3 for shake flask data, n = 3 for bench scale bioreactor data). Solid and dashed lines represent pairs of cell culture formats displaying the most similar performance. Experiments performed as described in Section 2.2.4.

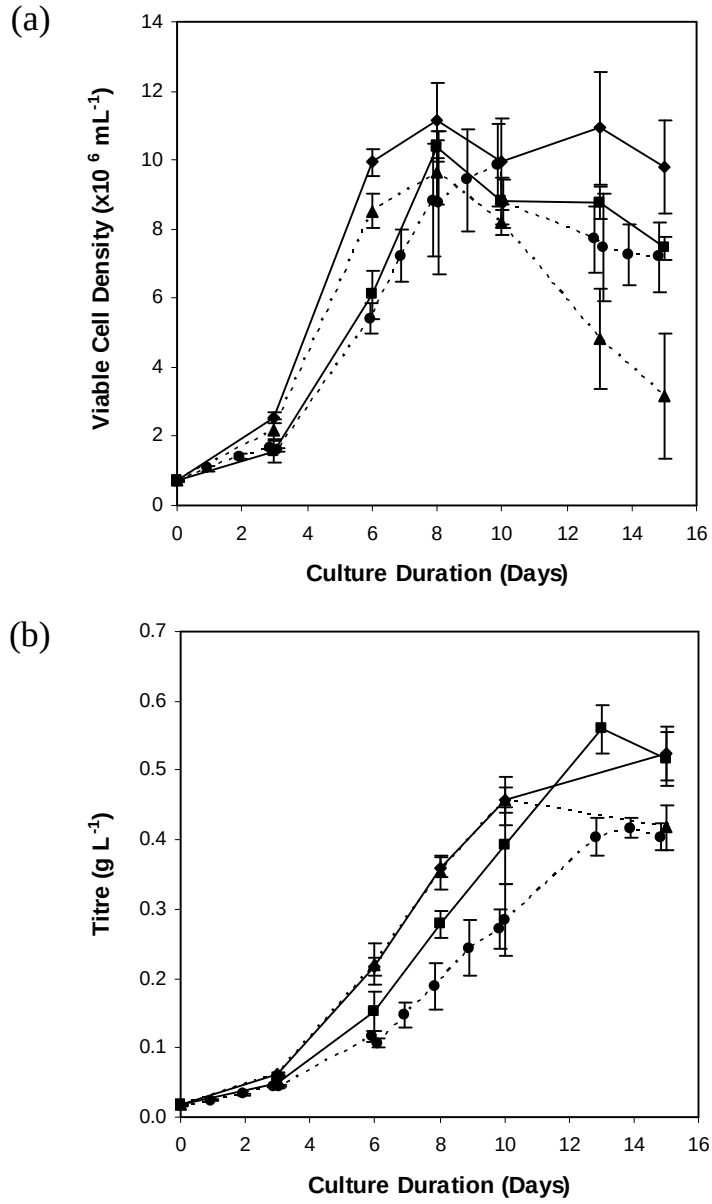

Figure 5.3. Cell culture kinetics for clone B1 in shake flask (■), PERC (♦) and REG (▲) µ24 plate formats and 1.5L wv bioreactors (●). Cell cultures performed as per Figure 5.1 Error bars represent one standard deviation about the mean (n = 6 for µ24 data; n = 3 for shake flask data, n = 3 for bench scale bioreactor data). Solid and dashed lines represent pairs of cell culture formats displaying the most similar performance. Experiments performed as described in Section 2.2.4.

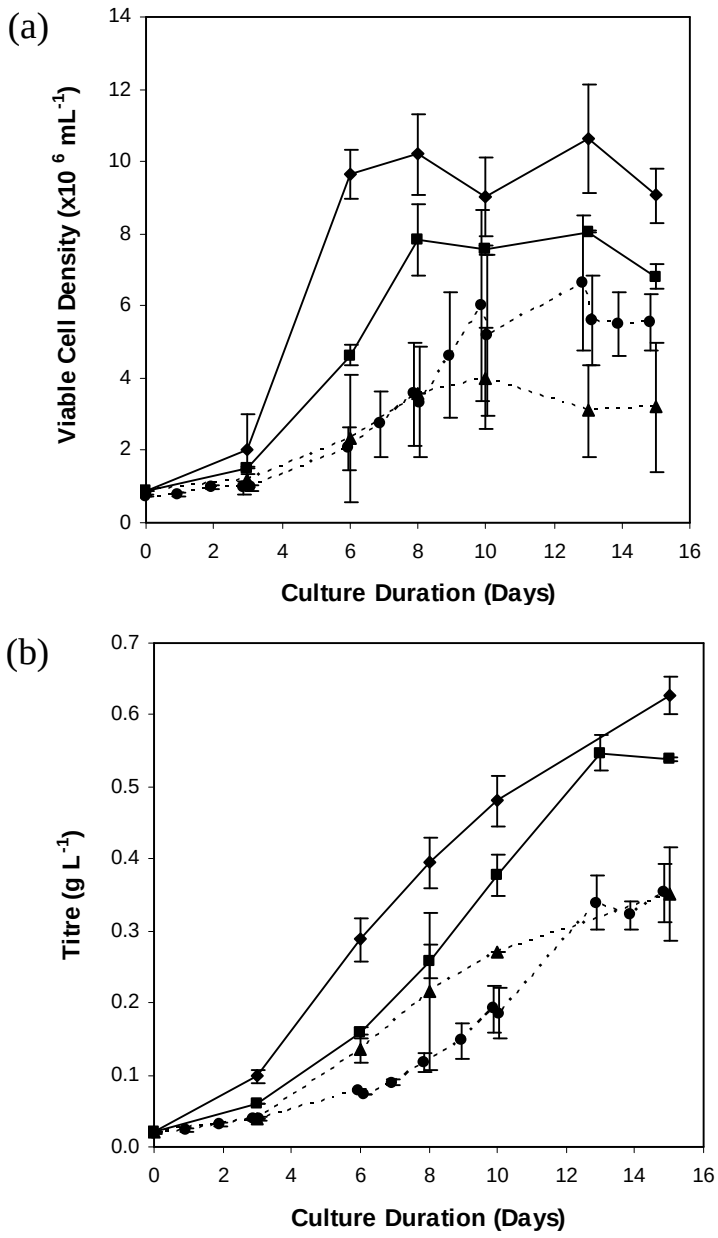

Figure 5.4. Cell culture kinetics for clone L6 in shake flask (■), PERC (♦) and REG (▲) µ24 plate formats and 1.5L wv bioreactors (●). Cell cultures performed as per Figure 5.1 Error bars represent one standard deviation about the mean (n = 6 for µ24 data; n = 3 for shake flask data, n = 3 for bench scale bioreactor data). Solid and dashed lines represent pairs of cell culture formats displaying the most similar performance. Experiments performed as described in Section 2.2.4.

In order to compare the key product titre data for all clones, Figure 5.5 summarises the day 15 titres for the four clones (see Figures 5.1 to 5.4 for full culture profiles). ANOVA analysis (raw data in Appendix F) indicates that there is a statistical difference between each of the cell culture formats for each of the clones. For all four of the clones investigated it is also apparent that the REG plate provides a much better indicator of STR performance than either shake flask or PERC plate formats (see p-values in Figure 5.5 calculated using an unpaired Student's T-test).

This study also indicates an interesting phenomenon with regards to the scalability of specific clones. The logic for the choice of each clone was described in Section 4.4. Briefly, this can be characterised as: BH7, lead clone in all formats; B1, poor clone in all formats; BH1, good performance in the REG plate format but poor performance in the PERC and shake flask formats; and finally L6 behaving in an opposite manner to BH1. As shown in Figure 5.5 and ANOVA data in Appendix F, clone B1 exhibits the smallest difference between PERC/Shake Flask day 15 titres and that of the REG/STR titre. This would imply that this clone is in fact robust, or scalable, in so far as being resistant to the energy dissipation caused by gas bubble bursting (Godoy-Silva et al., 2010), as opposed to, for example, clones L6 and BH7. Along with the ability to use the REG plate format as a better cell line selection tool, or in this case a bioreactor mimic, this type of analysis may be invaluable in terms of rapidly selecting robust, scalable clones that would perform predictably, i.e. with similar growth kinetics and final product titre, when scaling the process to manufacturing scale STR. Conversely, a high ranking clone selected by a shake flask screening process, for example L6, would not necessarily ensure selection of the best clones in terms of STR performance (Figure 5.5).

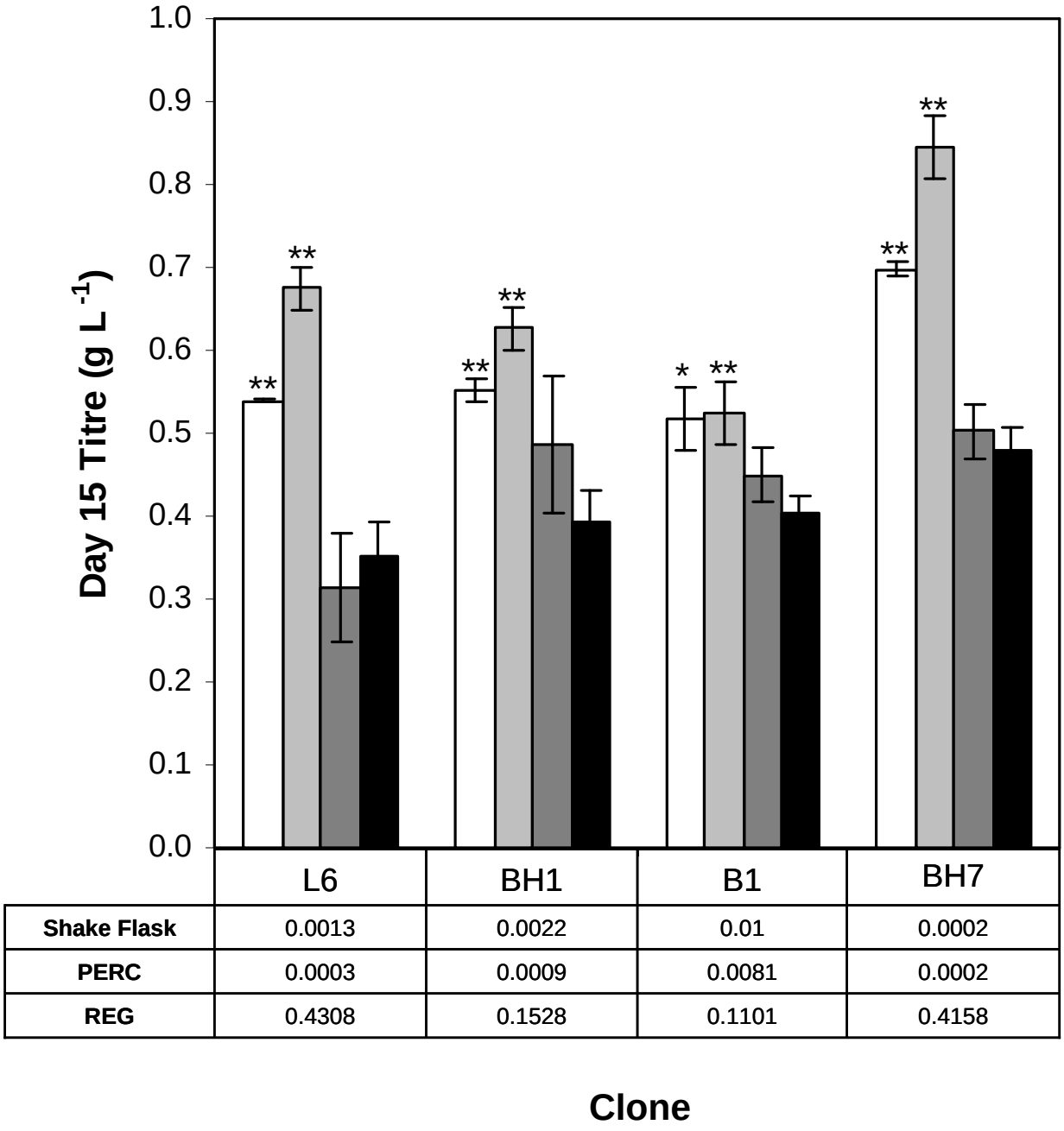

	L6	BH1	B1	BH7
Shake Flask	0.0013	0.0022	0.01	0.0002
PERC	0.0003	0.0009	0.0081	0.0002
REG	0.4308	0.1528	0.1101	0.4158

Figure 5.5. Graph comparing day 15 antibody titre data for the selected four clones across the different cell culture formats for shake flask (*white*), PERC (*light grey*) and REG (*dark grey*) µ24 plate formats and 1.5L wv bioreactors (*black*). Experimental conditions as per Figures 5.1 to 5.4. Error bars represent one standard deviation about the mean (n = 6 for µ24 data; n = 3 for shake flask data, n = 3 for bench scale bioreactor data. p-values for each of the cell culture formats as compared to the STR data are displayed in a table below the chart and are highlighted in the chart as * = $P < 0.05$, ** = $P < 0.01$). Experiments performed as described in Section 2.2.4.

5.3 Scale translation of m24 bioreactor broth harvesting characteristics

In addition to matching cell growth and product formation kinetics in the μ24 REG plate formats and larger scale STR it is important for further scale-down studies that the cell culture broth displays similar physico-chemical properties that might impact on primary product recovery steps.

This work will investigate the downstream processing of cell culture material for the clones used in Section 5.2. Downstream processing, and product recovery, is a crucial factor in the overall biopharmaceutical manufacturing process. For mammalian cell culture processes, filtration is now frequently used for cell removal and primary product recovery as opposed to centrifugation, for example (Liu et al. 2010). Consequently, established Ultra Scale-Down methods for depth filtration processes, as described in Section 2.6, were applied here to examine broth downstream processing characteristics. These have the advantage that they can operate with just 3-5 mL of material and so are compatible in scale with the broth volumes harvested from parallel μ24 cultures. Key process metrics will be filter capacity and the level of solids remaining (Lau et al. 2013).

As the nature of the cell culture broth will directly influence this process step, it would appear important to also investigate this effect in the overall context of cell line selection and process development. Similarly, the nature of the engineering environment, in which the cells are cultured, will greatly affect the cell morphology and therefore influence the ease of processing this material downstream of the cell culture phase. As shown in Figure 5.6, predicted filter capacity appears to be relatively similar

across the cell culture formats (29 ± 7 L m^{-2}). The filter capacity values, whilst lower than might be expected in industry (100 – 175 L m^{-2} (Pegel et al. 2011)), are comparable to values obtained from other small scale studies (24 – 45 L m^{-2} (Lau et al. 2013)). It is evident that the REG and STR systems show similar and lower % solids remaining values compared to the shake flask and PERC formats. The μ24 PERC plate format and shake flask systems exhibit a high degree of similarity with regard to the amount of solids remaining post depth filtration in comparison to both the REG plate format and the STR data. As can be seen in Table 5.2 this trend holds true for all but clone BH7.

These findings mirror the cell culture kinetics described in Section 5.2. Again, it appears that there are pairs of data; the REG and STR exhibit similarly low % solids remaining values as opposed to the relatively high values from the shake flask and PERC data. The low solids remaining values in the case of the REG plate and STR cell culture systems may be as a result of the presence of a dispersed gas phase in the cell culture process. This phenomenon has been reported previously with regard to USD centrifugation (Tait et al. 2009); indicating similar findings where cells that have been exposed to high levels of cell damage during the cell culture phase actually exhibit a more robust cell morphology. In this work, due to gas bubbles in the dispersed gas phase present in the STR and REG plate formats, cells cultured in these systems may be more robust than those from the PERC or shake flask formats. In this scenario, it is feasible that fragile cells may be broken open when filtered, thus allowing a greater degree of solids through the filter into the permeate during the filtration process, as seen in the PERC and shake flask USD depth filtration data (Figure 5.6).

It is clear that the downstream processing of the REG plate samples are much more

comparable to that of the STR than the PERC plate or shake flask samples. This again highlights the fact that it is the presence of the dispersed gas phase that is necessary in order to truly replicate the engineering environment of the STR cell culture format.

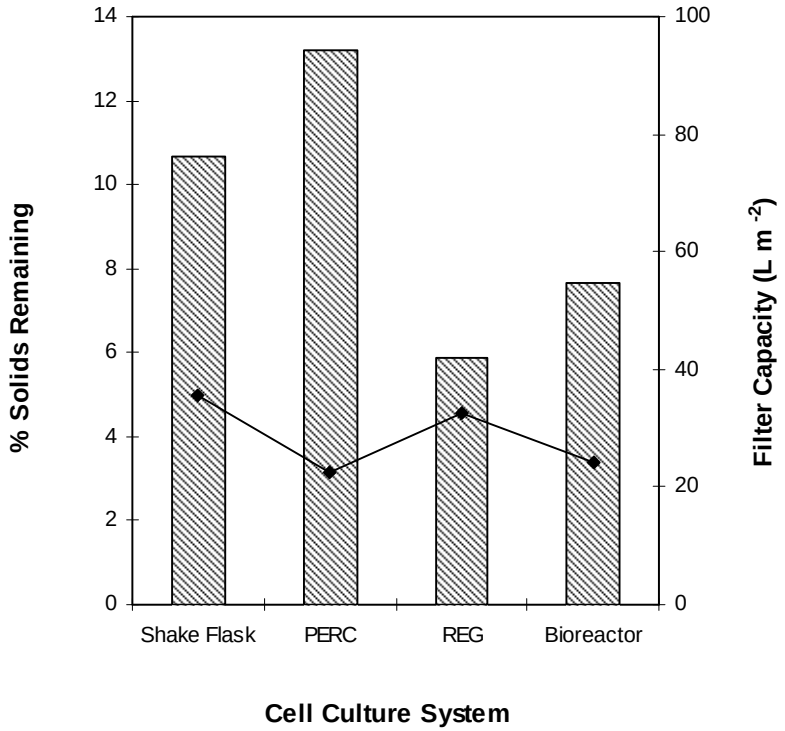

Figure 5.6. USD depth filtration data displaying the percentage of solids remaining (bars) and predicted filter capacity (diamonds) for clone BH1 across the cell culture formats. Experimental conditions: 05SP filters of an effective filter area of 0.28 cm^2 run at 300 mbar, cultures harvested approximately between 50 – 60% viability. Experiments performed as described in Section 2.6.

Table 5.2. USD depth filtration data presenting the percentage of solids remaining and predicted filter capacity for all clones across the cell culture formats. Experiments performed as described in Figure 5.6 and Section 2.6.

Clone	Cell Culture System	% solids remaining	Predicted filter capacity (L m^2)
BH1	Shake Flask	11	36
	PERC	13	22
	REG	6	32
	Bioreactor	8	24
BH7	Shake Flask	4	14
	PERC	9	21
	REG	9	27
	Bioreactor	3	21
B1	Shake Flask	19	51
	PERC	17	36
	REG	2	32
	Bioreactor	11	37
L6	Shake Flask	10	45
	PERC	20	36
	REG	4	32
	Bioreactor	3	35

5.4. Scale translation of m24 bioreactor product quality attributes

A biopharmaceutical product not only needs to display actual therapeutic effect but also product purity, safety and efficacy (Section 1.3). Manufactured commercially, the product needs to be made in consistent batches; differences in product quality can greatly impact on the previously stated factors. Divergent engineering environments will affect cell culture kinetics and in turn alter the ensuing product quality attributes (Hossler et al., 2009); therefore it is imperative to achieve comparable engineering environments across scales of cell culture formats. Such is the importance of optimal and consistent product quality profiles, it has been proposed that quality screening should occur even in early stage cell line selection in addition to typical cell growth and productivity analysis (Walsh and Jefferis, 2006).

Having shown that choice of μ24 cell culture format greatly influences culture performance and predictability of scaled-up performance, it is appealing to also distinguish how product quality attributes vary in the different bioreactor formats. In this work, product quality analysis has been performed on the mAb formed in each of the different cell culture systems to identify any additional effects the engineering environment may have on product formation. To this end, key product quality attributes were determined experimentally as described in Section 2.4.

As shown in Figure 5.7, for clone BH1, overall there is very good comparison in product quality across all the different bioreactor formats and scales of production. The presence of non-glycosylated heavy chain (NGHC) in a drug product may affect the efficacy of the biopharmaceutical (Wong et al. 2012). As can be seen in Figure 5.7 (a)

there is a relatively low level of this attribute across the cell culture formats. In addition, there is not a significant difference in this product quality characteristic between the different formats.

The product glycosylation profile for this IgG1 mAb is shown in Figure 5.7 (b). A legend of typical mAb glycan residues is illustrated in Figure 5.8. One of the key aspects of glycosylation for a mAb is the degree of galactosylation; a ratio of G0, G1 and G2 species with an increasing number of galactose residues. A consistent product glycoform profile is essential due to regulatory requirements (Hossler et al. 2009). Again, as shown in Figure 5.7 (b) there is little difference between the proportions of these fractions. The proportions of G1 and G2 species are highest for the STR system, thus potentially, and as might be expected, this is highlighting that this format can achieve the most uniform and consistent engineering environment, providing the most ideal conditions for cells to incorporate the utmost amount of glacatose residue additions.

Finally, Figure 5.7 (c) illustrates the proportion of monomer, low molecular weight fragments and aggregate species in the samples from the different cell culture formats. Overall there is a high degree of monomer species in the samples, with very little aggregate present. This is most important as aggregate species are most often non-functional and can cause issues with product immunogenicity (Filipe et al. 2012). The most significant result in this work is the presence of a high degree of low molecular weight species in the REG plate sample (Figure 5.7 (c)). Elevated levels of low molecular weight species are also found in REG plate samples for two of the other three clones (Table 5.3). Protein A positive, low molecular weight species occur as a result of mAb product fragmentation. A high degree of low molecular weight species may

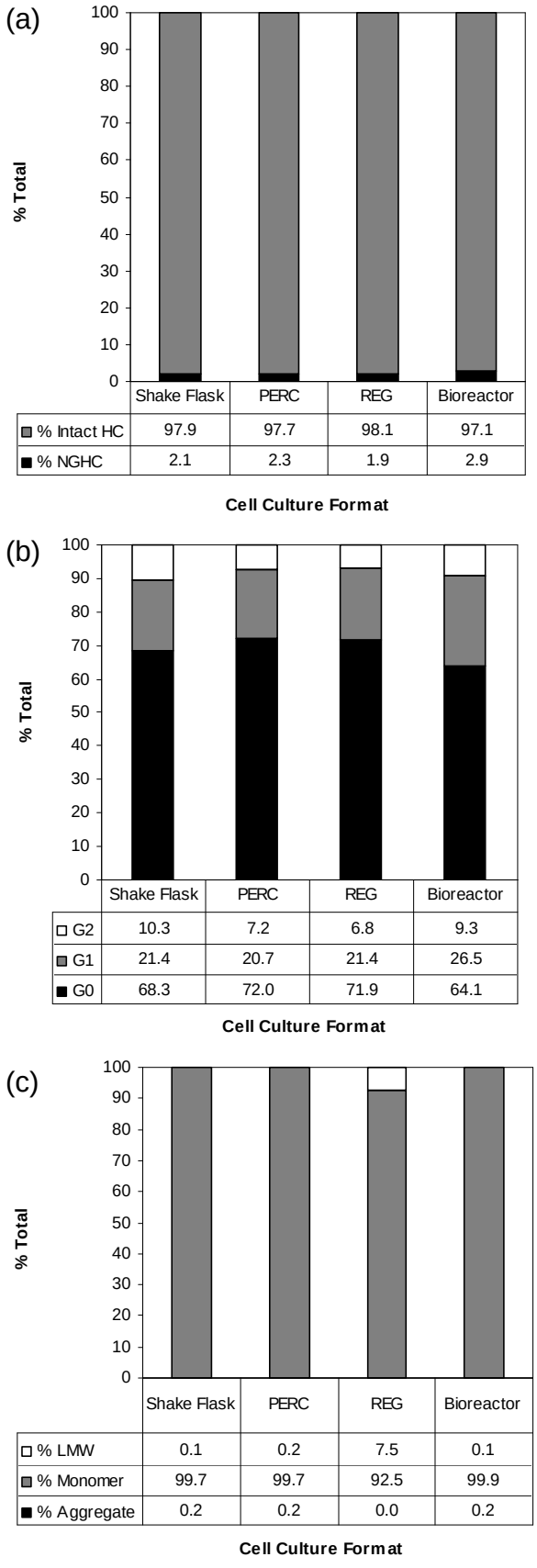

Figure 5.7. Product quality analysis for clone BH1 product generated in Section 5.2 showing (a) non-glycosylated heavy chain content, (b) glycosylation profile and (c) antibody aggregates and fragments. Experiments performed as described in Section 2.4. Product quality attributes measured as described in Section 2.4. Abbreviations: HC: Heavy chain, NGHC: Non-glycosylated heavy chain; G0-G2: ratio of galactose residues; LMW: Low molecular weight species.

indicate a greater presence of protease enzymes in the sample (Janeway et al., 2005). This is an interesting observation which reflects on the cell culture environment in the REG plate format. While the cell culture kinetics illustrated in Figures 5.1 to 5.4 indicate very similar profiles between the REG and STR formats, this observation may point towards subtle differences. Amplified protease levels in the REG plate sample may indicate a greater level of cell death, or more specifically necrotic cell death experienced in this cell culture format, thus leading to the release of proteases into the cell culture broth.

Product quality profiles from all the clones investigated are shown in Table 5.3. The same overall trends can be seen across the other three clones investigated in this work; in general there are very comparable product quality profiles across the different cell culture formats.

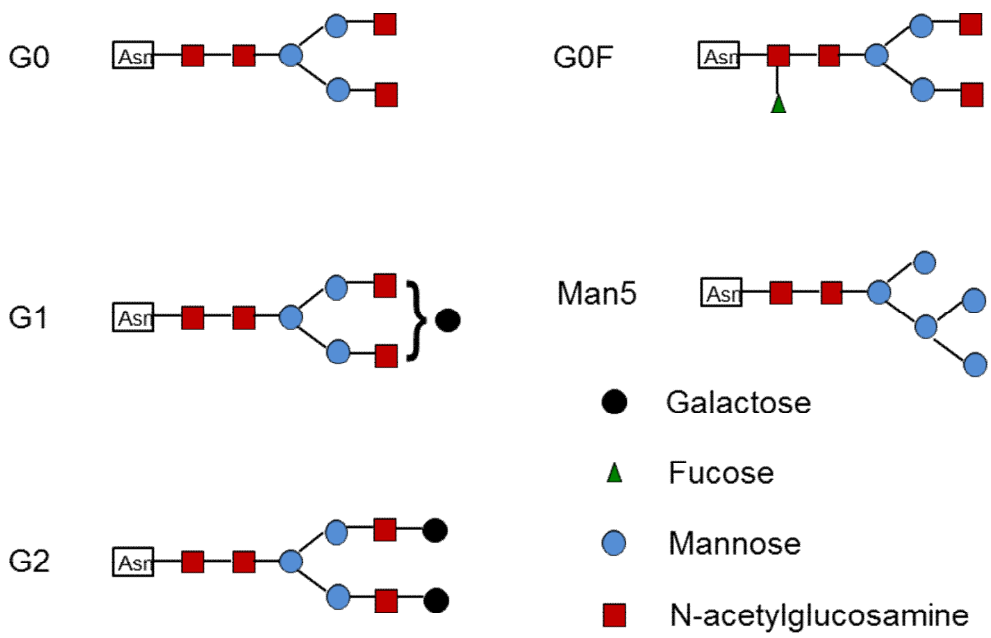

Figure 5.8. Index of typical mAb N-linked glycan residues.

Table 5.3. Product quality analysis summary for material generated in Section 5.2. Experiments performed as described in Section 2.4. Product quality attributes measured as described in Section 2.4.

Clone	Culture Format	Antibody Aggregates/Fragments			Non-glycosylated Heavy Chain		Glycosylation Profile		
		% Aggregate	% Monomer	% LMW	% NGHC	% Intact HC	G0	G1	G2
BH1	Shake Flask	0.2	99.7	0.1	2.1	97.9	68.3	21.4	10.3
	PERC	0.2	99.7	0.2	2.3	97.7	72.0	20.7	7.2
	REG	0.0	92.5	7.5	1.9	98.1	71.9	21.4	6.8
	Bioreactor	0.2	99.9	0.1	2.9	97.1	64.1	26.5	9.3
BH7	Shake Flask	0.2	99.6	0.2	1.2	98.8	74.6	18.7	6.7
	PERC	0.2	99.6	0.2	9.2	90.8	72.7	20.2	7.1
	REG	0.3	99.6	0.1	2.3	97.7	59.8	30.7	9.5
	Bioreactor	0.2	99.7	0.2	4.1	95.9	66.0	24.9	9.0
B1	Shake Flask	0.2	99.6	0.2	1.1	98.9	74.5	18.8	6.7
	PERC	0.0	99.8	0.2	1.2	98.8	71.2	20.8	8.1
	REG	0.2	98.3	1.5	1.0	99.0	72.5	20.5	7.0
	Bioreactor	0.2	99.7	0.2	1.4	98.6	58.3	30.5	11.3
L6	Shake Flask	0.2	99.5	0.3	1.1	98.9	73.1	19.9	7.0
	PERC	0.2	99.6	0.2	1.0	99.0	73.0	19.6	7.3
	REG	1.2	65.1	33.7	2.4	97.6	55.1	32.1	12.8
	Bioreactor	0.2	99.4	0.4	1.4	98.6	66.6	25.0	8.4

5.5. Summary

Work carried out in Chapter 4 demonstrated the use of the miniature bioreactor system as a platform cell line selection tool. In this Chapter, work illustrates the versatility of the miniature bioreactor system by demonstrating its scalability using matched mixing times as a scaling criterion and, critically, using the different plate designs, the fact that the presence of a dispersed gas phase is necessary in order to accurately recreate the bioreactor environment at small scale. This is shown in Figure 5.2 which illustrates that there is a 5 – 24% difference in day 15 titre values between the bioreactor and dispersed gas phase miniature bioreactor format across 4 clones, as opposed to 30 – 92% difference between the bioreactors and headspace sparged miniature bioreactor format.

Subsequently, the quality of the cell culture broth itself is analysed using an Ultra Scale-Down primary recovery depth filtration system. Taking advantage of the small volume required for this technique it was possible to identify how comparable the culture broth is to the bench scale STR system. Whilst there appears to be no significant difference in the estimated filter area required, there is a clear trend in the % solids remaining post filtration. For this attribute, it would appear that the relatively gentle engineering environments in the PERC and shake flask formats yield fragile cells and subsequently large amounts of solids post filtration, conversely, the comparatively harsh environments in the STR and REG plate formats result in more sturdy cells and thus lower levels of solids post filtration.

Finally, work was undertaken to understand the product quality attributes of the expressed product across the different cell culture systems, in particular the non-glycosylated heavy chain content (Figure 5.7 (a)), the glycosylation profile (Figure 5.7 (b)) and the proportion of product aggregates and fragments (Figure 5.7 (c)). Overall there is a high degree of similarity between the different profiles for all the systems. Potentially the most emphatic effect illustrated here is that the host cell line appears to be reasonably robust; despite significant differences in the cell culture kinetics (Figures 5.1 to 5.4; and Figure 5.5) this product quality analysis highlights only slight differences in the expressed Protein A positive product species. There is however an interesting finding in terms of the relative proportion of low molecular weight species present in the REG plate format samples. The next chapter will discuss the overall conclusions that can be made from this thesis and potential directions for future work.

Chapter 6. Conclusions and future work

6.1. Conclusions

The work carried out in this thesis undertakes a detailed engineering characterisation of a miniature bioreactor system which is used to establish a novel methodology for selecting robust cell lines with predictable cell growth and heterologous protein production kinetics in larger scale bioreactors. These were the main aims of this thesis as described in Section 1.11. This thesis demonstrates, for the first time, that a REG plate cell culture format is capable of predicting titre in large scale CHO cultures. Moreover, this is performed for a number of industrially relevant CHO cell clones.

A thorough engineering characterisation of the different cell culture systems was carried out in Chapter 3. The necessity is to first characterise the small and large scale formats to establish a suitable engineering basis on which to scale between the systems. By doing so, greater understanding of the cells growing in the different scales will be achieved thus leading to greater ability to predict how the cells will behave in the large scale culture format and thus improving process scale up and shortening development times. Under typical operating conditions, the existing 1.5 L scale-down STR model was shown to have k_La values >30 hr^{-1} (Figure 3.2; Table 3.3) and mixing times ≤7 s (Figure 3.3; Table 3.4). In the case of the 24-well miniature bioreactor system two different plate designs were investigated; the PERC plate, implementing headspace sparging, and the REG plate, in which gas is sparged directly into the cell culture, thereby generating a dispersed gas phase (Figure 2.1). Here it was shown that the sparged and non-sparged vessels exhibited similar engineering parameters; under typical operating conditions, dynamic mixing times were in the range of 0.8 – 13 s

(Table 3.5) and apparent $k_{LL}a$ values in the range 5 – 50 hr^{-1} (Figure 3.5). Following on from the work carried out by Silk et al. (2010), matched mixing time was used as a scaling criterion for cell culture studies.

Initial cell culture studies (Section 4.2.1.) explored the practical methodologies that were necessary to implement in order to achieve accurate and reproducible cell culture kinetics across the small scale system. Work then investigated the effect of the dispersed gas phase on cell culture kinetics (Section 4.2.4.). In general it was shown that the presence of the dispersed gas phase retarded cell growth, leading to a 38% decrease in IVC (Table 4.1). This decreased growth was associated with a typical 40% decrease in final antibody titre (Figure 4.3).

Crucially, in order to be relevant to industrial applications, a small scale cell culture format, such as the one investigated in this thesis, must be a platform system. As such, work investigated whether the results generated in Section 4.2 using a mAb expressing cell line in a non-chemically defined fed-batch cell culture process could be replicated for a different mAb expressing cell line in a chemically defined fed-batch cell culture process (Figure 4.4). This work illustrates that results are reproducible between such cell lines and processes.

Using this chemically defined process, 24 clonal lines expressing a range of cell culture and productivity characteristics were selected in order to assess the miniature scale bioreactor as a cell line selection tool (Section 4.4). Work undertaken shows how the headspace sparged plate format is able to accurately reproduce the clone ranking effect of a conventional shake flask system, while the direct sparged plate format does not (Figure 4.6). The ‘ideal’ environment offered by the PERC plates appears best suited for

cell line selection studies under precisely controlled suspension culture conditions. Here the small scale of the μ24 format with the PERC plate design offers around a 5-30 fold reduction in scale and approximately a threefold increase in throughput, in terms of laboratory footprint, compared to commonly used shake flask systems.

Chapter 5 investigates how a number of clones from the work undertaken in Section 4.4 perform when scaled up to a bench scale STR format. All systems were scaled using a matched mixing time as a scaling criterion (Section 2.2.5); it is shown that the presence of the dispersed gas phase in the REG plate design makes this format more representative of a laboratory or pilot scale stirred bioreactor (Figures 5.1 to 5.4). The PERC plate design was shown to consistently over predict sparged bioreactor performance, consequently use of this format for cell line selection could lead to identification of non-robust, less scalable cell lines. The REG plate is a valuable culture format for early stage cell culture process development studies and the ranking of clones under process relevant conditions, as is shown for a number of clones investigated in this work (Figure 5.5). In this context, the miniature 24-well format provides approximately a 200 fold reduction in scale and in the perspective of laboratory footprint, approximately a twentyfold increase in throughput as compared to an equivalent number of bench scale STR systems.

Finally, to enable rapid and robust process development pathways, upstream cell line selection and process operating conditions must also be informed by downstream processing studies. However, with small scale upstream technologies, there comes a new challenge in reduced amounts of material for such downstream processing studies. In Section 5.3, work was undertaken to show that it is possible to couple two small scale, high throughput process technologies, one for upstream mammalian cell culture

and the other for primary recovery to generate industrially relevant data for primary recovery purposes in terms of filter sizing and the degree of solids removal. In this case it was demonstrated that the presence of a dispersed gas phase in the cell culture system was necessary in order to reproduce the nature of the cell culture broth for primary recovery studies (Table 5.2). Finally, work was undertaken to investigate how the cell culture format impacts on key product quality characteristics. It is known that changes in the cell culture process can affect product quality of expressed CHO mAb products. However, work carried out in this thesis demonstrates that there is very little change in the product quality attributes with varying cell culture format (Table 5.3). Overall this work has provided novel insights into cell culture performance in miniature bioreactor formats and has established predictive methodologies for identification and scale-up of robust cell lines and cell culture processes. The generic nature of these findings have also been demonstrated on two different cell culture processes establishing the wider applicability of the work and also helping to establish the use of the specific miniature bioreactor platform in 'Quality by Design' driven bioprocess development approaches (this is explored further in Appendix A).

6.2. Future work

The implementation of this work at GlaxoSmithKline demonstrates the industrial application of such small scale, high throughout cell culture systems for the rapid selection of robust and scalable cell lines, ultimately, for biopharmaceutical production at manufacturing scale. However, there are a number of areas where further work could be carried out either to provide more fundamental insights into bioreactor performance or to establish the miniature bioreactor format as an industrial high throughput bioprocess development tool.

In terms of the engineering fundamentals there are a number of areas that might benefit from additional experimental techniques or the application of other approaches. For example, the literature correlations for shaken well formats (Section 3.3) do not necessarily hold true for this plate system due to significant differences in the well geometry, fill volume, typical agitation rates and orbital diameter throw of the shaker platform. As such, it would be most informative to apply a Computational Fluid Dynamics (CFD) approach, as previously used for different shaken well formats (Zhang et al., 2005; Zhang et al., 2008) for this miniature bioreactor system. Experimental mixing time and $k_L a$ values determined in this work could be used to validate the computational model. The model could then be used to determine energy dissipation rates and shear forces within the cell culture system providing additional engineering insights that are not directly measureable. Also, whilst the iodine decolourisation method has been widely used for mixing time determination, alternative methods such as Particle Image Velocimetry (Odeleye et al., 2014) can be employed to accurately determine the mixing throughout a bioreactor system. This would help to understand the fundamental fluid dynamics of the small scale system and could help to highlight any significant differences between the two plate formats.

As discussed in Section 4.2.4. two assumptions are made as to why shake flask titre values are as high as the PERC plate data, which represents the ‘ideal’ culture conditions. To test the first of these theories, that shake flask cell viability decreases towards the end of the culture, thus allowing the release of antibody fragments, mass spectrometry or SEC could be used to identify such species. Similarly, the second assumption, that the pH drifts in a shake flask, could be tested with a standard pH probe

in a modified shake flask vessel. If the pH profile was captured, this could be replicated in a pH controlled system to determine if such a pH profile increases cell productivity.

In a similar vein, a more thorough theoretical or experimentally verified understanding of how gas-liquid interfaces interact with cells would be beneficial. Gas bubbles are believed to interact with cells in a number of ways; for example, as a dispersed gas phase within the cell culture system, as a foam layer on the cell culture surface and at the point when bubbles disengage at the liquid-air interface. Investigation of these phenomena on a fundamental level would help to distinguish the most important of these factors and as such this element could be independently introduced to a small scale bioreactor system to increase the comparability of data generated with larger scale STR formats.

In terms of establishing the industrial adoption of the miniature bioreactor system it would also be necessary to explore operation in a more high throughput manner since, at present, the methodology is practically still a large burden in terms of operator workload. It would therefore be interesting to explore options for automation as this would reduce the workload for the operator whilst also improving liquid handling accuracy and reducing the chance for contamination.

As discussed in Section 5.4, the cell line used appears to be fairly robust in terms of the product quality profile of the expressed product across the different scales. Thus, whilst there is a large range of engineering environments in the different cell culture systems, there are only fairly limited product quality differences. In this context it would be more interesting to use a less robust cell line/product to see if any changes to the engineering environment changes are reflected in the cellular product assembly and processing.

Building on the scale-up results here, obtained under a single set of process conditions, it would also be necessary to explore whether comparable performance is achieved over a wider area of process design space. As such, the miniature bioreactor system examined in this thesis would provide an excellent cell culture tool in a Quality by Design setting implementing a Design of Experiments style approach to explore the process space. This type of application would require further work in order to understand whether the miniature bioreactor system maintains it's accuracy in replicating bench scale STR data when at the limits of the process design space.

Finally, following on from this type of application, it would be industrially valuable to construct a full small scale process mimic. Work undertaken in this thesis demonstrated coupling the small scale cell culture system to a USD primary recovery technique in order to assess processing of the cell culture material generated from the different cell culture systems. Future work might include using this USD tool in a preparative manner, generating material for a second filtration step, or proceeding directly to, for example, a preparative, small scale, chromatography step, which was itself also implemented in this thesis (Section 2.4.1). By combining such technologies alongside automated liquid handling systems, complete process pathways can be mapped out at small scale to provide whole bioprocessing data. As a QbD tool in this manner, this would generate a greater degree of knowledge earlier in the process development pathway such that, for example, clones could be selected not only on cell culture performance but also in a more holistic approach, accounting for any issues that might be discovered from such primary recovery, and further downstream, small scale studies.

Appendix A. Industrial implementation and economic comparison of the miniature bioreactor system as a cell line selection tool or bioreactor mimic[‡]

A.1. Introduction and aim

As discussed in Chapters 4 and 5, it has been shown that the small scale bioreactor platform investigated in this work has potential applications both as a cell line selection tool but also a scale-down bioreactor mimic, dependent on the plate type used. However, such applications will not be realised unless there is an economic driver for the relevant company to adopt such technologies. There will be an obvious degree of inertia in replacing existing technologies that are tried and tested due to the fact that any delays in the process development pathway will have a major impact on the commercial viability of the product in question.

The aim of this chapter is to explore the industrial implementation and economic feasibility of adopting this technology as either a cell line selection tool (during cell line development) or as a scale-down bioreactor mimic (during cell culture process development). Specific objectives are:

- To investigate how this miniature bioreactor system might fit into a traditional cell line selection/cell culture process development pathway.

[‡] This Chapter is included as part of the UCL requirements for award of the EngD in Bioprocess Engineering Leadership

- To examine the economic viability of implementing a small scale cell culture tool to replace traditional bench scale bioreactor systems.
- To explore the use of a small scale, high throughput system within a ‘Quality by Design’ context.

A.2. Practical implementation analysis

Figure A.1. illustrates a typical process flow diagram for a standard mammalian cell culture process for the manufacture of a biopharmaceutical product. Typically, transfection of the host cell line is followed by an initial cell culture period before single cell sorting. Single cells, or clones, are then typically cultured in static microwell plates. Rounds of cell line selection then occur with only the highest producing lines being transferred onto the next cell culture format.

As is shown in Figure A.1., the majority of bioreactor formats used for cell growth during cell line selection differ significantly from that of the final cell culture format for product manufacture. Therefore, the clones that perform well at the initial cell line selection phases may not necessarily be the ‘best’ clones from the entire pool of available cells. As illustrated in Chapters 4 and 5, there is an opportunity to introduce the small scale bioreactor format, investigated in this thesis, much earlier in the process development process in order to help ensure that robust and scalable clones are actually being selected.

At the shaken microwell stage there is an opportunity to utilise the PERC plate format as this would enable cells to be selected under more precisely controlled culture

conditions than in conventional microwell plates. However, there are still a vast number of clones that need to be screened at this point. Therefore, economically, the PERC system may not be feasible both in terms of consumables costs (PERC plates are over 100 times more expensive than a conventional microwell plate), but also in terms of capital costs for the number of base units required. Subsequent to this, the PERC plate format is well suited (as demonstrated in Section 4.4) to replace the shake flasks stage of the process because of the more realistic numbers involved. Alternatively, the REG plate system may be suited to utilisation at this stage in order to provide a more realistic screening method, selecting the most robust and scalable cell lines. (Section 4.4) Most companies will have small scale STR's as validated scale-down models of their production processes; the REG plate is ideal to be implemented alongside these systems. In this manner the REG plate can be used to perform high throughput experimentation, reducing the burden on the STR format and reducing the number of experiments that are required at the larger scale.

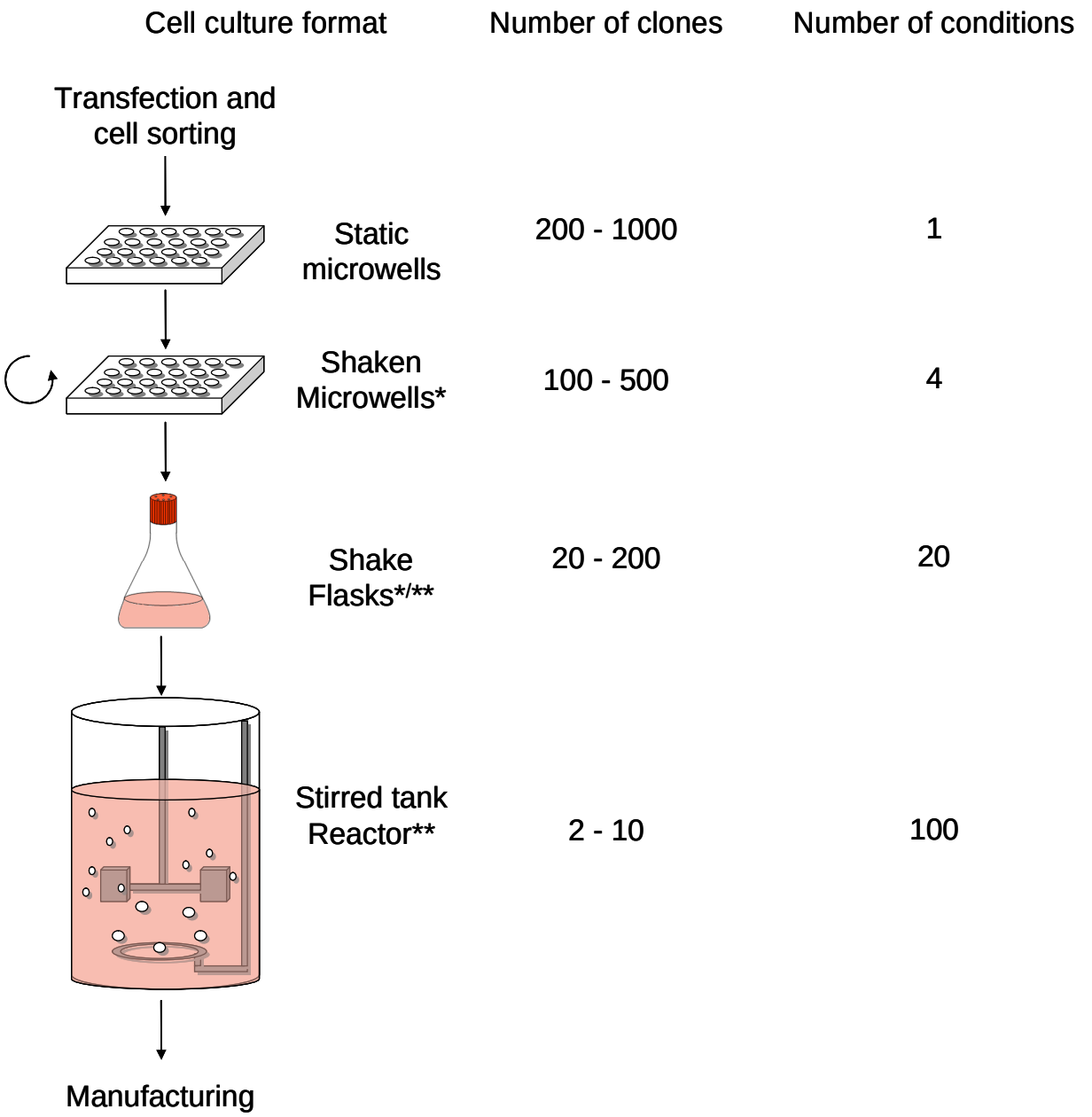

Figure A.1. Typical process flow diagram for a mammalian cell culture biopharmaceutical product. * represents where the PERC μ24 may be implemented and similarly ** represents potential implementation of the REG μ24 bioreactor format.

A.3. Economic feasibility analysis

No matter the practical utility of a process development tool, like the commercially available μ24 system, there must also be a clear economic incentive in order for companies to adopt the technology in practice. Table A.1. presents results from a preliminary economic model to help guide decision making. Data is normalised relative

to a bench scale bioreactor values. Raw data, assumptions and factors not included in the model are included in Appendix B.

In this analysis there is a clear decrease in cost per experiment from right to left, i.e. with decreasing culture volume. This trend is due to the relatively high price for media which dominates the costing side of the model. The small scale systems are all single use, thus they also have lower labour costs in terms of turning the cell culture format around and prepping for a next experiment. Importantly they also do not have associated CIP/SIP costs. The combination of these two factors results in significantly lower experimental costs for the small scale systems.

In order to compare absolute experimental costs across cell culture formats, two scoring parameters are introduced; information content and format utility. In the case of information content, this is based upon the percentage difference in average day 15 titre for the four clones investigated in Section 5.2 as compared to the bench scale STR. This actual experimental data is used to quantify how accurately each of these systems can predict cell culture performance; relative to the bench scale STR. Information content scoring values for the microwell format and the pilot and manufacturing scale STRs are assumed. A low information content value for the microwell format is a result of significant differences to the engineering environment of the bench scale STR and small culture volumes which reduces the amount of online and offline analysis that can be performed. Conversely, successively high values for the pilot and manufacturing scale STRs is a consequence of the fact that these systems will include full process instrumentation and automation as well as the fact that at a larger volume there will be

further opportunity to perform process relevant DSP studies or toxicology studies, for example.

The second scoring parameter, format utility, attempts to reflect the flexibility of the cell culture system. All values are assumed in this case. The small culture volume in the microwell system necessitates sacrificial sampling, or end point sampling, thus reducing format flexibility. Microwell and shake flask systems are penalised as they have no online process monitoring or control capabilities, which therefore limits these systems to experimentation at a limited range of process parameters, a single temperature set point, for example. All the small scale systems are penalised due to the fact that they are not automated in any way, thus reducing the complexity of experimentation that can be performed. The larger scale STR formats have an advantage in this criterion in that they will have a greater degree of instrumentation and process control, therefore increasing the utility of the system.

Scoring parameters are combined to exaggerate the requirement of having an accurate, yet functional bioreactor system. Absolute and relative cost per experiment values can be generated (described in Appendix Table B.1.). Accounting for data value and system flexibility, as described above, the REG plate miniature bioreactor system is highlighted as an economically viable alternative to a bench scale bioreactor system; used in a high throughput manner this system could reduce the number of experiments required at the bench scale (Table A.1.). This type of analysis also highlights that a shake flask system, might in principle at least, return valuable experimental data for less expenditure than the PERC plate miniature bioreactor system. This is particularly interesting and again highlights the need to effectively balance data value alongside economic burden.

Table A.1. Economic comparison of typical cell culture formats in mammalian cell culture process development.

Factor	Cell culture format						
	Microwell	**Shake Flask**	**PERC**	**REG**	**Bench scale STR**	**Pilot scale STR**	**Manufacturing scale STR**
Throughput	24	1	24	24	1	1	1
Throughput (per unit capital)	30	24	1	1	1	1	1
Total number of runs possible per year	23	23	23	23	18	18	15
Total number of experiments possible per year	16,560	552	552	552	18	18	15
Capital costs (per experiment) (£)	0.06	1.8	13	13	97	1,541	19,334
Consumables costs (per experiment) (£)	0.12	9.1	10	10	87	8,700	435,000
Turn around cost (per experiment) (£)	14	14	29	29	58	175	3,260
Labour cost (per experiment) (£)	101	101	202	202	404	808	1,212
Total cost (per experiment) (£)	**116**	**126**	**253**	**253**	**646**	**11,224**	**458,805**
Information content score*	*0.06*	*0.58*	*0.36*	*0.93*	*1*	*4*	*10*
No. of runs to be confident in data*	18	2	3	2	1	1	1
Format utility score*	0.10	0.25	0.50	0.50	1	2	4
Absolute cost factoring in scores (per experiment) (£)	19,825	867	1,414	545	646	1,403	11,470
Relative cost factoring in scores (per experiment) (£)*	**30.67**	**1.34**	**2.19**	**0.84**	**1**	**2.17**	**17.75**

*Relative to bench scale STR

A.4. Utility as a 'Quality by Design' tool

Whilst one of the primary aims of this thesis was to evaluate a small scale system for use as a tool in the rapid selection of robust and scalable cell lines (Section 1.11) it is interesting to also explore the option of using this device in a 'Quality by Design' driven, bioprocess development scenario (Section 5.1; Section 6.2). Given the fact that the miniature bioreactor, using mixing times as a scaling criterion and implementing a dispersed gas phase, accurately replicates cell culture kinetics, broth harvesting and product quality performance of the bench scale STR format (Chapter 5), the small scale system could in the future be utilised for process design space exploration. Due to the online monitoring and control capabilities, the high throughput nature of the format and the ability to integrate with DSP unit operations (Section 5.3) the miniature bioreactor system would be ideal, as a platform technology, by which to investigate process operating ranges within a QbD approach.

One of the major validation issues faced in a process design/optimisation scenario is that of experimental consistency. As a living organism is used to generate the biopharmaceutical product, there will be an inherent degree of variability in the process. Cell culture processes make use of monitoring and control systems in order to maintain the experiment within set critical process parameters that are designed to manufacture a product to set critical quality attributes; which are typically regarded as the cell growth and viability, expressed product titre, product quality (e.g. charge heterogeneity; correctly assembled or folded forms; non-aggregated/truncated forms and correctly glycosylated forms) and process impurity levels (e.g. amount of product aggregates formed in the processing; levels of host cell protein or DNA within the final product

form). To this extent, a significant validation issue lies in creating and maintaining a process such that it produces consistent batches of material of the desired critical quality attributes; thus process control and sensitivity is critical.

With regard to process validation, there is a move towards developing manufacturing processes that are based upon a Quality by Design foundation. As such, rather than having strict, and sometimes arbitrary, process control limits, temperature must be controlled to 37°C ± 1°C, for example, a Quality by Design developed process will have explored the process design space in order to gain better process/product understanding and thus build a set of operating conditions that may have greater degrees of tolerance (Shimoni et al, 2014). Thus even if an individual parameter moves outside of a set limit, this could be mitigated by a second parameter which remains within its own limit. Poor process/product understanding can lead to a lack of control, low productivity/product quality and failed manufacturing batches.

Use of a small scale, high throughput bioreactor model will enable the rapid evaluation of the process design space. Integrating this alongside small scale DSP unit operations, for example, will add further value to the exercise. As a QbD tool in this manner, this would generate a greater degree of process/product knowledge earlier in the process development pathway, thus reducing product development timelines and yielding more robust manufacturing processes in the long term (Shimoni et al, 2014; Tescione et al, 2014).

A.5. Summary

The aim of this chapter was to explore the practical and economic feasibility of integrating the miniature bioreactor system examined in this thesis into a traditional process development pathway and to investigate further use of this system in a Quality by Design format.

Figure A.1. illustrates a standard process development pathway and highlights the position that either the PERC or REG plate small scale bioreactor format may integrate into these screening stages. As highlighted, there is an opportunity to replace up to three elements of a traditional process with the miniature scale bioreactor system. As discussed in Section 4.4, cell line ranking differs significantly between the REG plate system and either the PERC plate format or a shake flask culture. The ability to select for robust and scalable cell lines, as demonstrated in Section 5.2, early in the cell culture process development pathway, is a unique ability of the miniature bioreactor system implementing a dispersed gas phase. As such it may be advantageous to perform industrial cell line screening using the REG plate miniature bioreactor format.

A preliminary economic analysis of typical cell culture formats used in cell culture process development was undertaken in Section A.3. Weighted experimental costs, relative to a bench scale STR system, indicated that the REG plate format was economically viable as a small scale cell culture model, which could reduce the number of experiments required at the bench scale (Table A.1.). Crucially, the model also revealed that the PERC plate system might generate relative bench scale STR data at almost double the financial burden as compared to the shake flask format.

Finally, Section A.4 investigated the concept of using a small scale cell culture format in a QbD scenario. Due to the comparable bench scale STR data, and the high throughput nature of the format, the system would be ideal to rapidly explore process design space. In this manner, product development timelines could be reduced as greater process/product knowledge could be gained early on in the product development pathway, and ultimately, more robust manufacturing processes could be designed.

Appendix B.

B.1. Economic model calculations

Factor	Calculation
Throughput	Culture format throughput
Throughput (per unit capital)	Number of systems that can be used in parallel per unit captial
Total number of batches possible per year	Number of working weeks per year/Experiment duration
Total number of experiments possible per year	Total number of batches possible per year*Throughput (per unit capital)
Capital costs (per experiment) (£)	(Capital cost/10)/Total number of experiments possible per year
Consumables costs (per experiment) (£)	Sum of all consumables
Turn around cost (per experiment) (£)	CIP/SIP costs (if applicable) plus associated labour hours
Labour cost (per experiment) (£)	Time per day*Experiment Duration
Total cost (per experiment) (£)	Sum capital, consumable, turn around and labour costs
Information content weighting	% difference in average day 15 titre (Section 5.2) relative to bench scale STR
Format utility	Assumed as described in Section A.I.3.
Weighted absolute cost (per experiment) (£)	Total cost/(Information content weighting*Format Utility)
Weighted relative cost (per experiment) (£)	Weighted absolute cost/Weighted absolute cost for the bench scale STR

Exponential 6/10 rule used to calculate capital costs with scale:
For example:
2 L STR = £17,500
200 L STR = $(200/2)^{0.6}$ × £17,500

B.2. Economic model raw data and assumptions

Data:

Capital Costs

System	Volume (L)	Costing	Total (£)
µ24	N/A	Quote	69995
Bench scale STR	2	Quote	17,500
Pilot scale STR	200	Exponential 6/10 rule	277,356
Manufacturing scale STR	10,000	Exponential 6/10 rule	2,900,147
Microwell/shake flask incubator	N/A	Quote	10,187

Consumables Costs

Item	Costing	Total (£)
Shake flask (50)	Quote	163.2
SRW microwell (100)	Quote	180
µ24 plate (6)	Quote	1170
µ24 caps (6)	Quote	156
Media (1 L CD-CHO)	Quote	58

Assumptions:

Throughput (per unit capital)
30 microwell plates per incubator (5 across, 2 deep, 3 tall)
24 shake flasks per incubator (8 across by 3 deep)

Total number of batches possible per year
Each experiment is 2 weeks
46 working weeks per year
0.5 week turnaround for bench/pilot scale STR; 1 week turnaround for manufacturing scale STR

Capital costs (per experiment) (£)
All equipment lasts 10 years and depreciation is linear per year

Turn around cost (per experiment) (£)
CIP/SIP for STR systems, assume £0.2/L

Labour costs
Assumes a wage of £30,000 p.a.

Labour cost (hour units)	**Cell Culture Format**						
Turnaround cost	**Microwell**	**Shake Flask**	**PERC**	**REG**	**Bench scale STR**	**Pilot scale STR**	**Manufacturing scale STR**
CIP					1	2	6
SIP					1	2	6
Prep	1	1	2	2	2	4	6
Total	*1*	*1*	*2*	*2*	*4*	*8*	*18*
Experiment cost	**Microwell**	**Shake Flask**	**PERC**	**REG**	**Bench scale STR**	**Pilot scale STR**	**Manufacturing scale STR**
Time per day	0.5	0.5	1	1	2	4	6
Total (per experiment)	*7*	*7*	*14*	*14*	*28*	*56*	*84*

Model does not consider:

- Installation costs
- Equipment maintenance costs
- Disposal of single use systems, disposal of contaminated waste streams
- Utilities
- Laboratory footprint and cost

Appendix C.

Table C.1. Global pharmaceutical industry sales (2001-2008) (IMS Health Market Prognosis).

Year	**2001**	**2002**	**2003**	**2004**	**2005**	**2006**	**2007**	**2008**
Total World Market (Current US$ in Billions)	393	429	499	560	605	648	715	773
Growth Over Previous Year ($Constant US$ Growth (%))	11.8	9.2	10.2	7.9	7.2	6.8	6.6	4.8

Appendix D.

Table D.1. Scrip's Pharmaceutical Company League Tables (2009)

Company	Total World Market Sales (US$ Millions)	R&D Expenditure (US$ Millions)	R&D Expenditure as a Percentage of Total Sales (%)
Pfizer	44174.00	7945.00	18.0
Roche	33315.71	7322.58	22.0
GlaxoSmithKline	37810.42	6828.92	18.1
Sanofi-Aventis	40561.90	6731.38	16.6
Novartis	33888.00	6383.00	18.8
AstraZeneca	31601.00	5179.00	16.4
Johnson & Johnson	24567.00	5095.00	20.7
Merck & Co	23619.90	4805.30	20.3
Takeda	14050.20	4394.55	31.3
Eli Lilly	19284.70	3840.90	19.9

Appendix E.

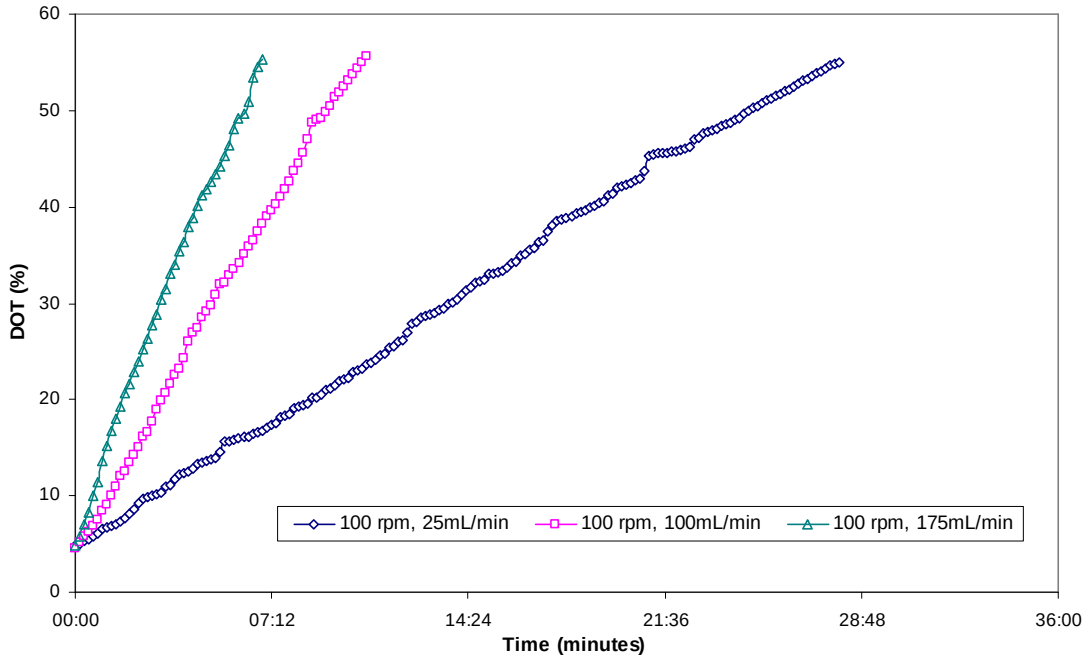

Figure E.1. Example DOT data from gassing out experiments as a function of aeration rate. $k_L a$ was determined using the static gassing out method described in Section 2.1.5.

Appendix F.

Table F.1. Raw ANOVA data used in Section 5.2.**L6**	SS	df	MS	F	P
Between:	0.453	3	0.151	73.771	1E-08
Within:	0.029	14	0.002		
Total:	0.481	17			
BH1	SS	df	MS	F	p
Between:	0.124	3	0.041	13.841	0.00018
Within:	0.042	14	0.003		
Total:	0.166	17			
B1	SS	df	MS	F	p
Between:	0.039	3	0.013	11.106	0.000537
Within:	0.016	14	0.001		
Total:	0.055	17			
BH7	SS	df	MS	F	p
Between:	0.454	3	0.151	145.575	0.0
Within:	0.015	14	0.001		
Total:	0.468	17			

References

Al-Rubeai, M., Oh, S. K. W., Musaheb, R. and Emery, A. N. (1990) Modified cellular metabolism in hybridomas subjected to hydrodynamic and other stresses. *Biotechnology Letters*, **12**, 323 – 328.

Amanullah, A., Buckland, B. and Nienow, A. (2004) In: Paul, E. L., Atiemo-Obeng, V. A. and Kresta, S. M. (ed.) Handbook of industrial mixing: Science and Practice. John Wiley and Sons.

Bailey, J. and Ollis, D. (1986) Biochemical engineering fundamentals. 2nd edition. McGraw Hill.

Barrett, T. (2008) Microwell Evaluation of Mammalian Cell Lines for Large Scale Culture. PhD Thesis, University College London.

Barrett, T., Wu, A., Zhang, H., Levy, S. and Lye, G. (2010) Microwell engineering characterization for mammalian cell culture process development. *Biotechnology and Bioengineering*, **105**, 2, 260 – 275.

Beckman Coulter website[1] (ViCell). Last accessed 12/02/13.

Betts, J. I. and Baganz, F. (2006) Miniature bioreactors: current practices and future opportunities. *Microbial Cell Factories*, **5**, 21, 1 – 14.

Betts, J. I., Doig, S. D. and Baganz, F. (2005) The characterisation and application of a novel miniature stirred bioreactor for the scale-down of industrially-relevant microbial fermentations. In Biochemical Engineering XIV: Frontiers and Advances in Biotechnology, Biological and Biomolecular Engineering British Columbia, Canada.

Betts, J. P. J., Warr, S. R. C., Finka, G. B., Uden, M., Town, M., Janda, J. M., Baganz,

[1] http://www.beckmancoulter.com/products/instrument/partChar/pc_vicell.asp

F. and Lye, G. J. (2014) Impact of aeration strategies on fed-batch cell culture kinetics in a single-use 24-well miniature bioreactor. *Biochemical Engineering Journal*, **82**, 105 – 116.

Birch, J. R. (1999). Suspension culture, animal cells. In: Flickinger, M. C., Drew, S. W. (ed.) Encyclopedia of Bioprocess Technology - Fermentation, Biocatalysis, and Bioseparation. John Wiley & Sons.

Birch, J. and Racher, A. (2006) Antibody production. *Advanced Drug Delivery Reviews*, **58**, 671 – 685.

Boychyn, M. Yim, S., Shamlou, P., Bulmer, M., More, J. and Hoare, M. (2001) Characterization of flow intensity in continuous centrifuges for the development of laboratory mimics. *Chemical Engineering Science*, **56**, 16, 4759 – 4770.

Brekke, O. and Sandlie, I. (2003) Therapeutic antibodies for human diseases at the dawn of the twenty-first century. *Nature Reviews Drug Discovery*, **2**, 52 – 62.

Büchs, J., Lotter, S. and Milbradt, C. (2001) Out-of-phase operating conditions, a hitherto unknown phenomenon in shaking bioreactors. *Biochemical Engineering Journal*, **7**, 2, 135 – 141.

Büchs, J., Maier, U., Milbradt, C. and Zoels, B. (2000) Power consumption in shaking flasks on rotary shaking machines. Part I. Power consumption measurement in unbaffled flasks at low liquid viscosity. *Biotechnology and Bioengineering*, **68**, 6, 589 – 593.

Bujalski, W., Takenaka, K., Paolini, S., Jahoda, M., Paglianti, A., Takahashi, K., Nienow, A. W. and Etchells, A. W. (1999) Suspension and liquid homogenization in high solids concentration stirred chemical reactors. *Chemical Engineering Research and Design*, **77**, 241 – 247.

Büntemeyer, H. (2007) Methods for off-line analysis of nutrients and products in mammalian cell culture. In: Pörtner, R. (ed.) Animal Cell Biotechnology: Methods and Protocols. Humana Press.

Butler, M. (2005) Animal cell cultures: recent achievements and perspectives in the production of biopharmaceuticals. *Applied Microbiology and Biotechnology*, **68**, 283 – 291.

Calderbank, P. (1958) Physical rate processes in industrial fermentation. The interfacial area in gas–liquid contacting with mechanical agitation. *Transactions of the Institution of Chemical Engineers*, **36**, 443 – 463.

Carroll, S., Naeiri, M. and Al-Rubeai, M. (2007) Monitoring of Growth, Physiology, and Productivity of Animal Cells by Flow Cytometry. In: Pörtner, R. (ed.) Animal Cell Biotechnology: Methods and Protocols. Humana Press.

CASY website[2]. Last accessed 01/02/12.

Catapano, G., Czermak, P., Eibl, R., Eibl, D. and Pörtner, R. (2009) Bioreactor Design and Scale-Up. In: Eibl, R., Eibl, D., Pörtner, R., Catapano, G. and Czermak, P. (ed.) Cell and Tissue Reaction Engineering. Springer.

Chen, A., Chitta, R., Chang, D. and Amanullah, A. (2009) Twenty-four well plate miniature bioreactor system as a scale-down model for cell culture process development. *Biotechnology and Bioengineering*, **102**, 1, 148 – 160.

Chen, W., Zhua, Z., Feng, Y. and Dimitrov, D. (2008) Human domain antibodies to conserved sterically restricted regions on gp120 as exceptionally potent cross-reactive HIV-1 neutralizers. *Proceedings of the National Academy of Sciences*, **105**, 44, 17121 – 17126.

Colangelo, J. and Orlando, R. (2001) On-target endoglycosidase digestion matrix-

[2] http://www.casy-technology.com/

Assisted laser desorption/ionization mass spectrometry of glycopeptides. *Rapid Communications in Mass Spectrometry*, **15**, 2284 – 2289.

Cui, Y.Q., van der Lans, R., Ch, K. and Luyben, A. (1996) Local power uptake in gas–liquid systems with single and multiple Rushton turbines. *Chemical Engineering Science*, **51**, 2631 – 2636.

DeFranco, A., Locksley, R. and Robertson, M. (2007) Immunity: The immune Response in Infectious and Inflammatory Disease. Oxford University Press.

Dimitrov, D. and Chen, W. (2008) Anti-HIV domain antibodies and method of making and using same. US Patent no. 61/019,426.

Dinnis, D. and James, D. (2005) Engineering mammalian cell factories for improved recombinant monoclonal antibody production: lessons from nature? *Biotechnology and Bioengineering*, **91**, 2, 180 – 189.

Doig, S., Baganz, F. and Lye, G. (2006) High throughput screening and process optimization, p. 293. In: Ratledge, C. and Kristiansen, B. (ed.) Basic Biotechnology, 3rd edition. Cambridge University Press.

Doig, S.D., Diep, A. and Baganz, F. (2005) Characterisation of a novel miniaturised bubble column bioreactor for high throughput cell cultivation. *Biochemical Engineering Journal*, **23**, 97 – 105.

Doig, S. D., Pickering, S. C. R. and Lye, G. J. (2005) Modelling surface aeration rates in shaken microtitre plates using dimensionless groups. *Chemical Engineering Science*, **60**, 10, 2741 - 2750.

Domantis Patent (2006) European Patent no. EP1517921B.

Doran, P. (1999) Bioprocess engineering principles. Academic Press.

Dübel, S. and Reichart, J. M. (2014) Therapeutic Antibodies - From Past to Future. In: Dubel, S. and Reichart, J. M. (ed.) Handbook of Therapeutic Antibodies. John Wiley & Sons.

Duetz, W. A., Ruedi, L., Hermann, R., O'Connor, K., Buchs, J. and Witholt, B. (2000) Methods for intense aeration, growth, storage, and replication of bacterial strains in microtiter plates. *Applied and Environmental Microbiology*, **66**, 2641 – 2646.

Dunn, I. J. and Einsele, A. J. (1975) Oxygen transfer coefficients by the dynamic method. *Journal of Applied Chemistry and Biotechnology*, **25**, 707 – 720.

Enever, C., Batuwangala, T., Plummer, C. and Sepp, A. (2009) Next generation immunotherapeutics - honing the magic bullet. *Current Opinion in Biotechnology*, **20**, 4, 405 – 411.

Farid, S. (2007) Process economics of industrial mAb manufacture. *Journal of Chromatography B*, **848**, 1, 8 – 18.

Filipe, V., Jiskoot, W., Basmeleh, A. H., Halim, A., Schellekens, H. and Brinks, V. (2012) Immunogenicity of different stressed IgG monoclonal antibody formulations in immune tolerant transgenic mice. *MAbs*, **4**, 740 – 752.

Flickinger, M. and Drew, S. (1999) Encyclopedia of bioprocess technology - fermentation, biocatalysis, and bioseparation. John Wiley and Sons.

GBI Research. (2012) Biopharmaceutical manufacturing in India, China and South Korea – regulatory framework, infrastructure support and discovery funding create an environment conducive to growth.

Genentech presentation given at Cell Culture Engineering X, Whistler, Canada, April 23-28, 2006.

Gill, N. K., Appleton, M., Baganz, F. and Lye, G. J. (2008a) Design and characterisation of a miniature stirred bioreactor system for parallel microbial fermentations. *Biochemical Engineering Journal*, **39**, 164 – 176.

Gill, N. K., Appleton, M., Baganz, F. and Lye, G. J. (2008b) Quantification of power consumption and oxygen transfer characteristics of a stirred miniature bioreactor for predictive fermentation scale-up. *Biotechnology and Bioengineering*, **100**, 6, 1144 – 1155.

Girard, P., Jordan, M., Tsao, M. and Wurm, F. (2001) Small-scale bioreactor system for process development and optimization. *Biochemical Engineering Journal*, **7**, 117 – 119.

Godoy-Silva, R., Berdugo, C. and Chalmers, J. (2010) Aeration, Mixing and hydrodynamics, animal cell bioreactors. In: Flickinger M. (ed.) Encyclopedia of Industrial Biotechnology: Bioprocess, Bioseparation, and Cell Technology. John Wiley and Sons.

Godoy-Silva, R., Chalmers, J., Casnocha, S., Bass, L. and Ma, N. (2009) Physiological responses of CHO cells to repetitive hydrodynamic stress. *Biotechnology and Bioengineering*, **103**, 6, 1103 – 1117.

Hacker, D., de Jesus, M. and Wurm, F. (2009) 25 years of recombinant proteins from reactor-grown cells — Where do we go from here? *Biotechnology Advances*, **27**, 1023 – 1027.

Hamilton, S. and Gerngross, T. (2007) Glycosylation engineering in yeast: the advent of fully humanized yeast. *Current Opinion in Biotechnology*, **18**, 5, 387 – 392.

Hanania, E., Fieck, A., Stevens, J., Bodzin, L., Palsson, B. and Koller, M. (2005) Automated in situ measurement of cell-specific antibody secretion and laser-mediated purification for rapid cloning of highly-secreting producers. *Biotechnology and Bioengineering*, **91**, 7, 872 – 876.

Harthun, S., Matischak, K. and Friedl, P. (1997) Determination of recombinant protein in animal cell culture supernatant by near-infrared spectroscopy. *Analytical Biochemistry*, **251**, 73 – 78.

Heath, C. and Kiss, R. (2007) Cell culture process development: advances in process engineering. *Biotechnology Progress*, **23**, 1, 46 – 51.

Hemrajani, R. and Tatterson, G. (2004) Mechanically stirred vessels. In: Paul, E., Atiemo-Obeng, V. and Kresta, S. (ed.) Handbook of industrial mixing: science and practice. John Wiley and Sons.

Henriques, J., Buziol, S., Stocker, E., Voogd, A. and Menezes, J. (2009) Monitoring mammalian cell cultivations for monoclonal antibody production using near-infrared spectroscopy, In: Rao, G. (ed.) Optical sensor systems in biotechnology. Springer.

Hermann, R., Lehmann, M. and Büchs, J. (2003) Characterization of gas-liquid mass transfer phenomena in microtiter plates. *Biotechnology and Bioengineering*, **81**, 2, 178 – 186.

Ho, Y., Varley, J. and Mantalaris, A. (2006) Development and analysis of a mathematical model for antibody-producing GS-NS0 cells under normal and hyperosmotic culture conditions. *Biotechnology Progress*, **22**, 6, 1560 – 1569.

Hoffman, T. (2006) Counting cells in Cell Biology: a laboratory handbook. Elsevier.

Holt, L., Herring, C., Jespers, L., Woolven, B. and Tomlinson, I. (2003) Domain antibodies: proteins for therapy. *Trends in Biotechnology*, **21**, 11, 484 – 490.

Hossler, P., Khattak S. F. and Li, Z. J. (2009) Optimal and consistent protein glycosylation in mammalian cell culture. *Glycobiology*, **19**, 936 – 949.

Hughmark, G. A. (1980) Power requirements and interfacial area in gas–liquid turbine agitated systems. *Industrial and Engineering Chemistry Process Design and Development,* **19**, 638–641.

IMS Health, 21st Century Pharma: Managing current challenges to ensure future growth. Article available online[3].

IMS Health, Biogenerics: A Difficult Birth. Article available online[4].

IMS Health Market Prognosis. Article available online[5].

IMS Health, Biotech market size and growth (2007) Article available online[6].

IMS Health, Press Release - Global biotech sales grew 12.5 percent in 2007, exceeding $75 Billion. Article available online[7].

Isett, K., George, H., Herber, W. and Amanullah, A. (2007) Twenty-four-well plate miniature bioreactor high-throughput system: Assessment for microbial cultivations. *Biotechnology and Bioengineering*, **98**, 1017 – 1028.

Jackson, N. B. (2011) Microscale approaches to the rapid evaluation and specification of microfiltration processes. PhD thesis, University College London.

Janeway, C. A., Travers, P., Walport, M. and Shlomchik, M. J. (2005) Immunobiology, 6th ed. Garland Sciences.

Jefferis, R. (2009) Recombinant antibody therapeutics: the impact of glycosylation on mechanisms of action. *Trends in Pharmacological Sciences*, **30**, 7, 356 – 362.

[3] http://www.imshealth.com/deployedfiles/imshealth/Global/Content/StaticFile/In_vivo_july_pharma_strategy_executive_summary.pdf.%20Last%20accessed%2024/02/2012
[4] http://www1.imshealth.com/web/content/0,3148,64576068_63872702_70261000_71026746,00.html
[5] http://www.imshealth.com/deployedfiles/imshealth/Global/Content/StaticFile/Top_Line_Data/Global_Pharma_Sales_2001-2008_Version_2.pdf
[6] http://www.imshealth.com/deployedfiles/imshealth/Global/Content/StaticFile/biotech_slides_for_internet.pdf
[7] http://www.imshealth.com/portal/site/imshealth/menuitem.a46c6d4df3db4b3d88f611019418c22a/?vgnextoid=bba69e392879a110VgnVCM100000ed152ca2RCRD&vgnextfmt=default

Ju, L.-K. and Chase, G. (1992) Improved scale up strategies of bioreactors. *Bioprocess Engineering*, **8,** 49 – 53.

Junker, B. (2004) Scale-up methodologies for Escherichia coli and yeast fermentation processes. *Journal of Bioscience and Bioengineering*, **97**, 6, 347 – 364.

Kantarci, N., Borak, F. and Ulgen, K. O. (2005) Bubble column reactors. *Process Biochemistry*, **40**, 2263 – 2283.

Kelley, B (2009) Industrialization of mAb production technology: The bioprocessing industry at a crossroads. *MAbs*, **1**, 5, 443 – 452.

Kong, S., Aucamp, J. and Titchener-Hooker, N.J. (2010) Studies on membrane sterile filtration of plasmid DNA using an automated multiwell technique. *Journal of Membrane Science*, **353**, 144 – 150.

La Merie, Top 20 Biologics, 2006. Article available online[8].

Lau, E. C., Kong, S., McNulty, S., Entwisle, C., Mcilgorm, A., Dalton, K. A. and Hoare, M. (2013) An ultra scale-down characterization of low shear stress primary recovery stages to enhance selectivity of fusion protein recovery from its molecular variants. *Biotechnology and Bioengineering*, **110**, 1973 – 1983.

Lee, S. and Lee, L. (2005) Encyclopaedia of Chemical Processing. CRC Press, London.

Legmann, R., Schreyer, B., Combs, R., McCormick, E., Russo, P. and Rodgers, S. (2009) A predictive high-throughput scale-down model of monoclonal antibody production in CHO cells. *Biotechnology and Bioengineering*, **104**, 6, 1107 – 1120.

[8] http://www.pipelinereview.com/index.php/2007021215649/free-Reports/Top-20-Biologics-2006-Sales-of-Antibodies-Proteins.html

Linek, V., Kordac, M., Fujasova, M. and Moucha, T. (2004) Gas–liquid mass transfer coefficient in stirred tanks interpreted through models of idealised eddy structure of turbulence in the bubble vicinity. *Chemical Engineering and Processing: Process Intensification*, **43**, 1511 – 1517.

Liu, H. F., Ma, J., Winter, C. and Bayer, R. (2010) Recovery and purification process development for monoclonal antibody production. *MAbs*, **2**, 480 – 499.

Lloyd, D., Holmes, P., Jackson, L., Emery, A. and Al-Rubeai, M. (2000) Relationship between cell size, cell cycle and specific recombinant protein productivity. *Cytotechnology*, **34**, 59 – 70.

Lodish, H., Berk, A., Matsudaira, P., Kaiser, C., Krieger, M., Scott, M., Zipursky, L. and Darnell, J. (2004) Molecular Cell Biology. W. H. Freeman and Company.

Mancia, F., Patel, S., Rajala, M., Scherer, P., Nemes, A., Schieren, I., Hendrickson, W. and Shapiro, L. (2004) Optimization of protein production in mammalian cells with a coexpressed fluorescent marker. *Structure*, **12**, 8, 1355 – 1360.

Markusen, J.F. and Robinson, D. K. (2010) Monoclonal Antibody Production, Cell Lines. In: Flickinger M. (ed.) Encyclopedia of Industrial Biotechnology. John Wiley and Sons.

Matasci, M., Hacker, D., Baldi, L. and Wurm, F. (2008) Recombinant therapeutic protein production in cultivated mammalian cells: current status and future prospects. *Drug Discovery Today: Technologies*, **5**, 37 – 42.

Mathews, C., van Holde, K. and Ahern, K. (2000) Biochemistry. Addison-Wesley.

Micheletti, M., Barrett, T., Doig, S., Baganz, F., Levy, M., Woodley J. and Lye, G. J. (2006) Fluid mixing in shaken bioreactors: Implications for scale-up

predictions from microlitre-scale microbial and mammalian cell cultures. *Chemical Engineering Science*, **61**, 9, 2939 – 2949.

Michel, B. J. and Miller, S. A. (1962) Power Requirements of Gas-Liquid Agitated Systems. *American Institute of Chemical Engineers*, **8**, 2, 262 – 266.

MicroReactor Technologies[9]. Last accessed 03/03/10.

Mockel, H. Weissgarber, H., Drewas, E., Rahner, H. (1990) Modelling of the calculation of the power input for aerated single and multistage impellers with special respect to scale-up. *Acta Biotechnologica*, **10**, 215 – 224.

Mollet, M., Ma, N., Zhao, Y., Brodkey, R., Taticek, R. and Chalmers, J. (2004) Bioprocess equipment: characterization of energy dissipation rate and its potential to damage cells. *Biotechnology Progress*, **20**, 1437 – 1448.

Nagata, S. (1975). Mixing: Principles and Applications. Halstead Press.

Nealon, A. J., O'Kennedy, R. D., Titchener-Hooker, N. J. and Lye, G. J. (2006) Quantification and prediction of jet macro-mixing times in static microwell plates. *Chemical Engineering Science*, **61**, 4860 – 4870.

Nelson, A. L., Dhimolea, E. and Reichert, J. M. (2010) Development trends for human monoclonal antibody therapeutics. *Nature Reviews Drug Discovery*, **9**, 767 – 774.

Nienow, A. (1997) On impeller circulation and mixing effectiveness in the turbulent flow regime. *Chemical Engineering Science*, **52,** 2557 – 2565.

Nienow, A. W. (1998) Hydrodynamics of stirred bioreactors. *Applied Mechanics Reviews*, **51**, 3 – 32.

[9] www.microreactor.com

Nienow, A. W. (2006) Reactor engineering in large scale animal cell culture. *Cytotehnology*, **50**, 9 – 33.

Nienow, A. W., Langheinrich, C., Stevenson, N. C., Emery, A. N., Clayton, T. M. and Slater, N. K. H. (1996) Homogenisation and oxygen transfer rates in large agitated and sparged animal cell bioreactors: Some implications for growth and production. *Cytotechnology*, **22**, 87 – 94.

Nienow, A. W., Rielly, C. D. and Brosnan, K. (2013) The physical characterisation of a microscale parallel bioreactor platform with an industrial CHO cell line expressing an IgG4. *Biochemical Engineering Journal*, **76**, 25 – 36.

Odeleye, A. O., Marsh, D. T., Osborne, M. D., Lye, G. J. and Micheletti, M. (2014). On the fluid dynamics of a laboratory scale single-use stirred bioreactor. *Chemical Engineering Science*, **111**, 299 – 312.

Oh, S. K. W., Nienow, A., Al-Rubeai, M. and Emery, A. N. (1989) The effects of agitation intensity with and without continuous sparging on the growth and antibody production of hybridoma cells. *Journal of Biotechnology*, **12**, 45 – 62.

Osman, J. J. (2001) Response of GS-NS0 mouse myeloma cells to pH fluctuations relevant to those found in large scale fermentation. PhD thesis, The University of Reading.

Patterson, G. K., Paul, E. L., Kresta, S. M. and Etchells, A. W. (2004) Mixing and chemical reaction. In: Paul, E. L., Atiemo-Obeng, V. A. and Kresta, S. M. (ed.) Handbook of industrial mixing: Science and Practice. John Wiley and Sons.

Pavlou, A. and Belsey, M. (2005) The therapeutic antibodies market to 2008. *European Journal of Pharmaceutics and Biopharmaceutics*. **59**, 3, 389 – 396.

Purvis, L. (2009) Biologics in perspective: The case for generic biologic drugs. AARP Public Policy Institute. Article available online[10].

Puskeiler, R., Kaufmann, K. and Weuster-Botz, D. (2005) Development, parallelization, and automation of a gas-inducing milliliter-scale bioreactor for high-throughput bioprocess design (HTBD). *Biotechnology and Bioengineering*, **89**, 512 – 523.

Rai, M. and Padh, H. (2001) Expression systems for production of heterologous proteins. *Current Science*, **80**, 9, 1121 – 1128.

Reimold, A., Iwakoshi, N., Manisk, J., Vallabhajosyula, P., Szomolanyi-Tsuda, E., Gravallese, E., Friend, D., Grusby, M., Altk, M. and Glimcher, L. (2001) Plasma cell differentiation requires the transcription factor XBP-1. *Nature*, **412**, 300 – 307.

Schröder, M. (2008) Engineering eukaryotic protein factories. *Biotechnology Letters*, **30**, 2, 187 – 196.

Schröder, M. and Kaufman, R. (2005) The mammalian unfolded protein response. *Annual Review of Biochemistry*, **74**, 739 – 789.

Scrip's Pharmaceutical Company League Tables (2009). Article available online[11].

Shimoni, Y., Goudar, C., Jenne, M. and Srinivasan, V. (2014) Qualification of Scale-Down Bioreactors: Validation of Process Changes in Commercial Production of Animal-Cell-Derived Products. *BioProcess International*, May 2014.

Shukla, A., Hubbard, B., Tressel, T., Guhan, S. and Low, D. (2007) Downstream processing of monoclonal antibodies - Application of platform approaches. *Journal of Chromatography B*, **848,** 28 – 39.

[10] http://assets.aarp.org/rgcenter/health/fs155_biologics.pdf
[11] http://www.scripnews.com/home/supplementsreports/Scrips-Pharmaceutical-Company-League-Tables---2009-178602

Sideman, S., Hortaçsu, Ö. and Fulton, J. W. (1966) Mass transfer in gas-liquid contacting systems. *Industrial and Engineering Chemistry*, **58,** 32 – 47.

Silk, N. (2014) High Throughput Approaches to Mammalian Cell Culture Process Development. EngD thesis, University College London.

Silk, N., Denby, S., Kuiper, M., Hatton, D., Field, R., Baganz, F. and Lye, G. (2010) Fed-batch operation of an industrial cell culture process in shaken microwells, *Biotechnology Letters*, **32**, 1, 73 – 78.

Sikora, K. (2007) Paying for cancer care - a new dilemma. *Journal of the Royal Society of Medicine*, **100,** 166 – 169.

Simcell website[12]. Last accessed 12/02/10.

Simoens, S. (2009) Health economics of market access for biopharmaceuticals and biosimilars. *Journal of Medical Economics*, **12**, 3, 211 – 218.

Smith, J., van't Riet, K. and Middleton, J. (1977) Scale up of agitated gas–liquid reactors for mass transfer. *Proceedings of 2nd European conference on mixing*, 51 – 66.

Stanbury, P. F. and Whitaker, A. (1984) Principles of fermentation technology. 1st edition. Pergamon Press Ltd.

Strobel, R., Bowden, D., Bracey, M., Sullivan, G., Hatfield, C., Jenkins, N and Vinci, V. (2001) High throughput cultivation of animal cells using shaken microplate techniques. In: Lindner-Olsson, E., Chatzissavidou, N. and Lüllau, E. (ed.) Animal cell technology: from target to market. Springer.

[12] http://www.seahorsebio.com/products/simcell/simcell.php

Szita, N., Boccazzi, P., Zhang, Z., Boyle, P., Sinskey, A. and Jensen, K. (2005) Development of a multiplexed microbioreactor system for high throughput bioprocessing. *Lab Chip*, **5**, 819 – 826.

Tait, A. S., Aucamp, J. P., Bugeon, A. and Hoare, M. (2009) Ultra Scale-Down Prediction Using Microwell Technology of the Industrial Scale Clarification Characteristics by Centrifugation of Mammalian Cell Broths. *Biotechnology and Bioengineering*, **104**, 321 – 331.

TAP Biosystems[13]. Last accessed 03/03/14.

Tecan[14]. Last accessed 03/03/12.

Tennekes, H. and Lumley, J. L. (1972) A first course in turbulence. MIT Press, Cambridge, p. 159.

Tescione, L., Lambropoulos, J., Paranandi, M. R., Makagiansar, H. and Ryll, T. (2014) Application of bioreactor design principles and multivariate analysis for development of cell culture scale-down models. *Biotechnology and Bioengineering*, Advanced online publication.

Tufts CSDD Press Release. Article available online[15].

Valentine, D. (2009) Single-Use Bioreactors: A Flexible Solution. Presentation at an IChemE meeting, November 2009.

Van't Riet, K. (1975) Turbine agitator hydrodynamics and dispersion performance. PhD thesis, University of Delft.

[13] http://www.tapbiosystems.com/
[14] www.tecan.com
[15] http://csdd.tufts.edu/NewsEvents/RecentNews.asp?newsid=69

Van't Riet, K. (1979) Review of measuring methods and results in nonviscous gas-liquid mass transfer in stirred vessels. *Industrial and Engineering Chemistry Process Design and Development*, **18**, 357 – 364.

Vilaca, P., Badino, A., Facciotti, M. and Schmidell, W. (2000) Determination of power consumption and volumetric oxygen transfer coefficient in bioreactors. *Bioprocess Engineering*, **22**, 261 – 265.

Villadsen, J., Nielsen, J. and Lidén, G. (2011) Bioreaction Engineering Principles. Springer.

Walsh, G. (2001) Proteins: biochemistry and biotechnology. John Wiley and Sons.

Walsh, G. and Jefferis, R. (2006) Post-translational modifications in the context of therapeutic proteins. *Nature Biotechnology*, **24**, 1241 – 1252.

Gary Walsh, G. (2014) Biopharmaceutical benchmarks 2014. *Nature Biotechnology*, **32**, 992 – 1000.

Waltz, E. (2005) GlaxoSmithKline cancer drug threatens Herceptin market. *Nature Biotechnology*, **23**, 12, 1453 – 1454.

Ward, E., Gussow, D., Griffiths, A., Jones, P. and Winter, G. (1989). Binding activities of a repertoire of single immunoglobulin variable domains secreted from E. coli. *Nature*, **341**, 544 – 546.

Warmoeskerken, M. (1986) Gas-liquid dispersing characteristics of turbine agitators. PhD thesis, University of Delft.

Weuster-Botz, D., Altenbach-Rehm, J. and Hawrylenko, A. (2001) Process-engineering characterization of small-scale bubble columns for microbial process development. *Bioprocess and Biosystems Engineering*, **24**, 3 – 11.

Wong, R. B., Ming, Z., An-Horng, L., Raju, T. S. and Kuang-Chuan, C. (2012) Functional Role of Glycosylation in a Human IgG4 Antibody Assessed by Surface Plasmon Resonance Technology. *Open Pharmacology Journal*, **6,** 27 – 33.

Woolley, J. and Al-Rubeai, M. (2009) The isolation and identification of a secreted biomarker associated with cell stress in serum-free CHO cell culture. *Biotechnology and Bioengineering*, **104**, 3, 590 – 600.

Wurm, F. (2004) Production of recombinant protein therapeutics in cultivated mammalian cells. *Nature Biotechnology*, **22**, 11, 1393 – 1398.

Xing, Z., Kenty, B., Li, Z. and Lee, S. (2009) Scale-up analysis for a CHO cell culture process in large-scale bioreactors. *Biotechnology and Bioengineering*, **103**, 4, 733 – 746.

Yang, J.-D., Li, C., Stasny, B., Henley, J., Guinto, W., Gonzalez, C., Gleason, J., Fung, M., Collopy, B., Benjamino, M., Gangi, J., Hanson, M. and Ille, E. (2007) Fed-batch bioreactor process scale-up from 3L to 2500L scale for monocolonal antibody production from cell culture. *Biotechnology and Bioengineering*, **98,** 1, 141 – 154.

Yeung, K., Hoare, M., Thornhill, N., Williams, T. and Vaghjiani, J. (1999) Near-infrared spectroscopy for bioprocess monitoring and control. *Biotechnology and Bioengineering*, **63**, 684 – 693.

Zhang, H., Williams-Dalson, W., Keshavarz-Moore, E. and Shamlou, P. (2005) Computational-fluid-dynamics (CFD) analysis of mixing and gas–liquid mass transfer in shake flasks. *Biotechnology and Applied Biochemistry*, **41**, 1 – 8.

Zhang, H., Lamping, S., Pickering, S., Lye, G. and Shamlou, P. (2008) Engineering characterisation of a single well from 24-well and 96-well microtitre plates. *Biochemical Engineering Journal*, **40**, 1, 138 – 149.

Zhang, X., Burki, C.-A., Stettler, M., de Sanctis, D., Perrone, M., Discacciati, M., Parolini, N., de Jesus, M., Hacker, D., Quarteroni, A. and Wurm, F. (2009) Efficient oxygen transfer by surface aeration in shaken cylindrical containers for mammalian cell cultivation at volumetric scales up to 1000L. *Biochemical Engineering Journal*, **45**, 41 – 47.

Zhang, Z., Szita, N., Boccazzi, P., Sinskey, A. and Jensen, K. (2006) A well-mixed polymer-based microbioreactor with integrated optical measurements. *Biotechnology and Bioengineering*, **93**, 286 – 296.

Zhu, Y., Bandopadhayay, P. and Wu, J. (2001) Measurement of gas–liquid mass transfer in an agitated vessel – a comparison between different impellers. *Journal of Chemical Engineering of Japan*, **34**, 579 – 584.